การเตรียมโฟมพอลิยูรีเทนแบบแข็งเร่งปฏิกิริยาด้วยสารประกอบเชิงซ้อนนิกเกิลและโคบอลต์

นางสาว ภัทรินทร์ แสงฝาก

วิทยานิพนธ์นี้เป็นส่วนหนึ่งของการศึกษาตามหลักสูตรปริญญาวิทยาศาสตรมหาบัณฑิต
สาขาวิชาปิโตรเคมีและวิทยาศาสตร์พอลิเมอร์
คณะวิทยาศาสตร์ จุฬาลงกรณ์มหาวิทยาลัย
ปีการศึกษา 2553

PREPARATION OF RIGID POLYURETHANE FOAM CATALYZED BY
NICKEL AND COBALT COMPLEXES

Miss Bhattarin Saengfak

ศูนย์วิทยทรัพยากร
จุฬาลงกรณ์มหาวิทยาลัย

A Thesis Submitted in Partial Fulfillment of the Requirements
for the Degree of Master of Science Program in Petrochemistry and Polymer Science
Faculty of Science
Chulalongkorn University
Academic Year 2010
Copyright of Chulalongkorn University

530594

Thesis Title   PREPARATION OF RIGID POLYURETHANE FOAM CATALYZED BY NICKEL AND COBALT COMPLEXES

By   Miss Bhattarin Saengfak

Field of Study   Petrochemistry and Polymer Science

Thesis Advisor   Associate Professor Nuanphun Chantarasiri, Ph.D.

Accepted by the Faculty of Science, Chulalongkorn University in Partial Fulfillment of the Requirements for the Master's Degree

....Dean of the Faculty of Science

(Professor Supot Hannongbua, Dr.rer.nat.)

THESIS COMMITTEE

.... Chairman

(Associate Professor Supawan Tantayanon, Ph.D.)

.... Thesis Advirsor

(Associate Professor Nuanphun Chantarasiri, Ph.D.)

.... Examiner

(Associate Professor Voravee P. Hoven, Ph.D.)

.... External Examiner

(Assistant Professor Toemsak Srikhirin, Ph.D.)

ภัทรินทร์   แสงฝาก: การเตรียมโฟมพอลิยูรีเทนแบบแข็งเร่งปฏิกิริยาด้วยสารประกอบ
เชิงซ้อนนิกเกิลและโคบอลต์. (PREPARATION OF RIGID POLYURETHANE FOAM
CATALYZED BY NICKEL AND COBALT COMPLEXES)
อ.ที่ปรึกษาวิทยานิพนธ์หลัก: รศ. ดร. นวลพรรณ จันทรศิริ, 107 หน้า.

งานวิจัยนี้เป็นการสังเคราะห์สารประกอบเชิงซ้อนของโลหะแทรนซิชัน   คือ $M(en)_2$,
$M(en)_2(sal)_2$, $M(trien)$ และ $M(trien)(sal)_2$ (M = Ni และ Co) เพื่อใช้เป็นตัวเร่งปฏิกิริยาสำหรับการ
สังเคราะห์โฟมพอลิยูรีเทนแบบแข็ง เวลาในการเกิดปฏิกิริยาของโฟม สมบัติทางกายภาพ และ
สมบัติเชิงกลของโฟมพอลิยูรีเทนจะถูกนำมาเปรียบเทียบกับโฟมที่เตรียมจากตัวเร่งปฏิกิริยาทาง
การค้า คือ ไดเมทิลไซโคลเฮกซิลแอมีน (DMCHA) การพิสูจน์เอกลักษณ์ของสารประกอบเชิงซ้อน
ของที่ใช้เป็นตัวเร่งปฏิกิริยาทำได้โดยใช้ยูวี-วิสสเปกโตรสโคปี ไออาร์สสเปกโตรสโคปี การ
วิเคราะห์ธาตุ และอะตอมมิกแอบซอฟชัน การหาปริมาณหมู่ไอโซไซยาเนตที่เกิดปฏิกิริยาและ
อัตราส่วนระหว่างพอลิไอโซไซยานูเรตต่อพอลิยูรีเทนในโฟมพอลิยูรีเทนทำได้โดยใช้เอทีอาร์ไอ
อาร์ ปฏิกิริยาการเกิดโฟมพอลิยูรีเทนเป็นปฏิกิริยาการคายความร้อนโดยอุณหภูมิของการ
เกิดปฏิกิริยาอยู่ในช่วง 114-125 องศาเซลเซียส ในช่วงเวลาการเตรียมโฟม ได้ศึกษาเวลาที่ของผสม
เป็นครีม เวลาที่ของผสมเป็นเจล เวลาที่ผิวหน้าของโฟมไม่เกาะติดกับวัสดุสัมผัส และเวลาที่โฟม
หยุดฟู ความหนาแน่นของโฟมพอลิยูรีเทนอยู่ในช่วง 42.3-73.9 kg/m^3 สารประกอบเชิงซ้อนของ
โคบอลต์สามารถเร่งปฏิกิริยาการเกิดโฟมได้ดีกว่าสารประกอบเชิงซ้อนของนิกเกิล ความทนทาน
ต่อแรงกดอัดของโฟมพอลิยูรีเทนที่เร่งปฏิกิริยาด้วย $Ni(trien)(sal)_2$ แสดงค่าสูงกว่าโฟมที่เตรียมจาก
DMCHA โฟมที่เตรียมได้จาก $Ni(en)_2$ และ $Co(en)_2$ แสดงค่าการสลายตัวทางความร้อนเท่ากับ
กับโฟมที่เตรียมจาก DMCHA โฟมที่เตรียมได้จาก Co(trien) and $Co(en)_2$ มีค่าการนำความร้อน
เทียบเท่ากับโฟมที่เตรียมได้จาก DMCHA

สาขาวิชา ปิโตรเคมีและวิทยาศาสตร์พอลิเมอร์ ลายมือชื่อนิสิต ภัทรินทร์ แสงฝาก
ปีการศึกษา   2553   ลายมือชื่อ อ. ที่ปรึกษาวิทยานิพนธ์หลัก

5172402023: MAJOR PETROCHEMISTRY AND POLYMER SCIENCE
KEYWORDS: METAL COMPLEX/ RIGID POLYURETHANE FOAM/ NCO CONVERSION

BHATTARIN SAENGFAK: PREPARATION OF RIGID POLYURETHANE FOAM CATALYZED BY NICKEL AND COBALT COMPLEXES THESIS ADVISOR: ASSOC. PROF. NUANPHUN CHANTARASIRI, Ph. D., 107 pp.

Transition metal complexes, namely $M(en)_2$, $M(en)_2(sal)_2$, $M(trien)$ and $M(trien)(sal)_2$ (M = Ni and Co), were synthesized and used as catalysts for the preparation of rigid polyurethane foams (PURFs). The reaction times, physical and mechanical properties of PURFs were investigated and compared to those prepared by commercial catalyst, N,N-dimethylcyclohexylamine (DMCHA). UV-vis spectroscopy, IR spectroscopy, elemental analysis and atomic absorption were used to characterize the transition metal complexes catalysts. ATR-IR technique was used to study isocyanate (NCO) conversion and polyisocyanurate/polyurethane (PIR/PUR) ratio in the PURFs. The polymerization reaction of foaming preparation is exothermic reaction. The maximum reaction temperature is in the range of 114-125°C. During the foam preparation, cream time, gel time, tack-free time and rise time were investigated. The results showed that the apparent density of PURFs was in the range 42.3-73.9 kg/m^3. Co complexes showed better catalytic activity than Ni complexes. Compressive strength of PURF prepared from $Ni(trien)(sal)_2$ was better than that prepared from DMCHA. PURFs obtained from $Ni(en)_2$ and $Co(en)_2$ showed similar thermal decomposition with that obtained from DMCHA catalyst. Thermal conductivity of PURFs showed that PURFs catalyzed by $Co(trien)$ and $Co(en)_2$ gave thermal conductivity similar to that catalyzed by DMCHA.

Field of Study: Petrochemistry and Polymer Science Student's Signature. Bhattarin Saengfak

Academic Year:_____2010_____ Advisor's Signature. Nuanphun Chantarasiri

ACKNOWLEDGEMENTS

CONTENTS

LIST OF TABLES

LIST OF FIGURES

ศูนย์วิทยทรัพยากร
จุฬาลงกรณ์มหาวิทยาลัย

LIST OF SCHEMES

LIST OF ABBREVIATIONS

%	percentage
ε	molar absorptivity
ATR-IR	Attenuated Total Reflectance-Infrared
cm	centimeter
cm^{-1}	unit of wavenumber
^{o}C	degree Celsius (centigrade)
Co	cobalt element
$Co(en)_2$	cobalt-ethylenediamine complex
$Co(en)_2(sal)_2$	cobalt-ethylenediamine-salicylate complex
$Co(OAc)_2$	cobalt acetate
$Co(trien)$	cobalt-triethylenetetramine complex
$Co(trien)(sal)_2$	cobalt-triethylenetetramine-salicylate complex
DBTDL	dibutyltin dilaurate
DMCHA	N,N-dimethylcyclohexylamine
EA	Elemental Analysis
en	ethylenediamine
FTIR	Fourier Transform Infrared Spectrophotometer
g	gram
h	hour
KBr	potassium bromide
kg	kilogram
kV	kilovolt
M	metal
m^3	cubic meter
MDI	4,4'-methane diphenyl diisocyanate
mg	milligram
min	minute
mL	milliliter
mm	millimeter
mmol	millimole
N	newton unit

Ni	nickel element
NCO	isocyanate
Ni(OAc)$_2$	nickel acetate
Ni(en)$_2$	nickel -ethylenediamine complex
Ni(en)$_2$(sal)$_2$	nickel -ethylenediamine-salicylate complex
Ni(trien)	nickel-triethylenetetramine complex
Ni(trien)(sal)$_2$	nickel-triethylenetetramine-salicylate complex
OHV	hydroxyl value
pbw	part by weight
PIR	polyisocyanurate
PMDI	polymeric 4,4'-methane diphenyl diisocyanate
ppm	part per million
PURFs	rigid polyurethane foam
rpm	round per minute
sal	salicylate
sec	second
SEM	Scanning Electron Microscope
t	time
TDI	toluene diisocyanate
TGA	Thermogravimetric Analysis
T$_{max}$	maximum core temperature
trien	triethylenetetramine
UV	ultraviolet

ศูนย์วิทยทรัพยากร
จุฬาลงกรณ์มหาวิทยาลัย

CHAPTER I
INTRODUCTION

Polyurethane foams are high molecular weight polymer based on the polyaddition of polyether or polyester polyol with polyisocyanates and some supplementary chemicals and catalysts. The main reactions are described in Scheme 1.1. A wide variety of properties can be tailored to fulfill the requirements of different applications from elastic to hard materials.

Blowing Reaction:

$$-NCO + H_2O \longrightarrow -NHCOOH \longrightarrow -NH_2 + CO_2 \uparrow$$

urea

Gelling Reaction:

$$-NCO + -OH \longrightarrow -NHCO-$$

urethane

Trimerization:

$$3(R-NCO) \longrightarrow$$

isocyanurate
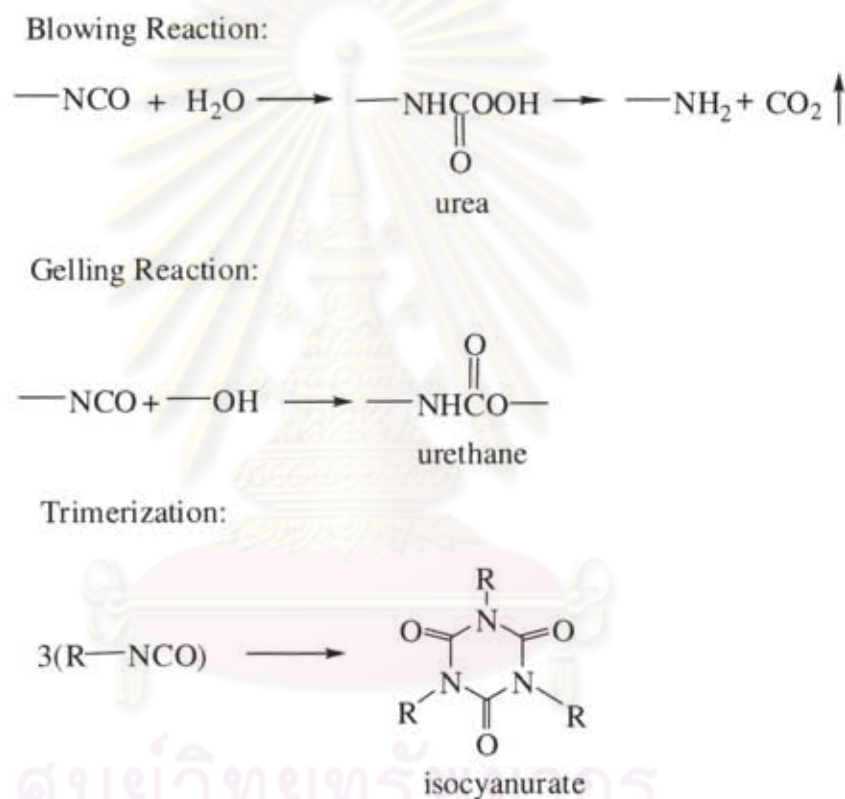
Scheme 1.1 Main reactions involved in polyurethane foam formation

Polyurethane foams (PURFs) account for the largest market among polymeric foams in the world. Polyurethane foams are categorized as flexible or soft, rigid or hard and semi-rigid according to their mechanical properties, such as their rigidity, stiffness, tensile, and compressive properties. Polyurethane foams feature excellent mechanical properties in relation to their low density, as well as low thermal conductivity which makes them generally suitable foe use as thermal insulation materials. Compared with other insulating materials, rigid polyurethane foam is

highly competitive. The air trapped within the honeycomb like structure develops passive insulation characteristics of foam in addition to polyurethanes heat absorption capacity.

Foaming occurs when a small amount of blowing agent is added during polymerization. Water (blowing agent) reacts with isocyanate groups giving carbamic acids, which spontaneously lose CO_2, thus generating the foam bubbles.

In the production of polyurethane foam, catalysts play an important role. With a good selection of the catalysts, the desired profile in reaction, foaming, flowability, and foam properties can be obtained. The reaction between polyisocyanate and polyol is very slow. Therefore tertiary amine and tin compound having excellent catalytic activity are used mainly as catalysts for polyurethane formation. In particular, dibutyltin dilaurate (DBTDL) has been used. However, tin is toxic to human beings. Accordingly, new catalytic systems are necessary to replace these catalysts.

Objective and scope of the research

The purposed of this study is to prepare rigid polyurethane foams catalyzed by transition metal complexes. Two types of metal complexes were prepared. Metal-amine complexes [M(en)$_2$ and M(trien)] were prepared from the reaction between metal acetates and amines (Schemes 1.2 and 1.3). Metal-amine-salicylate complexes [M(en)$_2$(sal)$_2$ and M(trien)(sal)$_2$] were prepared from the reaction between metal acetates, amines and salicylic acid (sal)$_2$ (Schemes 1.4 and 1.5). Metal acetates employed were nickel (II) acetate tetrahydrate ($Ni(OAc)_2.4H_2O$) and cobalt (II) acetate tetrahydrate ($Co(OAc)_2.4H_2O$). Amines employed were ethylenediamine (en) and triethlylenetetramine (trien).
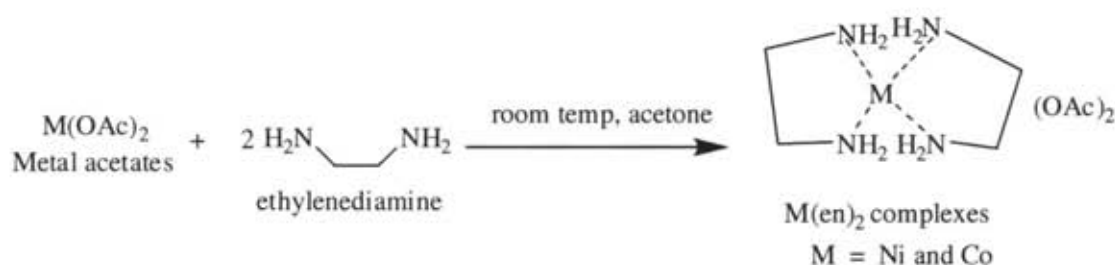
Scheme 1.2 Synthesis of M(en)$_2$ complexes
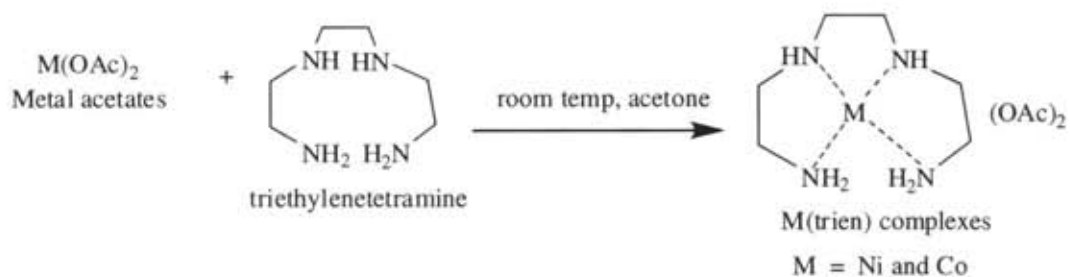
Scheme 1.3 Synthesis of M(trien)$_2$ complexes
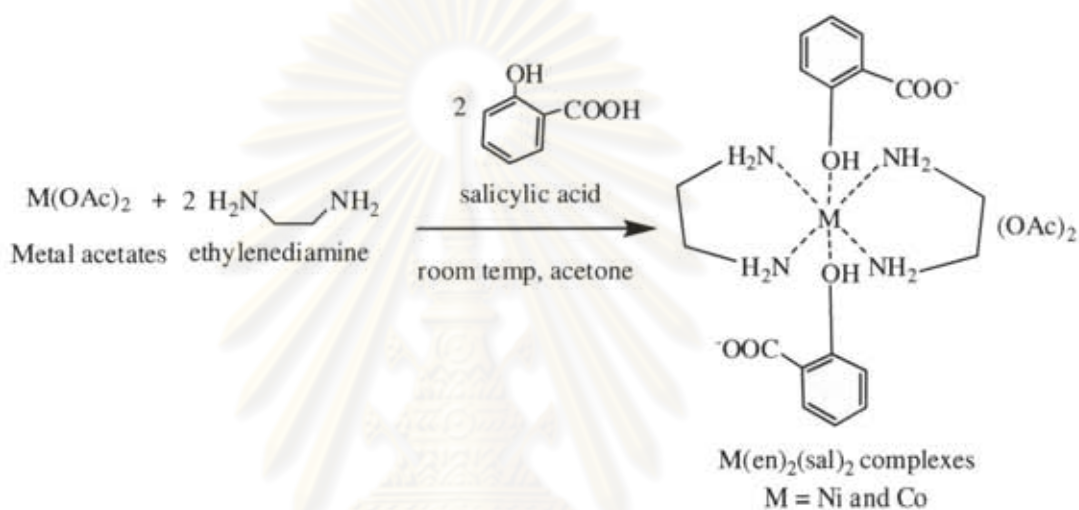
Scheme 1.4 Synthesis of M(en)$_2$(sal)$_2$ complexes
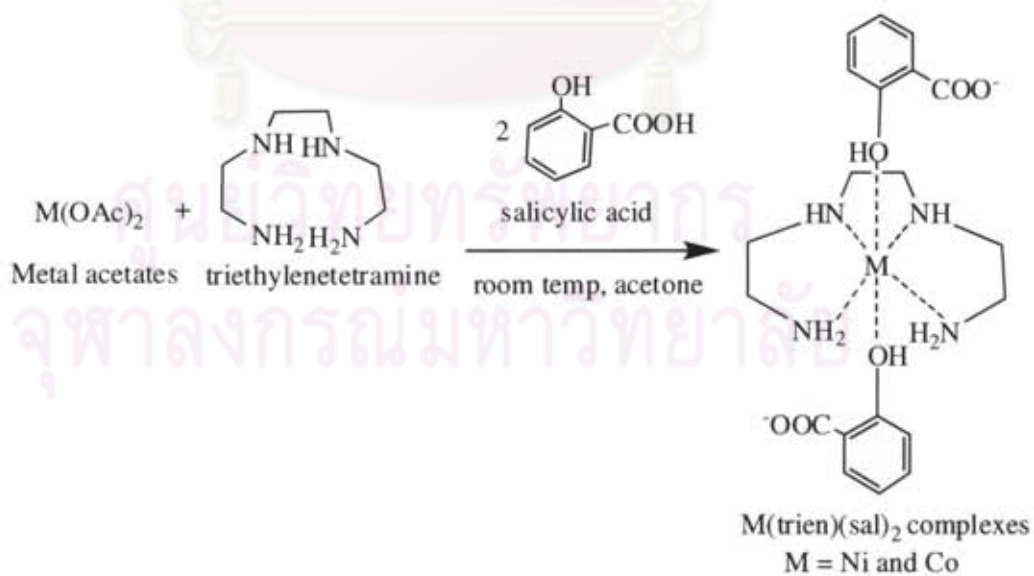
Scheme 1.5 Synthesis of M(trien)$_2$(sal)$_2$ complexes

The method to prepare the foam was a premix of the polyol, catalyst, water (blowing agent) and surfactant. The isocyanate was finally added and the mixture was mixed with a high speed mixer. Subsequently, the exothermic polyurethane formation took place which was accompanied by a large volume expansion and a temperature rise from foam formation.

For comparison, a reference foam system was prepared by use of N,N-Dimethylcyclohexylamine (DMCHA) as a catalyst. DMCHA is normally used as a catalyst in commercial rigid polyurethane foam system. It was found that rigid polyurethane foam catalyzed by nickel and cobalt complexes had good physical and mechanical properties comparable to the foam prepared from DMCHA catalyst.

CHAPTER II
THEORY AND LITERATURE REVIEWS

A cellular polymer is defined as a polymer the apparent of which is decrease substantially by the presence of numerous cells disposed throughout its mass [1]. Cellular polymers, or polymeric foams, are multi-phase materials consisting of a minimum of two phases. Synthetic foams are specialized typed of foam which are true composite three phase systems comprising hollow polymeric, ceramic, or glass microspheres dispersed in the continuous polymer matrix phase. The first commercial man-made cellular polymer was sponge rubber, introduced between 1910 and 1920 [2].

According to their complex nature, cellular polymers have been classified in a variety of ways, usually in term of either the cellular morphology mechanical behavior or composition. With respect to the cell structure, cellular polymers can be divided into two general classes:

2.1 Closed cell foams

The gas is dispersed in the foam of discrete gas bubble (figure 2.1) and the polymer matrix exists as only continuous phase. Gas transport takes place by diffusion through the cell wall. Closed cell foams are generally formed by high pressure technique.
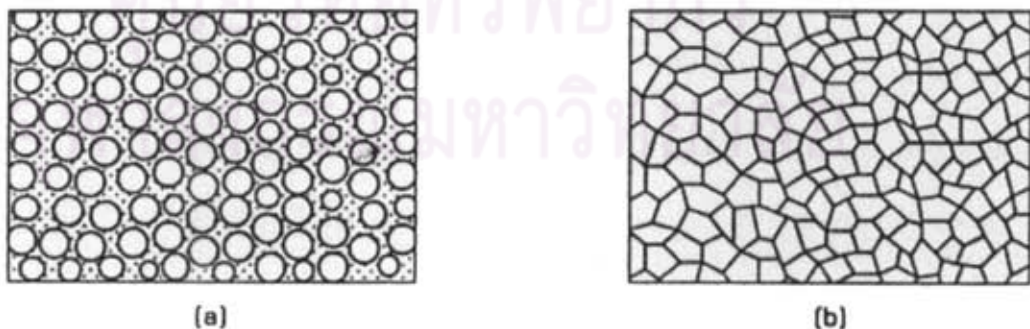
Figure 2.1 Closed cell foam structures (a) discrete cell dispersed in foam e.g. syntactic foam (b) cells in contact with each other. [3]

2.2 Open cell foams

The void (gas cell) coalesces so that the combined solid and gaseous phases are continuous. Therefore, the gas is able to flow through the polymer matrix under the action of some driving force. Open cell foams are generally formed during processing under ambient, i.e. low pressure, atmospheric conditions.

In practice, the two cellular morphological form co-exist so that a polymer foam does not always completely open or completely closed cells. The main physical difference between the two types of cell, i.e. open and closed cell, is depicted in Figure 2.2.

Figure 2.2 (a) Open gas structural element (b) Closed gas structural element [3]

The open cell structure, Figure 2.2(a), consists of a lattice of struts, whereas for the closed cell structure, Figure 2.2(b), in addition to the struts there are windows or membranes of base polymer between the strut faces. These membranes are usually significantly thinner than the dimensions of the struts themselves but provide addition support and therefore stiffness and strength to the cell.

Cellular polymers can also be classified according to their stiffness, the two extremes being rigid and flexible depending on the chemical composition, the rigidity of the polymer backbone, the degree of crystallinity and the degree of crosslink (if any).

2.3 Rigid foams

The polymers exist as hard materials. Typical examples include most polyolefins, polystyrene (PS), phenolics (PFs), polycarbonates (PC), and some polyurethane (PU) foams.

2.4 Flexible foams

The polymers exist as soft materials. Typical examples include rubber foams, flexible PU foams, and plasticized poly(vinyl chloride) (pPVC) foams.

Intermediate between these two extremes is a class of cellular polymer known as semi-rigid foams. Although these materials have an elastic modulus higher than that of flexible foams, the stress-strain behavior is nevertheless closer to that of flexible systems than that exhibited by rigid foams.

The most widely used system of producing foamed polymer involves (i) the nucleation of gas bubble in the liquid polymer, (ii) the growth and stabilization of these bubbles, and (iii) the solidification of the polymeric phase by crosslinking or cooling to give s structurally stable cellular system.

2.5 Bubble Formation

In the general case describe above, the first step in producing foam is the initiation of gas bubble in the liquid system. This process is known as nucleation. In many cases, it is necessary to add nucleating agents such as and chemical silica to control cell size and cell distribution. Several techniques are used to entrain the gas in the liquid polymer before expansion

(a) Blowing due to an 'in stitu' chemical reaction

Gas is formed by reaction of two chemicals and evolution occurs simultaneously with polymerization and crosslinking. This is an important process for the manufacture of PU foams.

(b) Thermal decomposition of a chemical blowing agent (CBA)

The solid blowing agent (BA) is intimately mixed with the polymer, preferably in the liquid state, and the mixture heated to a temperature at which the BA decomposition to give off an inert gas such as carbon dioxide (CO_2) or nitrogen (N_2). The polymer is then hardened either by gelation at this temperature (thermosetting plastics) or by cooling to room temperature (thermoplastics).

(c) Blowing by vapor from a volatile liquid

The liquid BA is incorporated into the polymer at atmospheric pressure and is converted into vapor by heat from a crosslink reaction. PU foams blown with CFCs are examples of this method.

2.6 Bubble Growth

Lowering of the melt pressure relieves the supersaturation of the material, after which no new bubbles are formed. The solubilized gas then diffuses into the existing bubbles, causing them to expand. The initial bubble is spherical in shape and grows as a resulting of the differential pressure (ΔP) between the inside and outside of the cell. At equilibrium, ΔP, the interfacial surface tension (γ), and radius (r) of the bubble are related as follow,

$$\Delta P = (2\gamma) / (r) \tag{1.1}$$

Saunders [4] report that a better bubble stability, a small average cell size, and more oven bubble size distribution is produced at low interfacial surface tension. Schematic representations of idealized cellular structures at different stages of bubble expansion are shown in Figure 2.2. The foam depicted in Figure 2.2 (a) shows the bubbles uniformly dispersed throughout the liquid medium and if stabilized in this condition the foam would clearly have a high density. As the gas volume faction

increase, Figure 2.2 (b), the foam density decreases. For spherical bubbles of uniform size, the lowest density is achieved when the bubble are closed packed.
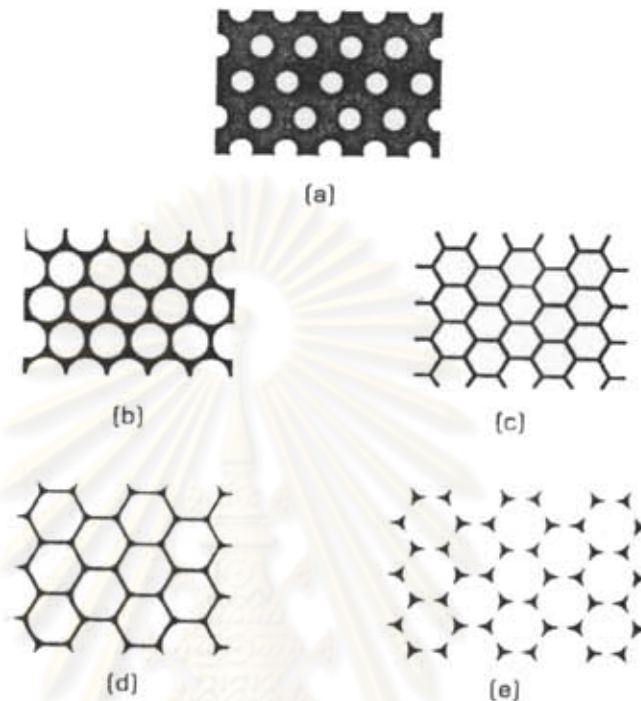
Figure 2.3 Schematic representations of cellular structures at different stages of foam expansion [3]

On further expansion, the bubbles eventually touch each other and the internal gas pressure presses the cells together causing the polymer to fill the interstices. Thus, the cells become bounded by polyhedra, often represented in an idealized form as a pentagonal dodecahedron with planes surfaces of uniform thickness, but simplistically shown in two dimensions as a hexagonal honeycomb (Figure 2.3(c)). Depending on the physical state of the liquid system, i.e. its viscosity and surface energy, gravitational and other force may cause the liquid material to concentrate at intersection of the elements of the associated cells as depicted in Figure 2.3(d). At this stage the foam is of low density and is closed cell. However, the membranes between the cell structures, which represent the interface between the gas bubbles, may become ruptured and give varying degrees of connectivity between the cells. This give rise to an open cell structure as represented in Figure 2.3(e).

2.7 Bubble Stabilization

Ultimate stabilization is due to either chemical reaction continuing to complete gelation effect of cooling below a melting point or softening point to prevent polymer flow. As complete solidification is approached the previously formed spherical bubble may become destroyed by the flow of foam or by gravity, with resultant anisotropy of cellular structure. Also, there is a tendency for the gas within the cell to equilibrate over of time at ambient temperature and pressure. This can resulting in changing properties with time as the balance between gas diffusion into the cell takes place as the foam ages. For obvious reasons the "ageing" stage is minimized when the expanding gas within the cell is the same as, or similar to, air.

2.8 General Properties of Cellular Polymer

Foaming dramatically alters the range of physical and mechanical properties of the base material. The mechanical properties of solid polymer exert a strong influence on the properties of the foam, which are also affected by processing techniques and conditions, molecular orientation, crosslink density (if applicable), additives and blowing agents used.

Density particularly affected the following parameters: (i) modulus, (ii) strength, and (iii) thermal conductivity. The term *foam density* can be defined as follows:

$$\text{Foam density} = \frac{\text{Mass}}{\text{Volume}}$$

(can change during the ageing process)

Foam typically have the following density ranges:

> 600 kg/m^3	= High density
100 – 600 kg/m^3	= Intermediate density
< 100 kg/m^3	= Low density

The mechanical properties of rigid foams differ markedly from those of flexible foams. Compressive properties are perhaps the most important mechanical properties of cellular polymers. Compressive energy absorption characteristics and deformation characteristics of foam depend mainly on density, type of the base polymer, and the predominance of either open or closed cells.

In simple terms, closed cell foam deformation involves cell wall bending/bucking, gas compression, cell wall stretching/yielding.
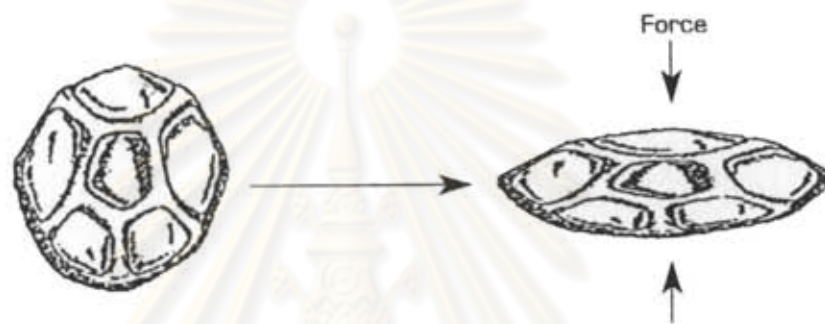
Figure 2.4 Schematic representation of closed cell deformation [3]

Closed cell rigid foams (e.g. PS and PU foams) exhibit from very limited to no yielding behavior. Consequently, gas compression and matrix strength play important roles during the mechanical deformation of rigid foams. In addition, cell rupture often occurs during the energy absorption process.

2.9 Application of Cellular polymers

Approximately 90% of total foam usage derives from their excellent thermal insulation and energy absorbing characteristic. Rigid closed cell foams are particularly suitable for thermal insulation because in addition to their low thermal conductivity they are easy to dispense and have low moisture absorption. PS and PU foams are extensively used for these applications.

2.10 Raw materials

2.10.1. Isocyanate

Several aromatic and aliphatic diisocyanates are available but some 95% of all polyurethane are based upon the two aromatic diisocyanate (MDI) and it derivatives. The consumption of MDI overlook that of TDI in 1984.

1. Toluene diisocyanate (TDI) (liquid, b.p. 120°C) TDI is the most commonly available as mixtures of 80:20 and 65:35 of the 2,4 and 2,6 isomers respectively.

2,4-TDI   2,6-TDI

Figure 2.5 Toluene diisocyanate isomers used for PU foam

TDI has a relatively high vapor pressure and gives rise to the risk of airborne exposure to workers. As a consequence, it is quite a difficult material to handle on site, in transport and in the laboratory, and therefore usage has been limited in favor of MDI which has a lower volatility.

2. Polymeric 4,4′ Diphenylmethane Diisocyanate (PMDI) (liquid, b.p. 330°C, flash point ≥ 204°C). Polymeric MDI is a polymethylene polyphenylisocyanate that contains MDI. PMDI is high reactivity, low viscosity and applicable to many foam processes, coatings, adhesieves and elastomers.
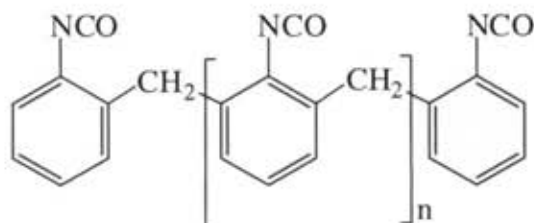
Figure 2.6 Molecular structure of PMDI

Alternatively, handling of PMDI can be facilitated by producing an oligomeric mixture containing approximately 55% MDI, 25% MDI trimer (functionality = 2 to 3) and 20% of polymeric MDI. This is known as polymeric MDI and is a liquid at ambient temperatures.

Cavender and Hawker[5] reported that the main reasons why TDI has been used for a long time (and still is) is because the cost of TDI production is considerably lower than for MDI and, more importantly, the final properties of the foam are relatively better for TDI systems than for MDI based systems. However, polymeric MDI and mixtures of MDI and TDI are becoming competitive in some areas such as self-skinning foams, high quality cushioning foams and high resilience foams. It should be noted that isocyanates are toxic materials necessitating great care in their use. The main health effects of isocyantes are on the respiratory system, i.e. they could induce bronchial spasms, sore throats, and tightness of the chest. MDI has the lowest toxicity rating of the isocyanates.

2.10.2 Polyols

A wide range of polyols is used in polyurethane manufacture. Most of the polyols used, however, fall into two class: hydroxyl-terminated polyether, or hydroxyl-terminated polyester. The structure of polyol plays a large part in determining the properties of the final urethane polymer. The molecular weight and functionality of the polyol are the main factors, but the structure of the polyol chains is important. Generally, flexible foam polyols have molecular weight of 1,000-6500 g/mol, functionality 2.0-3.0 and hydroxyl value 28-160 mg KOH/g , whereas rigid foam polyols have molecular weight 150-1000 g/mol, functionality 2.5-8.0 and

hydroxyl value 250-1000 mg KOH/g. The rigid of the foam can be increased by reducing the chain segment length between junction points-this effectively produces more tightly crosslinked networks. Specifications of commercial polyols include hydroxyl values which are used in stoichiometric formulation calculation. Examples are shown in Table 2.1.
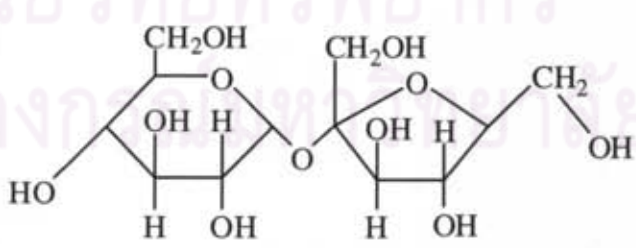
1. Polyether Polyols

Approximately 90% of polyols used in PU foam production are hydroxyl-terminated polyether due to their low cost and ease of handling. Polyether-based foams have better resilience and resistance to hydrolysis than polyester-based foams. They are produced by ring opening of alkylene oxides using a polyfunctional starter or initiator. Ethylene or propylene oxide are the most commonly used polyols. The polyols used for making rigid foams have molecular weight approximately 500 g/mol in order to reduce the distance between crosslinks.

2. Polyester Polyols

Saturated polyesters with terminal hydroxyl groups are used to make both flexible and rigid polyurethane polymers. Compare with polyether polyols, polyester polyols tend to be more reactive, produced foam with better mechanical properties, are less susceptible to yellowing in sunlight and are less soluble in organic solvents. However, they are more expensive, more viscous and therefore more difficult to handle. Consequently, they are only used in application that require their superior properties. Polyester polyols are made by condensation reaction between diols (triols) and dicarboxylic acids.

Table 2.1 Specifications of commercial polyols including functionality values

Alcohol	Chemical structure	Functionality
Ethylene glycol (EG)	$HO-CH_2-CH_2-OH$	2
Glycerol	H_2C-OH $HC-OH$ H_2C-OH	3
Trimethylol propane (TMP)	H_2C-CH_2-OH $HC-CH_2-OH$ H_2C-CH_2-OH	3
Pentaerythritol	H_2C-OH $HO-CH_2-C-CH_2-OH$ H_2C-OH	4
Sorbitol	(structure of sorbitol)	6
Sucrose	(structure of sucrose)	6

2.10.3 Catalyst

Catalysts play a very important role in the reaction of isocyanates. A number of catalysts can be used for the reaction of isocyanate with polyols and with water and these include aliphatic and aromatic tertiary amines, and organo-metallic compound, especially tin compounds. Alkali metals salts of carboxylic acids and phenols, and symmetrical triazine derivatives are used to promote the polymerization of isocyanates. Catalyst exerts an influence upon the rates of competing reaction and has a major effect on the ultimate properties of the final foam.

Tertiary amines are the catalysts most widely used in making polyurethane foams. The mechanism of catalysis by a tertiary amine involves he domination of electron by the tertiary nitrogen to the carbonyl carbon of the isocyanate group thus forming a complex intermediate. The catalytic activity of tertiary amine depends on its structure and its basicity. The catalytic effect increase with increasing basicity but is reduced by steric hindrance of the aminic nitrogen. The choice of catalysts for making rigid, closed-cell, polyurethane foams from polymeric MDI is usually concerned with obtaining the glation/foam rise profile and cure rate most suitable for the process application.

2.10.4 Blowing Agents

Blowing agents, sometime referred to as foaming agents, are used to generate cells in polymeric materials. They are generally classification based on the mechanism by which gas created.

     1. Physical Blowing Agents (PBAs) - are gases or compounds that produce gases as a result of physical processes such as evaporation, desorption at elevated temperature, or reduced pressure.

Table 2.2 Amine catalysts used in commercial foam systems

1. N,N-Dimethylcyclohexylamine, (DMCHA)

Liquid with an intense odor. Rigid foams, polyester-based flexible foams and some semi-rigid foams.

$H_3C-N-CH_3$

2. Diaminobicyclooctane (DABCO)

Solid, soluble in water, glycols and polyethers. Maybe used in most types of polyurethanes.

3. Dibutyltin dilaurate (DBTDL)
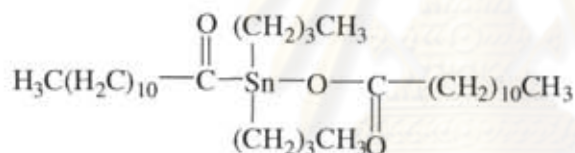
Microcellular foams, RIM, two-pot molding systems, elastomers.

4. Tetramethylbis(aminoethyl)ether (ZF-20)
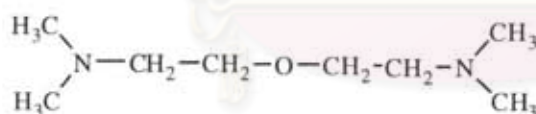
A general purpose, high efficient blowing catalyst used in urethane flexible foams and rigid packaging foams

5. N,N-Dimethylaminoethanol

$(CH_3)_2NCH_2CH_2OH$

Inexpensive, low-odor, isocyanate reactive, mobile liquid catalyst used in polyether-based flexible foams.

6. Methylene-bis-dimethylcyclohexylamine
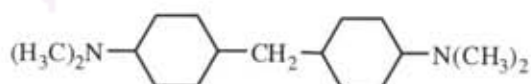
Low-volatility liquid with much lower odor than 2. Used in polyester-based flexible foams and potting compounds.

7. Stannous octoate
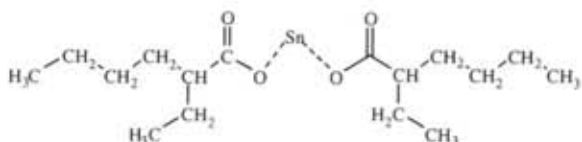
Slab stock polyether-based flexible foams, molded flexible foams.

8. Lead octoate   Urethane chain extension catalyst
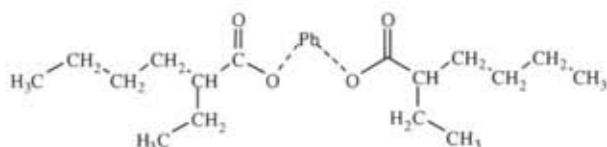
2. Chemical Blowing Agents (CBAs) – are individual compounds or mixtures of compounds that produce gas as a result of a chemical reaction. The chemical change is usually brought about by thermal decomposition or as a result of chemical reaction with other components of the formulation. Water acts as a blowing agent – it produces CO_2 gas by reaction with a diisocyanate. Typical water concentrations are 3-5 parts of water per 100 parts of polyester polyol and 1.8-5 parts per 100 parts of polyether polyol. The reaction of water with an isocyanate is exothermic.

2.10.5 Surfactant

Surfactants are essential additives used in PU foam formulations. They assist in mixing incompatible component of the formulation, controlling cell size, open cell content, and uniformity through reduced surface tension [6,7]. The most important surfactants are based on water-soluble polyether siloxanes. It has been found that increasing the level of surfactant in the PU foam formulation causes a reduction in the rate of foam rise [8]. This can be explained by the fact that increasing he surfactant level will effectively reduce functional group concentration. Consequently, the rate of foam rise , temperature rise, and overall reaction rate reduced. There is a critical level of surfactant below which the foam produce will suffer foam coarse cell structure and collapse. Just above this critical level, good open cell foam is produced. At higher silicone levels, foams with closed cells are produced.

Polyurethane chemistry is based on the high reactivity of the isocyanate group with any compound containing active hydrogen. Most polyurethanes [9,10] are

formed by exothermic reaction between di- or polyfunctional isocyanate and di- or polyfunctional hydroxyl species.

2.11 Primary Reactions of Isocyanates

Primary isocyanate reactions are very fast reactions. They produce urethane, amine and substituted ureas, all of which still contain active hydrogen atoms. In the presence of suitable catalysts at elevated temperatures, controlled secondary reactions occur which strongly influence the physical properties of the foam by introducing chain branching and crosslinking.

Reaction with Hydroxyl compounds – the reaction between an isocyanate and a polyol produces a urethane,

$$R-NCO + R'-OH \longrightarrow R-NH-\underset{\underset{O}{\|}}{C}-OR'$$

Isocyanate   Hydroxyl   Urethane
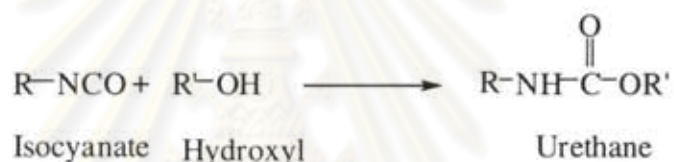
This reaction is known as the *'gelling reaction'*. Since it is an exothermic reaction it must be temperature controlled. The rate of polymerization is affected by the chemical structure the isocyanate and polyol. A catalyst is used to accelerate the reaction rate.

Reaction with water – the reaction between an isocyanate and water releases carbon dioxide and an amine via a transient unstable carbamic acid,

$$R-NCO + H_2O \longrightarrow R-NH-\underset{\underset{O}{\|}}{C}-OH \longrightarrow R-NH_2 + CO_2 \uparrow$$

Isocyanate   Water   Carbamic acid   Amine
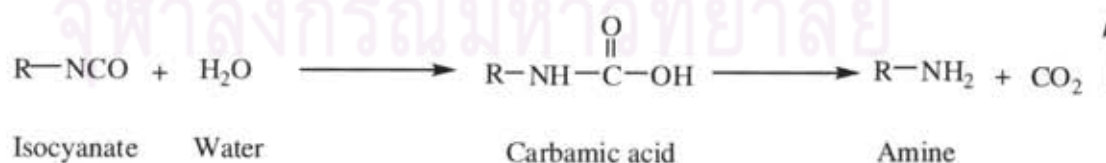
This reaction is known as the *'blowing reaction'* because the CO_2 gas produced is used for blowing the foam.

Reaction with amines – the reaction of an isocyanate with an amine forms a urea linkage,

$$R-NCO \quad + \quad R'-NH_2 \quad \longrightarrow \quad R'-NH-\overset{\overset{\displaystyle O}{\|}}{C}-NH-R$$

Isocyanate   Amine   Substituted urea
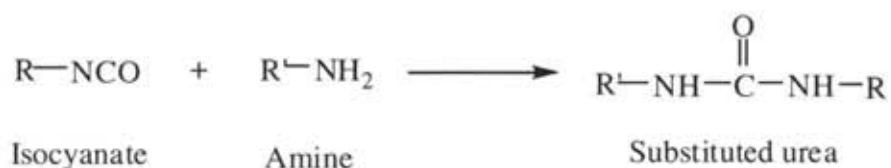
Reaction of unhindered isocynates with primary amine occur approximately 100-1000 times faster than with primary alcohols[11].

2.12 Secondary Reactions of Isocyanates

Isocyanate may react, under suitable conditions, with the active hydrogen atoms of urethane and urea linkage from the primary reaction as shown follows:

Reaction with urethanes - isocyanate can react with the active hydrogen atoms of urethane linkages to form branched allophonates,

$$R-NCO \quad + \quad R'-NH\overset{\overset{\displaystyle O}{\|}}{-C}-OR'' \quad \longrightarrow \quad R-NH-CO-\underset{\underset{\displaystyle COOR''}{|}}{NR'}$$

Isocyanate   Urethane   Allophanate
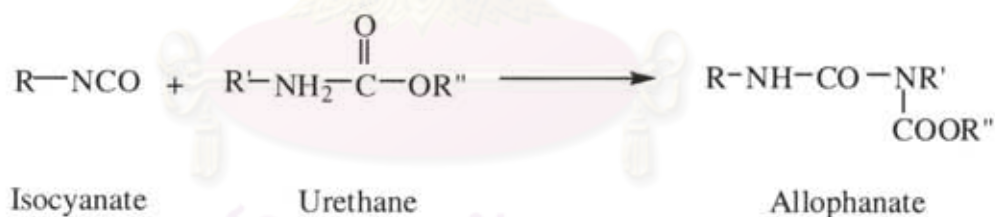
Reaction with Urea – isocyanate can also react with the active hydrogen atoms of substituted ureas to form branched (biuret) structure,

$$R-NCO \quad + \quad R'-NH\overset{\overset{\displaystyle O}{\|}}{-C}-NH-R'' \quad \longrightarrow \quad R-NH-CO-\underset{\underset{\displaystyle CO-NH-R''}{|}}{NR'}$$

Isocyanate   Substituted urea   Biuret
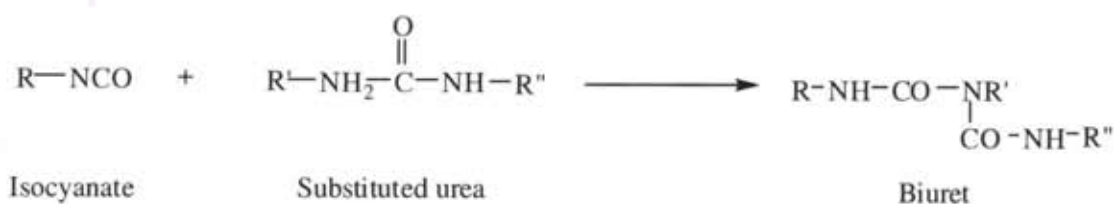
Reactions of isocyanate with both urethanes and ureas produce crosslinking. At temperature below 100°C these reactions are some 100 times shower than the

primary reactions [12]. Generally, reaction of isocyanates with urea groups are significantly faster and occur at low temperature than with urethane groups.

1. Isocyanate Dimer and Trimer Formation

Uretidinedione (isocyanate dimers) can only be produced form aromatic isocyanates and are inhibited by ortho substituents. Thus, 2,4- and 2,6-TDI do not form dimmers at normal temperatures but 4,4' diphenylmethane diisocyanate (MDI) slowly dimerises when left to stand at room temperature. Isocyanurates can be formed on heating either aliphatic or aromatic isocyanates.

Uretidiendione (dimers)   Isocyanurate (trimers)
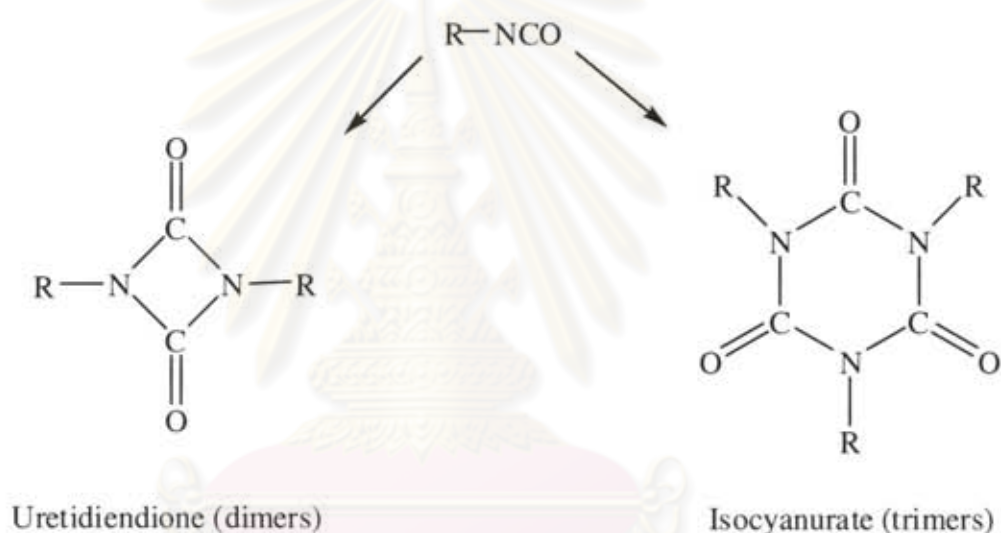
Figure 2.7 Chemical structure of isocyanate dimer and trimer

The amount of isocyanate required to react with the polyol and any other reactive additive, is calculated in the usual way to obtain the chemically stoichiometric amount of isocyanate may then be adjusted upwards or downwards, depending on polyurethane system, the properties required of the polymeric product and known effects such as the scale of manufacture and the ambient conditions.

2.13 Isocyanate Index (Index number)

The number of isocyanate used relative to the theoretical equivalent amount, is known as the *Isocyanate index* or sometime *Index number*.

$$\text{Isocyanate index} = \frac{\text{actual amount of isocyanate}}{\text{Theoretical amount of isocyanate}} \times 100$$

For example, an isocyanate index between 103 and 108 is 3% to 8% excess of isocyanate.

The conventional way of calculating the ratio of the components required for polyurethane manufacture is to calculate the number of parts by weight of the isocyanate that are required to react with 100 parts by weight (pbw) of polyol and proportionate amounts of additives. The analytical data required for calculation are the isocyanate value of the isocyanate and hydroxyl value, residual acid value and water content of the polyol and other reactive additives.

2.14 Isocyanate value

The isocyanate value is the weight percentage of reactive – NCO groups:

$$
\begin{aligned}
\text{Isocyanate value} \quad &= \% - \text{NCO groups} \\
&= \frac{42 \times \text{functionality} \times 100}{\text{molar mass}} \\
&= \frac{4200}{\text{equivalent weight}}
\end{aligned}
$$

2.15 Hydroxyl value (Hydroxyl number)

The hydroxyl value (OHV) sometime called the hydroxyl number of the polyol, is express in mg KOH/g of polyol. This convention arises from the method of determining hydroxyl values by acetylation with pyridine and acetic anhydride in which the result is obtained as the difference between two titrations with KOH solution. The OHV may thus be defined as the weight of KOH in milligrams that will neutralize the acetic capable of combining by acetylation with 1 g of the polyol. Polyols are sometime characterised by quoting the weight percentage hydroxyl groups. This related to OHV:

$$\% \text{ Hydroxyl groups} \quad = \frac{OHV}{33}$$

$$\text{Hydroxyl value} \quad = \frac{56.1 \times \text{functionality} \times 1000}{\text{molar mass}}$$

$$= \frac{56.1 \times 1000}{\text{equivalent weight}}$$

2.16 Water content

Water reacts with two – NCO groups and the equivalent weight of water is thus:

$$\text{Equivalent weight} = \frac{\text{molar mass}}{\text{functionality}} = \frac{18}{2}$$

2.17 Isocyanate conversion (α)

Isocyanate conversion (α) is the ratio between urethane absorbance at time = t and urethane absorbance at time = 0 :

$$\alpha = \left[1 - \frac{NCO^f}{NCO^o} \right] \times 100$$

α : isocyanate conversion (%)

NCO^f : the area of isocyanate absorbance peak at time t or final isocyanate

NCO^0 : the area of isocyanate absorbance peak at time 0 or initial isocyanate

2.18 Literature reviews

The polyurethane industry has progressed rapidly, and reaction of polyols and isocyanates are well known technological processes. However, the reaction rate of isocyanate on preparations of polyurethane is very slow. Therefore, tertiary amines

and tin compound, having excellent catalytic activity, are used mainly as catalysts for polyurethane formation. In particular, dibutyltin dilaurate (DBTDL) has been used. However, tin is toxic to human beings. Accordingly, a new catalysts or catalytic system is necessary to replace this catalyst.

Inoue *et al* [13] studied amine-metal complexes as efficient catalysts for polyurethane syntheses. Since the reaction of aliphatic isocyanates in the preparation of polyurethane is very slow compared with aromatic isocyanates. In this research, they prepared the complexes of $M(acac)_n$ [M = Mn, Fe, Co, Ni and Cu] and tertiary amines as new catalysts for the reaction between hexamethylene diisocyanate (HDI) and polyols. They found that $Mn(acac)_n$-TEDA complex showed better catalytic activity than other $M(acac)_n$ complexes and showed comparable catalytic activity as DBTDL catalyst.

Maris and coworkers [14] studied catalytic activities of various tertiary amines for isocyanate reaction. This activity relates to the catalysis of the gel and blow reaction and also the allophanate, biuret and trimerization reactions. They suggested the activation mechanism of urethane reaction in the presence of a tertiary amine and metal catalyst. The mechanism of tertiary amine catalysts are shown in Scheme 2.1. In general, the tertiary amine coordinate to the positive electron charged carbon of the NCO group or hydrogen of the OH group and forms a transition state to activate urethane formation reaction.

Baker mechanism

Farka mechanism

Scheme 2.1 Reaction mechanism of tertiary amine catalysts

The following catalytic mechanism of tin (II) salts has been proposed [15] (Scheme 2.2). The isocyanate, polyol and tin catalyst form a ternary complex, which then gives the urethane product. In the first one the tin first adds to the polyol then the isocyanate. In the second one the tin adds to the oxygen of the isocyanate the reacts with the polyol.

The proposed mechanisms for tin (IV) catalysts, dialkyltin dicarbonates and dialkyltin dialkylthiolates, is the reaction of the tin with a polyol forming a tin alkoxide, which can then react with the isocyanate to form a complex [15] (Scheme 2.3). Transfer of the alkoxide anion onto the coordinated isocyanate affords an N-stannylurethane, which then undergoes alcoholysis to produce the urethane group and the original tin alkoxide. A synergy between tin and amine catalysts is also observed. One of the proposed mechanisms is given in Scheme 2.4. Metal complexes (metal-based catalysts) acted as a Lewis acid, primarily coordinated to the oxygen atom of the NCO group and activated the electrophilic nature of the carbon and amine interacting with the proton of hydroxyl group in polyol, which then reacts with the isocyanate.

Strachota and coworkers [16] studied commercially available amines, including N-substituted morpholines, as single catalysts and as catalyst mixtures for

polyurethane foam preparation. The motivation was to search for economically and environmentally replacements of "classical" catalysts as diazabicyclooctane, dibutyltindilaurate (DBTDL) and N,N-bis(2-dimethylaminoethyl)methylamine (DMAEMA). Especially interesting point was DBTDL replacement and also the possibility of using reactive catalyst derivatives that would be incorporated into polyurethanes, thus reducing the content of volatile organic compounds in the polymer. Tertiary amines and tin compounds did not support isocyanate side reactions, and show varying selectivity for the "gelation" vs. "foaming" reactions. Generally, PU catalysts can be divided according to their function into gel catalysts, blow catalysts, and skin cure catalysts. In this work, tin(II) 2-ethyl-hexanoate (SnOct), as well as combinations of these catalysts were tested in simple PU mixtures (bulk as well as foams) in order to evaluate their activity and selectivity. The well-established gelling catalysts, diaminobicyclooctane (DABCO) and DBTDL, and the classical foaming catalyst DMAEMA were used for comparative tests. In foam tests, DABCO and the mixtures DMCHA-SnOct and DABCO-SnOct-DMAEMA showed the best catalytic results on the reference system.

Scheme 2.2 Mechanism of tin (II) salts catalyst
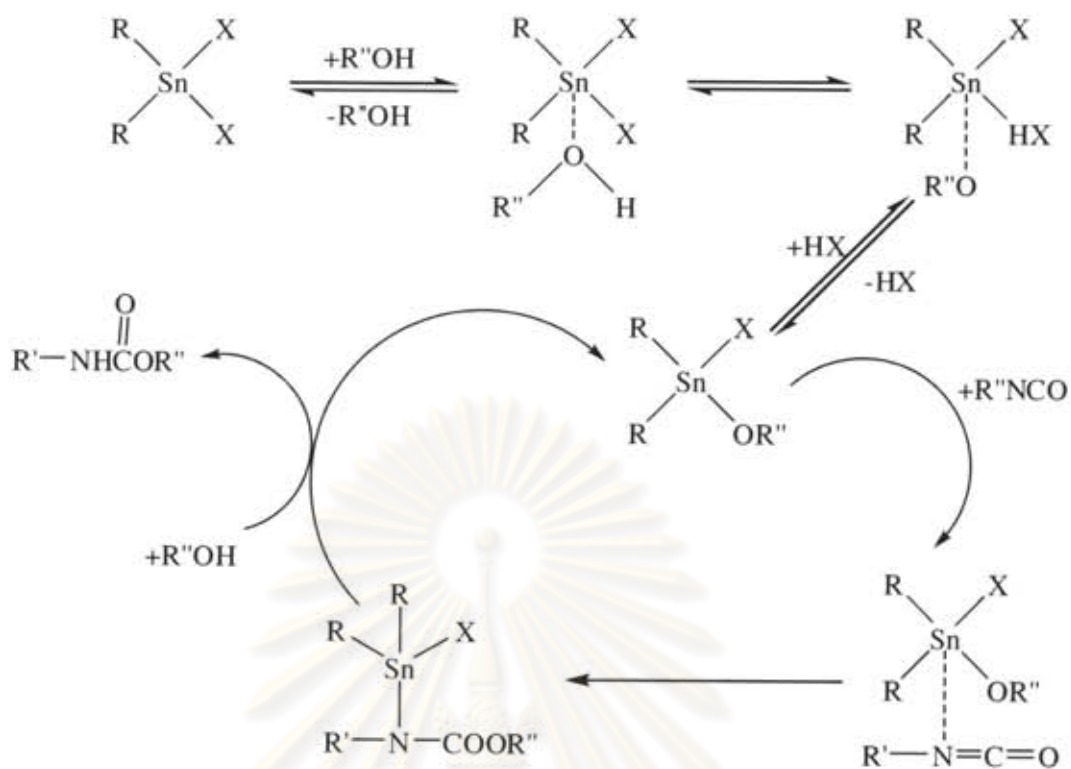
Scheme 2.3 Mechanism of tin (IV) salts catalyst

Mechanism I

R—N=C=O $\xrightleftharpoons{\text{MX}_2}$ $\left[\begin{array}{c} \text{R-N=C=}\overset{\oplus}{\text{O}}\text{-}\overset{\ominus}{\text{MX}_2} \\ \Updownarrow \\ \text{R-N=}\overset{\oplus}{\text{C}}\text{-O-}\overset{\ominus}{\text{MX}_2} \end{array}\right]$

$\xrightarrow{\text{R'OH}}$ $\left[\begin{array}{c} \text{R—N=}\overset{\oplus}{\text{C}}\text{—O} \\ | \\ \text{H—}\overset{\oplus}{\text{O}}\text{—MX}_2 \\ | \\ \text{R'} \end{array}\right]$

R·N=C=O

Mechanism II

H—O—R' + MX$_2$ $\xrightleftharpoons{}$ $\left[\begin{array}{c} \overset{\ominus}{\text{MX}_2} \\ | \\ \text{R'—O—H} \\ \oplus \end{array}\right]$

$\left[\begin{array}{c} \overset{\text{H}}{\text{R—N—}}\overset{\bullet}{\text{C}}\text{=O} \\ | \\ \text{O} \quad \text{MX}_2^{\ominus} \\ | \\ \text{R'} \\ \Updownarrow \\ \text{R—}\overset{\bullet}{\text{N}}\text{=C—O} \\ \text{H} \quad | \\ \text{O} \quad \overset{\ominus}{\text{MX}_2} \\ | \\ \text{R'} \end{array}\right]$

$\xrightleftharpoons{}$ R—NH—C$\begin{array}{c} \text{O} \\ \| \\ \\ \text{O—R'} \end{array}$ + MX$_2$
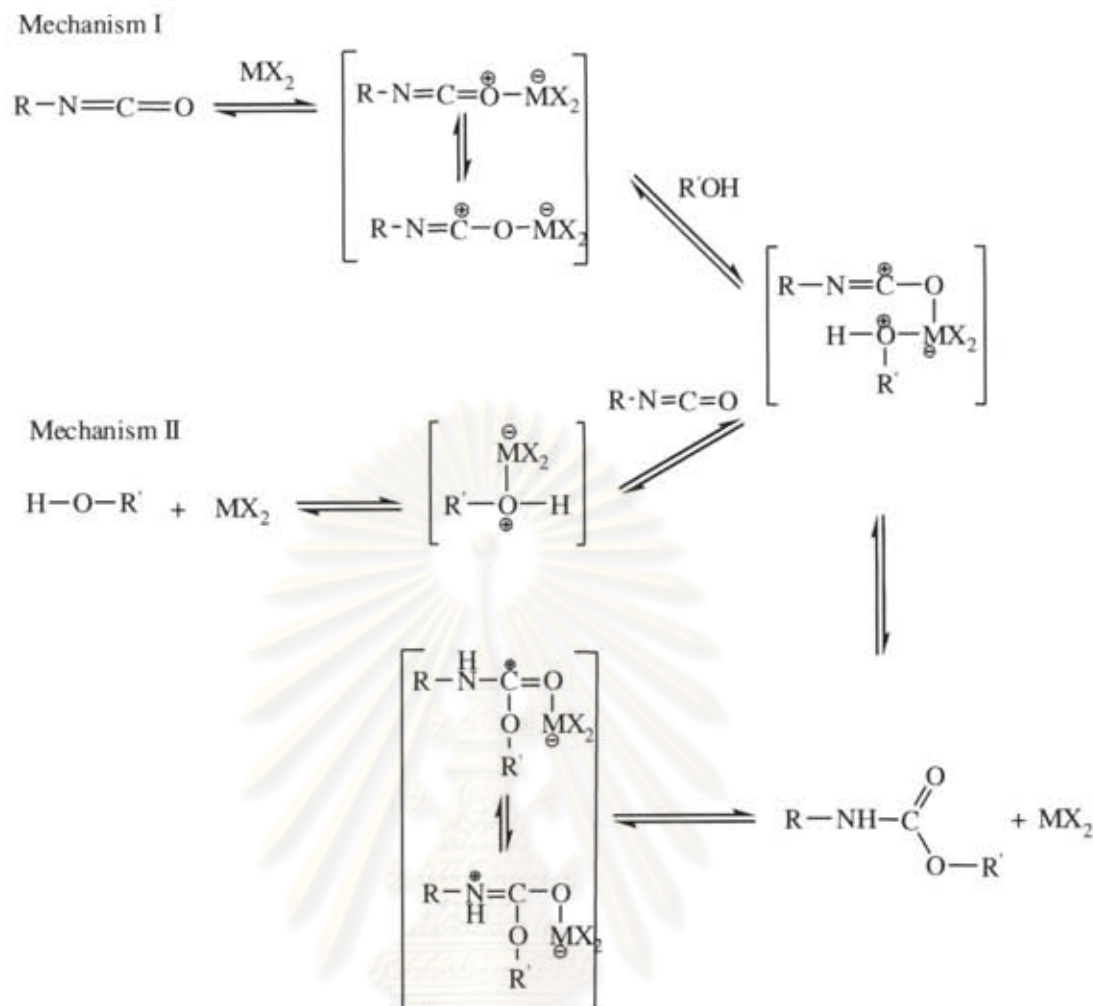
Scheme 2.4 Reaction mechanisms of metal-based catalyst

Sardon and coworkers [17] studied of the catalytic activity of tin and zirconium compounds in the polymerization of isophorone diisocyanate (IPDI)-based waterborne polyurethanes. Zirconium acetyl acetonate is much less toxic than the commonly used dibutyltin diacetate but it is deactivated in the presence of acid groups. Isophorone diisocyanate based waterborne polyurethanes was synthesized using zirconium acetyl acetonate. This catalyst had a relatively low toxicity about 10 to 20 times less toxic than comparable tin compounds. Therefore, it was a good candidate in this application to replace the general use of tin catalysts. The results showed that in the presence of triethyl amine, tin catalyst showed a higher reactivity towards the secondary isocyanate group than to the primary group, while zirconium catalyst showed the same reactivity to both isocyanate groups. These results confirmed that zirconium catalyst was a good alternative to replace tin compounds.

Okuzono and coworkers [18] studied new polyisocyanurate catalysts which exhibit high activity at low temperature. The combination of other tertiary amine catalysts could improve the flowability, however, the flammability of the foam would be a hazard because the isocyanurate reaction has not fully progressed. For the improvement of the above-mentioned problems, Tosoh Corp. has developed several new quaternary ammonium salt compounds, such as Toyocat-TR20. TR20, however, should be used in conjunction with an alkali metal co-catalyst. Presently, Tosoh has succeeded in developing another new catalyst having even higher catalytic activity at low temperature, which can replace the use of the alkali metal catalyst. The new catalyst provides the low temperature dependency in the isocyanurate reaction activity compared to the traditional isocyanurate catalysts. The new catalyst provides the following advantages:

1. The catalytic activity is high.
2. The isocyanurate reaction activity at low temperature is high.
3. The initial foaming reaction is improved, thereby the rise profile is now smooth.

Kurnoskin [19] synthesized metal-containing epoxy polymers by crosslinking of diglycidyl ether of bisphenol A (DGEBA) with transition metal complexes (M = Mn, Fe, Co, Ni, Cu, Zn and Cd) and aliphatic amines (ethylenediamine, diethylenetriamine, triethylenetetramine and cyanoethylated diethylenetriamine) as shown in Figure 2.8. The reactivity of the complexes in reactions with DGEBA and its dependence on the structure of the metal complexes was investigated. It was found that metal-containing epoxy polymers had good strength and heat resistance.

$$M(en)_2 \qquad M(trien) \qquad M(en)_2(OHC_6H_4COO)_2 \qquad M(trien)(OHC_6H_4COO)_2$$

M = Mn, Fe, Co, Ni, Cu, Zn, Cd
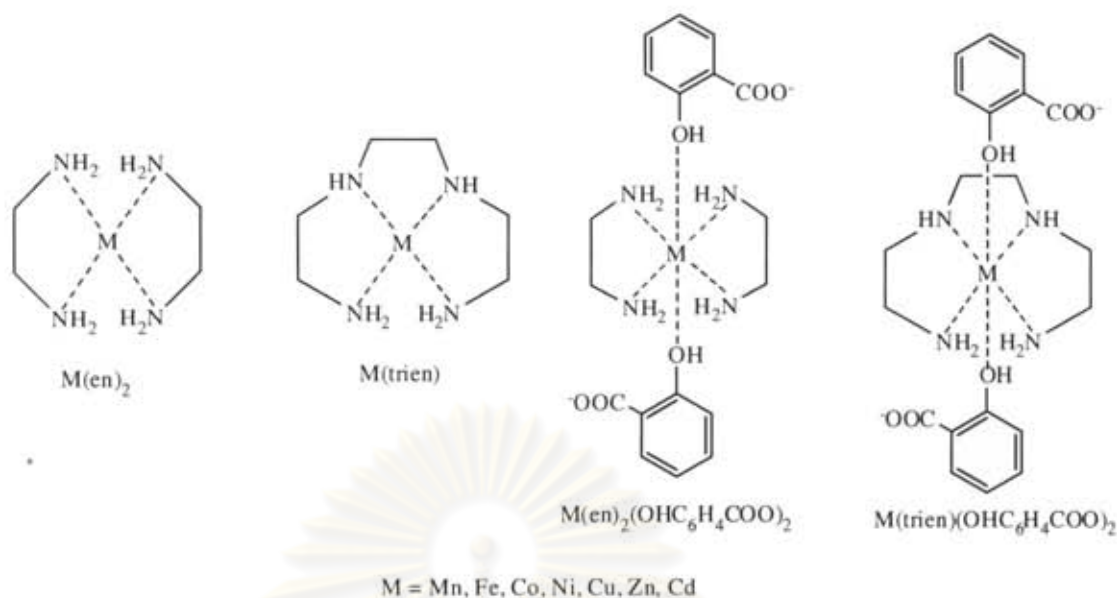
Figure 2.8 Metal complexes used in Kurnoskin's work

From the above research works, metal complexes of transition metals and amines could be used to catalyze urethane formation. Therefore, the aim of this work was to use the metal complexes from Kurnoskin's work, which were previously used to prepared metal-containing epoxy polymers, as catalysts for rigid polyurethane foam preparation.

CHAPTER III
EXPERIMENTAL

3.1 Raw materials

The raw materials employed in the preparation of rigid polyurethane foam are as follows:

- Polymeric methane diphenyl diisocyanate (PMDI): MR 200 (South City Petrochem Co., Ltd.); NCO % = 31.0; average functionality = 2.7
- Sucrose based polyether polyol (Raypol 4221): South City Petrochem Co., Ltd.); OH No. = 440 mg KOH/g; average functionality = 4.3
- Surfactant agents: polysiloxane-polyether copolymer: (Tegostab B8460) (South City Petrochem Co., Ltd.).
- Blowing agent: water was used as a chemical blowing agent.
- Catalysts: transition metal complexes employed were metal-amine complexes [$M(en)_2$ and $M(trien)$] and metal-ethylenediamine-salicylate complexes [$M(en)_2(sal)_2$ and $M(trien)(sal)_2$]. These metal complexes were synthesized from metal acetates, amines and salicylic acid.

3.2 Synthesis of transition metal complexes

Metal complexes of transition metal (M = Ni and Co) and amines [ethylenediamine (en) and triethylenetetramine (trien)] were prepared following the method reported in the literature [19].

3.2.1 Synthesis of metal-amine complexes

3.2.1.1 Synthesis of nickel-ethylenediamine complex [$Ni(en)_2$]

$Ni(en)_2$ were synthesized from the reaction between nickel (II) acetate and ethylenediamine (en) in acetone to give nickel-ethylenediamine complex [$Ni(en)_2$] (Scheme 3.1).
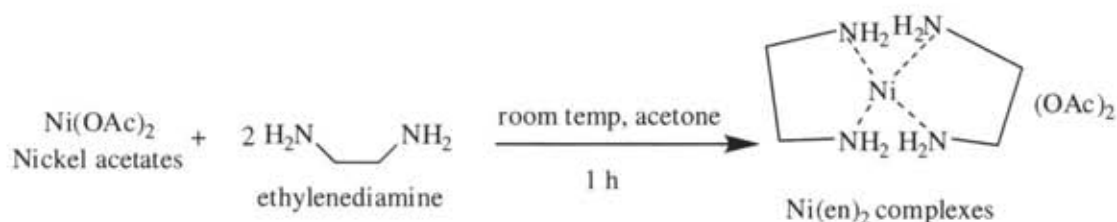
Scheme 3.1 Synthesis of nickel-ethylenediamine complex

The preparation of nickel-ethylenediamine complexes [Ni(en)$_2$] was performed as follows: a solution of nickel (II) acetate monohydrate (0.67 g, 2.69 mmol) was stirred in acetone (20 ml) at room temperature. A solution of ethylenediamine (0.33 ml, 4.94 mmol) in acetone (10 ml) was added drop wise to nickel acetate solution over a period of 15 minutes and stirred at room temperature for 1 hour. Precipitate of Ni(en)$_2$ complexes was dried under vacuum. Ni(en)$_2$ was obtain as a purple-red powder. (0.68 g, 68%): IR (KBr, cm^{-1}); 3460, 3275 (NH stretching), 2946, 2944, 2890 (CH stretching), 1572 (asymmetric C=O stretching), 1408 (symmetric C=O stretching), 1333 (CN stretching), 1024 (CO stretching). UV; λ_{max} (H$_2$O) = 344 nm, molar absorptivity (ε) = 60. Anal. Calcd. For NiC$_8$O$_4$H$_{22}$N$_4$: C 32.37; H 7.42; N 18.88; found C 32.37; H 7.42; N 17.73. AAS. Calcd. For NiC$_8$O$_4$H$_{22}$N$_4$: Ni 19.79; found Ni 19.80.

3.2.1.2 Synthesis of cobalt-ethylenediamine complex [Co(en)$_2$]

Co(en)$_2$ were synthesized from the reaction between cobalt (II) acetate and ethylenediamine (en) (Scheme 3.2) in acetone gave cobalt complexes [Co(en)$_2$].
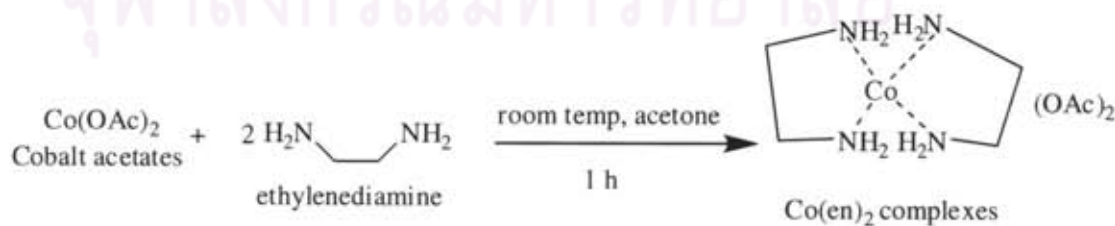
Scheme 3.2 Synthesis of cobalt-ethylenediamine complex

The experiment of Co(en)$_2$ was carried out according to described in experiment 3.2.1.1 employing cobalt (II) acetate tetrahydrate (Co(OAc)$_2$.4H$_2$O) (0.67 g, 2.69 mmol) instead of nickel (II) acetate tetrahydrate (Ni(OAc)$_2$.4H$_2$O). A solution of ethylenediamine (0.33 ml, 4.94 mmol) in acetone (10 ml) was added dropwise to nickel acetate solution. Precipitate of Co(en)$_2$ complexes was dried under vacuum. The yield of Co(en)$_2$ was obtain as a deep-red powder (0.74 g, 74%): IR (KBr, cm^{-1}); 3484 , 3216 (NH stretching), 2946 , 2966 (CH stretching), 1568 (asymmetric C=O stretching), 1400 (symmetric C=O stretching), 1340 (CN stretching), 1055 (CO). UV; λ_{max} (H$_2$O) = 470 nm, molar absorptivity (ε) = 40. Anal. Calcd. For CoC$_8$O$_4$H$_{22}$N$_4$: C 32.33; H 7.41; N 18.86; found C 29.73 ; H 6.97; N 12.89. AAS. Calcd. For CoC$_8$O$_4$H$_{22}$N$_4$: Co 19.85; found Co 19.80.

3.2.1.3 Synthesis of nickel-triethylenetetramine complexes [Ni(trien)]

Ni(trien) were synthesized from the reaction between nickel (II) acetate and triethylenetetramine (trien) (Scheme 3.3) in acetone gave nickel complexes [Ni(trien)].
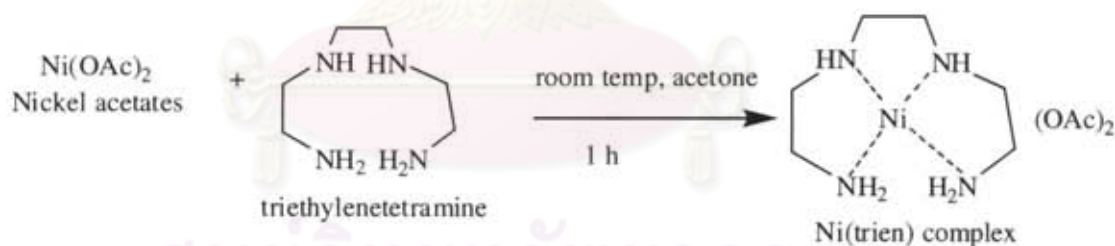
Scheme 3.3 Synthesis of nickel-triethylenetetramine complexes

The preparation of Ni(trien) were synthesized form nickel (II) acetate tetrahydrate (Ni(OAc)$_2$.4H$_2$O) (0.63 g, 2.53 mmol) was stirred in acetone (20 ml). The solution of triethylenetetramine (0.37 ml, 2.47 mmol) in acetone (10 ml) was added dropwise to nickel acetate solution over a period of 15 minutes and stirred at room temperature for 1 hour. The solution was evaporated and dried under vacuum. Ni(trien) complexes was obtained as a purple viscous liquid. (0.94 g, 94%): IR (KBr, cm^{-1}); 3441, 3409 (NH stretching), 2938 (CH stretching), 1546 (asymmetric C=O

stretching), 1466 (symmetric C=O stretching), 1402 (CN stretching), 1024 (CO stretching). UV; λ_{max} (H$_2$O) = 348 nm, molar absorptivity (ε) = 46.

3.2.1.4 Synthesis of cobalt-triethylenetetramine complexes [Co(trien)]

Co(trien) were synthesized from the reaction between nickel (II) acetate and triethylenetetramine (trien) (Scheme 3.4) in acetone gave cobalt complexes [Co(trien)].
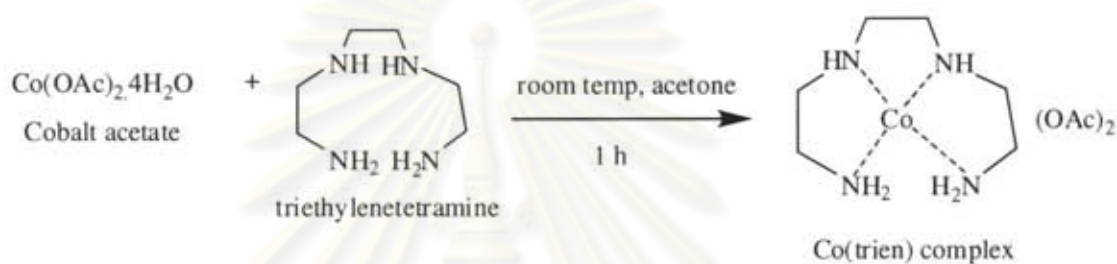
Scheme 3.4 Synthesis of cobalt-triethylenetetramine complexes

The experiment of Co(trien) was carried out according to described in experiment 3.2.1.3 employing cobalt (II) acetate tetrahydrate (Co(OAc)$_2$.4H$_2$O) (0.63 g, 2.53 mmol) instead of nickel (II) acetate tetrahydrate (Ni(OAc)$_2$.4H$_2$O) was stirred in acetone (20 ml) and using triethylenetetramine (0.37 ml, 2.47 mmol). The light-brown viscous liquid was obtain by evaporation and dried under vacuum. (0.95 g, 95%): IR (KBr, cm^{-1}); 3414, 3213 (NH stretching), 2986 (CH stretching), 1573 (asymmetric C=O stretching), 1409 (symmetric C=O stretching), 1056 (CO stretching). UV; λ_{max} (H$_2$O) = 505 nm, molar absorptivity (ε) = 40.

3.2.2 Synthesis of metal-amine-salicylic complexes

3.2.2.1 Synthesis of nickel-ethylenediamine-salicylate complex
[Ni(en)$_2$(sal)$_2$]
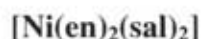
Ni(en)$_2$(sal)$_2$ were synthesized from the reaction between nickel (II) acetate, ethylenediamine (en) and salicylic acid (Scheme 3.5).

The preparation of Ni(en)$_2$(sal)$_2$ was carried out according to the method reported in the literature [19]. The mixture of nickel (II) acetate tetrahydrate (Ni(OAc)$_2$.4H$_2$O) (0.38 g, 1.57 mmol) and ethylenediamine (0.2 ml, 3.52 mmol) was stirred in acetone (20 ml) at room temperature for 1h. Finally added salicylic acid (0.42 g, 3.11 mmol) solution to the previous mixture and continuously stirred the same condition. Ni(en)$_2$(sal)$_2$ as a yellow-brown viscous liquid was obtained by evaporation and dried under vacuum. (0.92 g, 92%): IR (KBr, cm^{-1}); 2972 (CH stretching), 1705 (C=O, salicylate stretching), 1595 (Ar-H stretching), 1462 (asymmetric C=O stretching, acetate), 1385 (CN stretching)1027, (CO stretching), 859, 768 (Ar-H stretching). UV; λ_{max} (H$_2$O) = 427 nm, molar absorptivity (ε) = 399. The experimental scheme of Ni(en)$_2$(sal)$_2$ as show in Scheme 3.5.
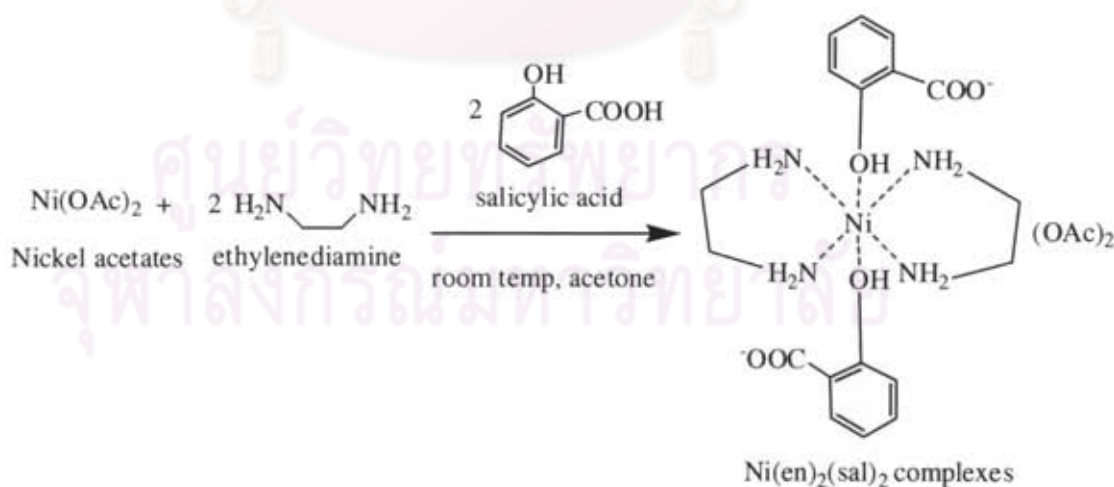
Scheme 3.5 Synthesis of nickel-ethylenediamine-salicylate complexes

3.2.2.2 Synthesis of cobalt-ethylenediamine-salicylate complex [Co(en)₂(sal)₂]

Co(en)$_2$(sal)$_2$ were synthesized from the reaction between cobalt (II) acetate, ethylenediamine (en) and salicylic acid (Scheme 3.6).
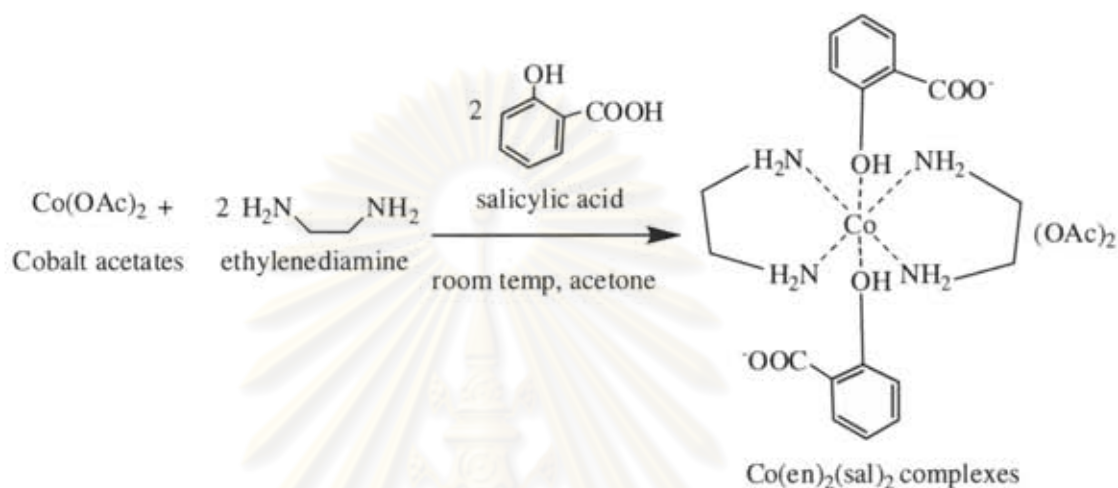
Scheme 3.6 Synthesis of cobalt-ethylenediamine-salicylate complexes

The experiment of Co(en)$_2$(sal)$_2$ was carried out according to described in experiment 3.2.2.1 employing cobalt (II) acetate tetrahydrate (Co(OAc)$_2$.4H$_2$O) (0.38 g, 1.57 mmol), ethylenediamine (0.2 ml, 3.52 mmol) and salicylic acid (0.42 g, 3.11 mmol). The red viscous liquid of Co(en)$_2$(sal)$_2$ was obtained by evaporation and dried under vacuum. (0.90 g, 90%): IR (KBr, cm^{-1}); 3262 (NH stretching), 1705 (C=O, salicylate stretching), 1586 (Ar-H stretching), 1494 (asymmetric C=O stretching, acetate), 1457 (symmetric C=O stretching, acetate), 1387 (CN stretching), 1246, 1148, 1059 (CO stretching), 855, 757 (Ar-H stretching). UV; λ_{max} (H$_2$O) = 497 nm, molar absorptivity (ε) = 452.

3.2.2.3 Synthesis of nickel-triethylenetetramine-salicylate complex [Ni(trien)(sal)$_2$]

Ni(trien)(sal)$_2$ were synthesized from the reaction between nickel (II) acetate, triethylenetetramine (trien) and salicylic acid (Scheme 3.7).
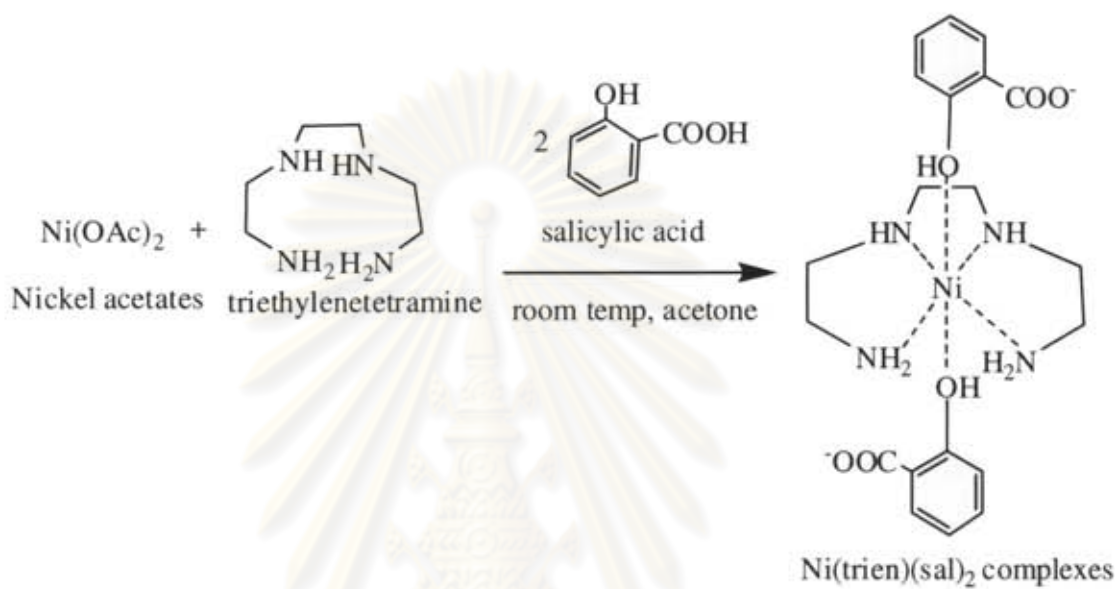
Scheme 3.7 Synthesis of nickel-triethylenetetramine-salicylate complexes

The preparation of Ni(trien)(sal)$_2$ was preformed according to the method reported in literature [19]. The mixture of nickel (II) acetate tetrahydrate (Ni(OAc)$_2$.4H$_2$O) (0.38 g, 1.57 mmol), triethylenetetramine (0.2 ml, 3.52 mmol) was stirred in acetone (20 ml) at room temperature for 1h. Finally added salicylic acid (0.42 g, 3.11 mmol) solution to the previous mixture and continuously stirred the same condition. The blue viscous liquid of Ni(trien)(sal)$_2$ was obtained by evaporation and dried under vacuum. (0.92 g, 92%): IR (KBr, cm^{-1}); 3218 (NH stretching), 2938 (CH stretching), 1721 (C=O, salicylate stretching), 1591 (Ar-H stretching), 1482 (asymmetric C=O stretching, acetate), 1471 (symmetric C=O stretching, acetate), 1380 (CN stretching), 1296, 1256, 1023 (CO stretching), 852, 764 (Ar-H stretching). UV; λ_{max} (H$_2$O) = 295 nm, molar absorptivity (ε) = 429.

3.2.2.4 Synthesis of cobalt-triethylenetetramine-salicylate complex [Co(trien)(sal)₂]

Co(trien)(sal)₂ were synthesized from the reaction between cobalt (II) acetate, triethylenetetramine (trien) and salicylic acid (Scheme 3.8).
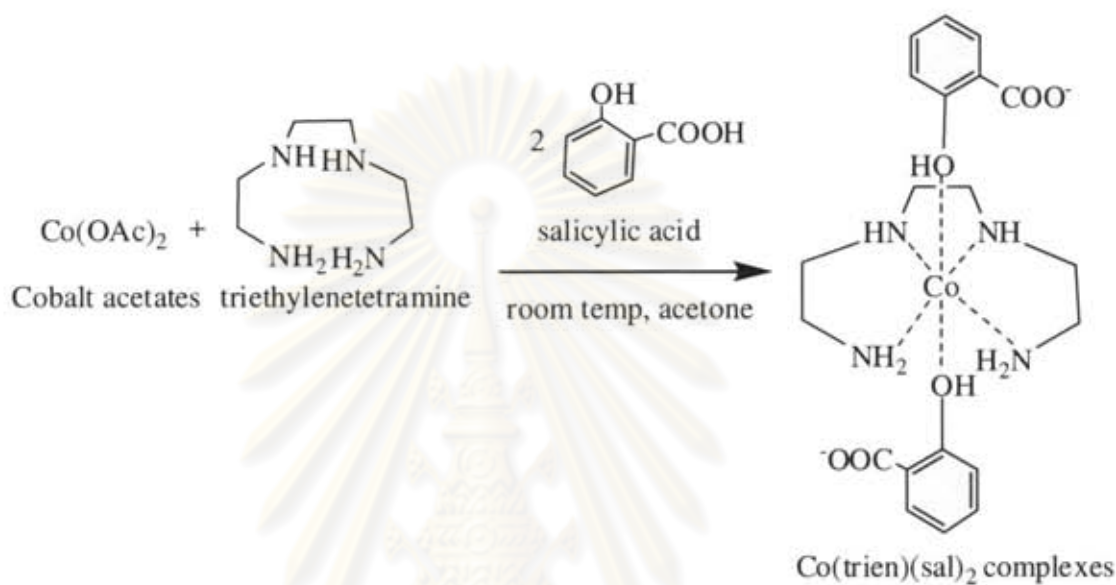

Scheme 3.8 Synthesis of cobalt-triethylenetetramine-salicylate complexes

The experimental of Co(trien)(sal)₂ was carried out according to described in experimental 3.2.2.3 employing cobalt (II) acetate tetrahydrate (Co(OAc)₂.4H₂O) (0.38 g, 1.57 mmol), ethylenediamine (0.2 ml, 3.52 mmol) and salicylic acid (0.42 g, 3.11 mmol). The red-brown viscous liquid of Co(trien)(sal)₂ was obtained by evaporation and dried under vacuum. (0.94 g, 94%): IR (KBr, cm⁻¹); 3090 (NH stretching), 2943 (CH stretching), 1717 (C=O stretching, salicylate), 1588 (Ar-H stretching), 1482 (asymmetric C=O stretching, acetate), 1460 (symmetric C=O stretching, acetate), 1387 (CN stretching), 1256, 1227 , 1074 (CO stretching), 862 , 761 (Ar-H). UV; λ_{max} (H₂O) = 496 nm, molar absorptivity (ε) = 521.

Compositions of starting materials in the preparation of all metal complexes are shown in Table 3.1.

Table 3.1 Composition of starting materials in the preparation of metal complexes

Metal complexes	Wt. of M(OAc)$_2$ (g)	Wt. of composition			Yield (%)	Appearance
		en (ml)	trien (ml)	salicylic acid (g)		
Ni(en)$_2$	0.67	0.33	-	-	68	purple-red powder
Ni(en)$_2$(sal)$_2$	0.38	0.20	-	0.42	92	yellow-brown viscous liquid
Ni(trien)	0.63	-	0.37	-	94	purple viscous liquid
Ni(trien)(sal)$_2$	0.38	-	0.20	0.42	92	blue viscous liquid
Co(en)$_2$	0.67	0.33	-	-	74	deep-red powder
Co(en)$_2$(sal)$_2$	0.38	0.20	-	0.42	90	red viscous liquid
Co(trien)	0.63	-	0.37	-	95	light-brown viscous liquid
Co(trien)(sal)$_2$	0.38	-	0.20	0.42	94	red-brown viscous liquid

en = ethylenediamine, trien = triethylenetetramine

3.3 Rigid polyurethane foam preparation

The foam formulations are reported in Table 3.2 and 3.3. We prepared foams characterization by two different isocyanate indexes (100 and 150). Moreover, we employed water as a blowing agent to study the influence of isocyanate index and mechanical properties. We prepared three sample of each kind of formulation and the results reported are the average values of the properties of the three samples. The polyol, surfactant, blowing agent and synthesized catalyst were mixed in paper cup (8.5 × 16.5 cm) by hand mixing technique and then PMDI was added. The total components of the formulation were mixed by mechanical stirrer (2000 rpm) for 30 seconds at room temperature. The preparation diagram was shown in Figure 3.1 and Scheme 3.9.

During the reaction, we measured the cream time, which is the time of the beginning of reaction, the gel time, namely the time needed for the mass to reach the gel point, tack free time and rise time (Table 4.4). After that, the foams were placed in an oven at room temperature for 24 h to the polymerization reaction completed and 7 days after foam preparation carrying out mechanical characterization.
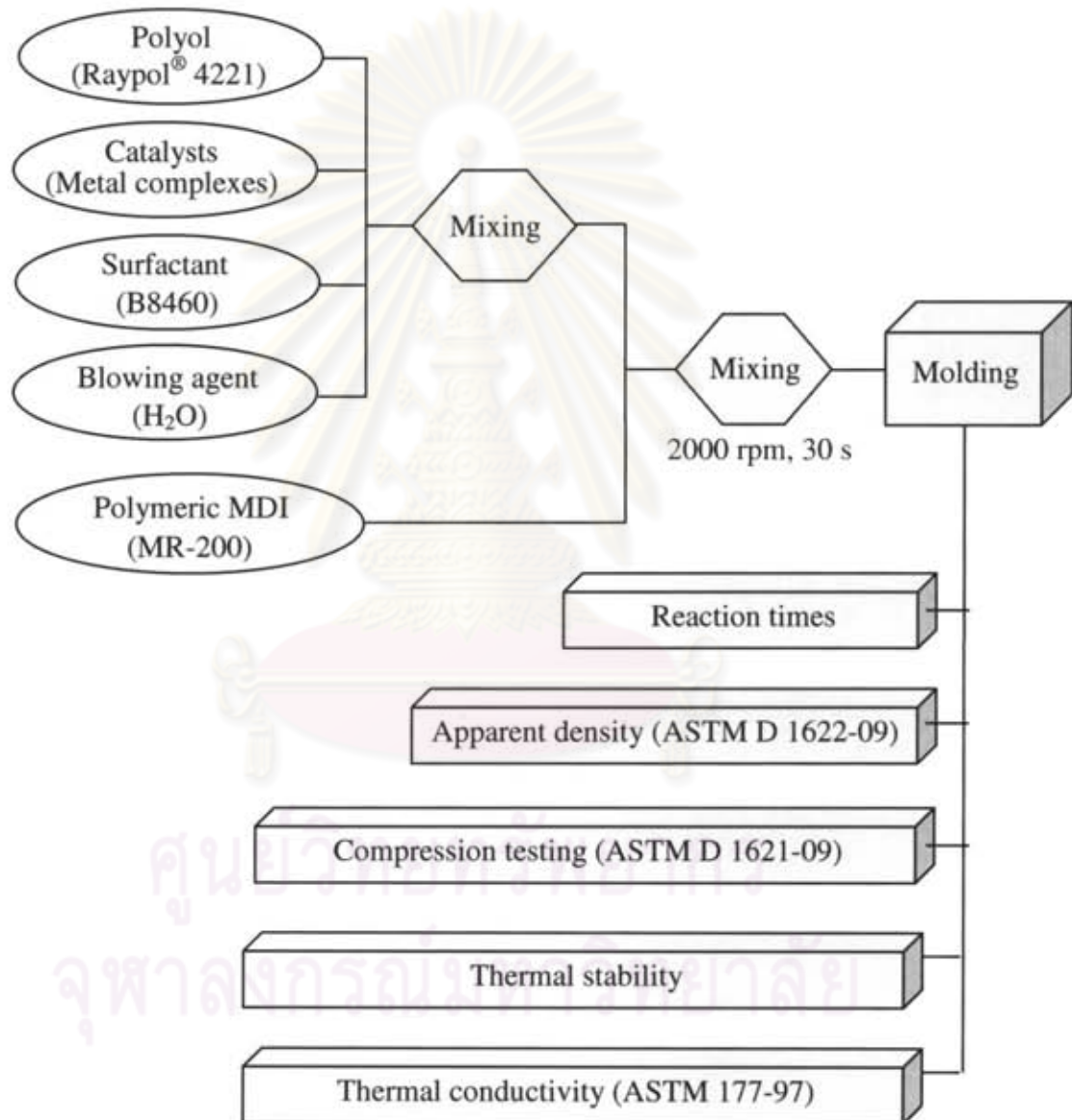
Figure 3.1 Diagram of preparation and analyzed of PURFs

Scheme 3.10 Diagram of preparation of rigid polyurethane foam

Table 3.2 PURFs formulations at different NCO indexes (in part by weight unit) [20]

Formulation (pbw)	NCO index	100	150
	NCO:OH	2.5:1	3.75:1
	(mole ratio)		
Polyols (Raypol®4221)		100	100
Catalysts (metal complexes and DMCHA)		1.2	1.2
Surfactant (TEGOTAB B8460)		2.5	2.5
Blowing agent (H_2O)		4.0	4.0
Polymeric MDI (MR-200)		133	249.6

Table 3.3 PURFs formulations at different NCO indexes (in gram unit cup test)

Formulation (pbw)	NCO index	100	150
	NCO:OH	2.5:1	3.75:1
	(mole ratio)		
Polyols (Raypol®4221)		10	10
Catalysts (metal complexes and DMCHA)		0.12	0.12
Surfactant (TEGOTAB B8460)		0.25	0.25
Blowing agent (H_2O)		0.4	0.4
Polymeric MDI (MR-200)		13.3	25.0

3.4 Measurements

3.4.1 UV-Vis analysis

UV spectra were performed in water on Cary 50 Probe, Varian ultraviolet and visible spectrophotometer at room temperature. The samples were scanned over the range of 800-200 nm at a medium speed.

3.4.2 FTIR and ATR-FTIR analysis

IR spectrum of catalyst was performed on a Perkin Elmer FTIR spectrometer spectrum RX I using neat samples and potassium bromide (KBr) disk at room temperature, the samples were scanned over the range of 500-4000 cm^{-1} at the resolution of 16 cm^{-1} and number of scan was 4. Rigid polyurethane foams were recorded on a Perkin-Elmer ATR-IR spectrophotometer at room temperature. The samples were scanned over range of 500-4000 cm^{-1} at the resolution of 16 cm^{-1} and number of scan was 16. The data, collected as transmittance values, were converted into absorbance. Frequency assignments for a typical PUR/PIR functional group are given in Table 3.4. The absorbance of the different groups was measured by employing a common baseline that crosses three anchor points at approximately 1470-1350-1160 cm^{-1} for trimer calculation and 2480-2015-985 cm^{-1} for the free isocyanate calculation. For the quantitative free isocyanate calculation, phenyl group was chosen as a reference group because phenyl absorption remained constant for a given formulation and was independent of the type of reaction.
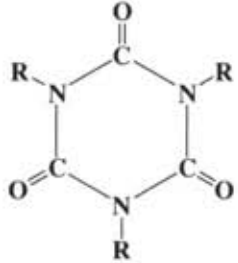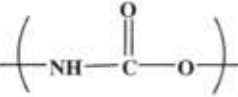
3.4.3 Cell morphology analysis

The Hitachi/S-4800 field emission scanning electron microscope (SEM) over the range ×40 – ×70 was used to study the morphology of rigid polyurethane foams. The samples were gold-coated before scanning in order to provide an electrically conductive surface. The accelerating voltage was 20 kV in order to avoid degradation of the sample.

3.4.4 Elemental analysis

Elemental analyses were carried out using a Perkin-Elmer EP 2400 analyzer.

Table 3.4 Wavenumber of typical PIR/PUR absorbance [21]

Functional groups	Wavenumber (cm^{-1})	Chemical structure
Isocyanate	2277	N=C=O
Phenyl	1595	Ar-H
Isocyanurate	1415	
Urethane	1220	

3.4.5 Thermal gravimetric analysis (TGA)

The thermogravimetric analyses (TGA) was carried out on a Netzsch STA 409C thermogravimetric analyzer. The weight of samples for all foams was kept within 3-5 mg and heated from 25 and 800°C at heating rate 20°C/min under N_2 atmosphere. The result of thermal stability was reported in percentage weight residue of rigid polyurethane foams. Initial decomposition temperature was taken at the temperature where 5 wt% loss of the rigid polyurethane foam occurred.

3.4.6 Reaction times

Cream time, gel time, tack free time and rise time during the foaming process were measured using a stopwatch. Foaming temperature and temperature profile was recorded by a dual thermocouple, Digicon DP-71.

3.4.7 Physical and Mechanical properties

The apparent density of rigid polyurethane foams was determined according to ASTM D 1622, the size of specimen was 3.0×3.0×3.0 cm (length×width×thickness) and the average values of three samples were done.

The compressive strength of the foams has been measured according to ASTM D 1621. At 10% strain in the perpendicular to the foam rise direction was performed using universal testing machine, Lloyd/LRX. The size of specimen was 3.0×3.0×3.0 cm (length×width×thickness), and the rate of crosshead movement was fixed at 2.54 mm/min for each sample and the preload cell used was 0.100 N.

The thermal conductivity of the foams has been evaluated according to ASTM 177-97 standard for which the size of the sample was 5.0×5.0×4.0 cm (length×width×thickness). Analyzed by Hot Disk Thermal Constant Analyzer TPS 2500 (Hot Disk AB) under room temperature condition. Disk type: Kapton Insulation (Sensor No. C7577, Radius = 2.001 mm.)

CHAPTER IV

RESULTS AND DISCUSSION

4.1 Synthesis of metal complexes as catalysts

4.1.1 Synthesis of metal-ethylenediamine complexes [M(en)$_2$]

M(en)$_2$ were synthesized from the reaction between metal (II) acetate and ethylenediamine (en) (Scheme 4.1) in acetone by modification of the synthetic method reported in the literature [19].
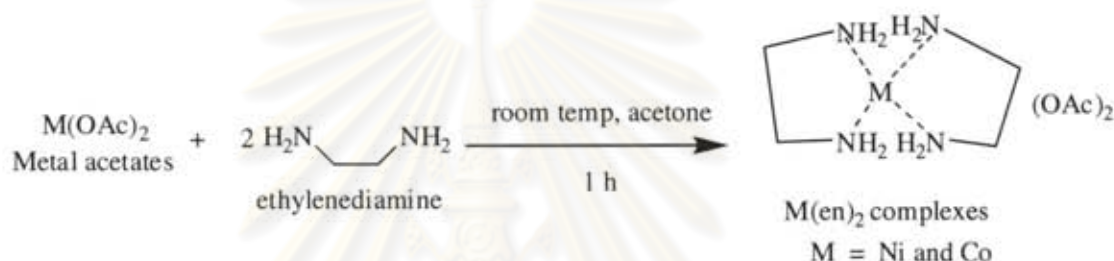
Scheme 4.1 Synthesis of metal-ethylenediamine complexes [M(en)$_2$]

Ni(en)$_2$ and Co(en)$_2$ complexes were obtained as purple-red and deep-red solid, respectively.

4.1.1.1 IR spectroscopy of M(en)$_2$ complexes

M(en)$_2$ complexes (where M = Ni and Co) showed similar IR spectra as shown in Figures 4.1 and 4.2. The important characteristic absorption bands were observed at 3216-3484 cm^{-1} (NH stretching), 2890-2966 cm^{-1} (CH stretching). The C=O stretching of carbonyl group in Ni(en)$_2$ and Co(en)$_2$ appeared at 1568 and 1572 cm^{-1} (asymmetric C=O stretching), 1400 and 1408 cm^{-1} (symmetric C=O stretching), respectively. The C=O stretching peaks of M(en)$_2$ were different from those of Ni(OAc)$_2$, which appeared at 1535 cm^{-1} (asymmetric C=O stretching) and 1417 cm^{-1} (symmetric C=O stretching) and Co(OAc)$_2$, which appeared at 1544 cm^{-1} (asymmetric C=O stretching) and 1422 cm^{-1} (symmetric C=O stretching). The absorption bands of Ni(en)$_2$ and Co(en)$_2$ exhibited C-O stretching at 1024 and 1055 cm^{-1}, respectively

which shifted from typical absorption band of Ni(OAc)$_2$ and Co(OAc)$_2$ at 1027 cm^{-1} and 1023 cm^{-1}, respectively. The peak of H$_2$O in Ni(OAc)$_2$.4 H$_2$O at 2900-3500 cm^{-1} (O-H stretching) was not found in Ni(en)$_2$. Since the IR peaks of metal complexes synthesized as catalyst shifted form those of M(OAc)$_2$ (M = Ni and Co), this suggested that the M(en)$_2$ complexes were formed.
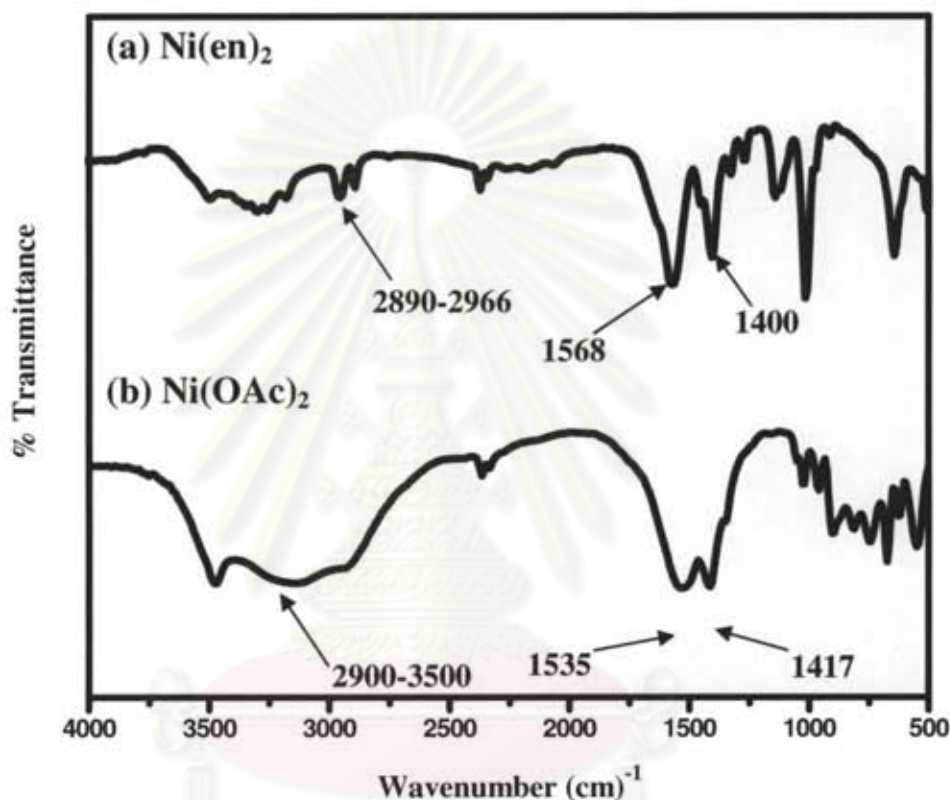
Figure 4.1 IR spectra of (a) Ni(en)$_2$; (b) Ni(OAc)$_2$

4.1.1.2 UV-Visible spectroscopy of M(en)$_2$ complexes

UV-Vis spectra of M(en)$_2$ complexes are shown in Figures 4.3 and 4.4. The maximum wavelength of Ni(en)$_2$ and Co(en)$_2$ complexes appeared at 344 and 470 nm, respectively. They are different form the maximum wavelength of Ni(OAc)$_2$ and Co(OAc)$_2$, which appeared at 394 and 513 nm, respectively. It was found that the maximum wavelength of Ni(en)$_2$ and Co(en)$_2$ complexes shifted from the typical

maximum wavelength of $Ni(OAc)_2$ and $Co(OAc)_2$, which indicated that the metal complexes were obtained.
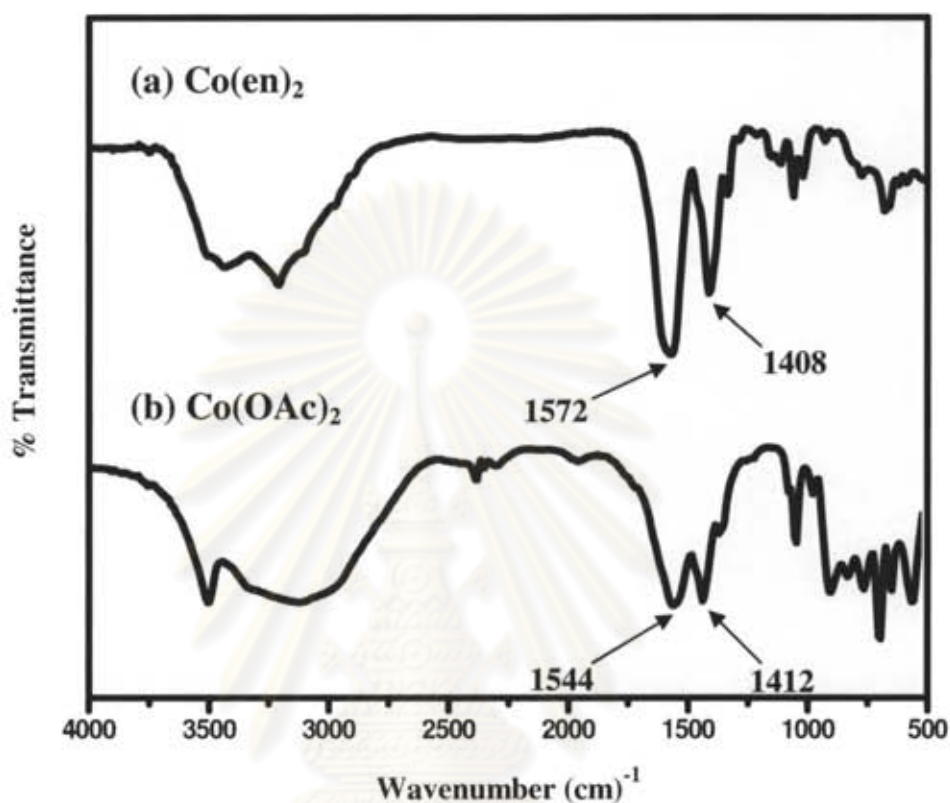
Figure 4.2 IR spectra of (a) $Co(en)_2$; (b) $Co(OAc)_2$

4.1.2 Synthesis of metal-ethylenediamine-salicylate complexes [M(en)₂(sal)₂]
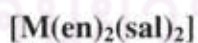
$M(en)_2(sal)_2$ were synthesized from the reaction between metal (II) acetate, ethylenediamine (en) and salicylic acid (Scheme 4.2) by modification of the synthetic method reported in the literature [19]. $Ni(en)_2(sal)_2$ and $Co(en)_2(sal)_2$ complexes were obtained as yellow-brown and red viscous liquid, respectively.
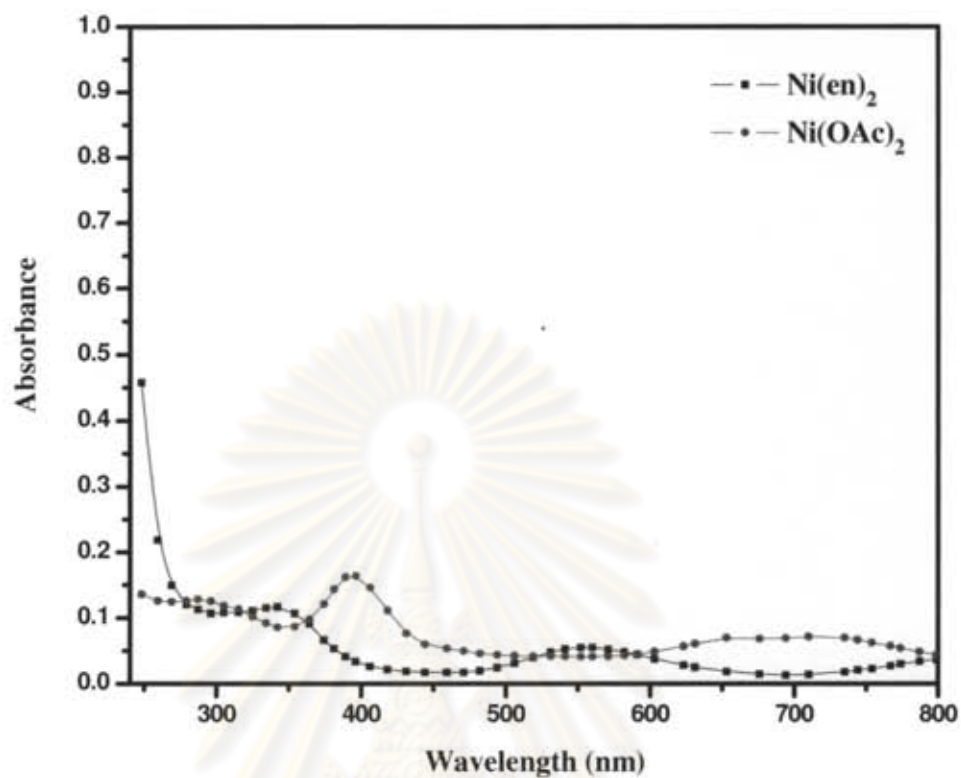
Figure 4.3 UV-Vis spectra of Ni(OAc)$_2$ and Ni(en)$_2$
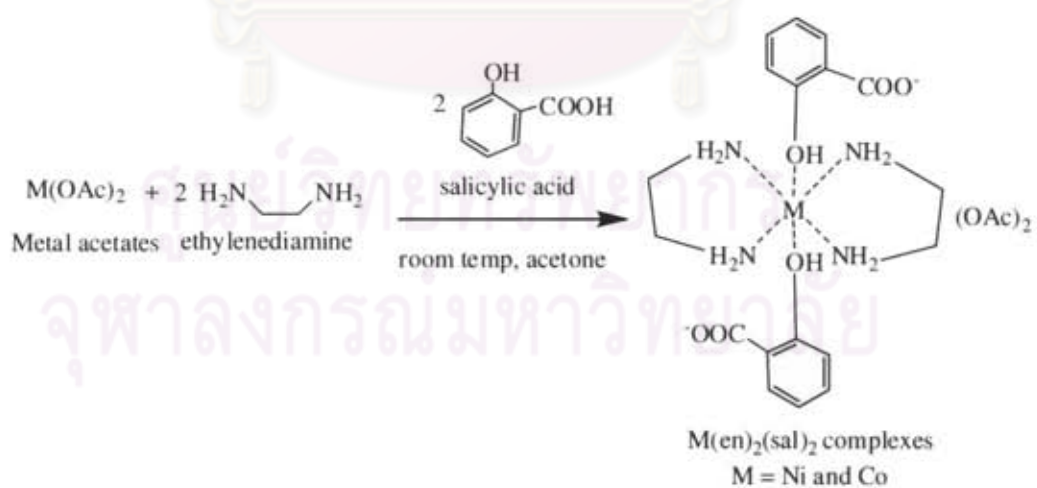
Scheme 4.2 Synthesis of metal-ethylenediamine-salicylate complexes [M(en)$_2$(sal)$_2$]

4.1.2.1 IR spectroscopy of M(en)$_2$(sal)$_2$ complexes

M(en)$_2$(sal)$_2$ complexes (where M = Ni and Co) showed similar IR spectra as shown in Figure 4.5. Absorption bands were observed at 3262 cm^{-1} (NH stretching), 2972 cm^{-1} (CH stretching), 1568-1595 cm^{-1} (Ar-H stretching), 1385-1387 cm^{-1} (CN stretching) and 757-859 cm^{-1} (Ar-H stretching). The carbonyl (C=O stretching) of M(en)$_2$(sal)$_2$ appeared in the range 1462-1455 cm^{-1} (asymmetric C=O stretching). The important absorption band of salicylate carbonyl was observed at 1719-1705 cm^{-1}.
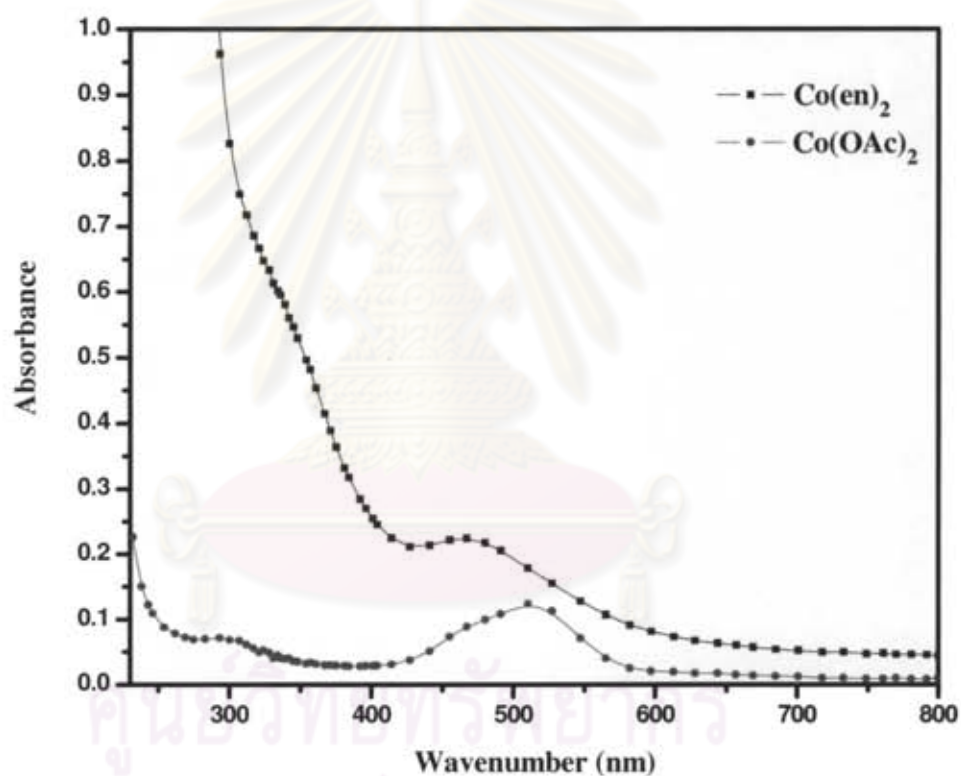
Figure 4.4 UV-Vis spectra of Co(OAc)$_2$ and Co(en)$_2$

4.1.2.2 UV-Visible spectroscopy of M(en)₂(sal)₂ complexes

UV-Vis spectra of M(en)$_2$(sal)$_2$ complexes are shown in Figures 4.6 and 4.7. The maximum wavelength of Ni(en)$_2$(sal)$_2$ and Co(en)$_2$(sal)$_2$ complexes appeared at 427 and 497 nm, respectively. They are different form the maximum wavelength of Ni(OAc)$_2$ and Co(OAc)$_2$, which appeared at 394 and 513 nm, respectively. It was found that the maximum wavelength of Ni(en)$_2$(sal)$_2$ and Co(en)$_2$(sal)$_2$ complexes shifted from the typical maximum wavelength of Ni(OAc)$_2$ and Co(OAc)$_2$, which indicated that the complexes were obtained.

4.1.3 Synthesis of metal-triethylenetetramine complexes [M(trien)]

M(trien) were synthesized from the reaction between metal (II) acetate and triethylenetetramine (trien) (Scheme 4.3) in acetone by modification of the synthetic method reported in the literature [19]. Ni(trien) and Co(trien) complexes were obtained as purple viscous liquid and light-brown solid, respectively.
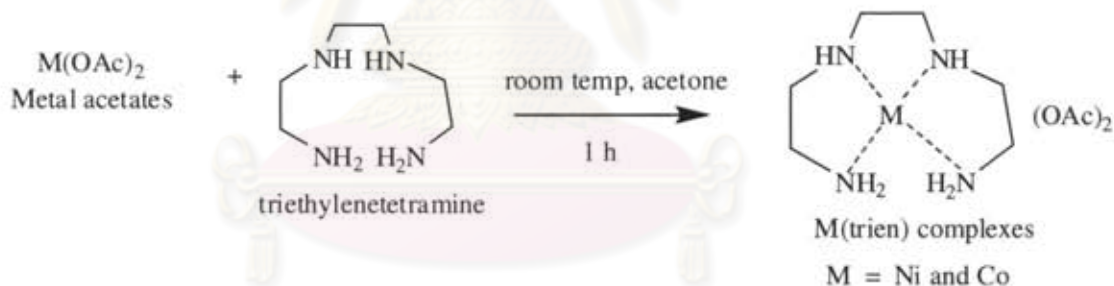
Scheme 4.3 Synthesis of metal-triethylenetetramine complexes [M(trien)]
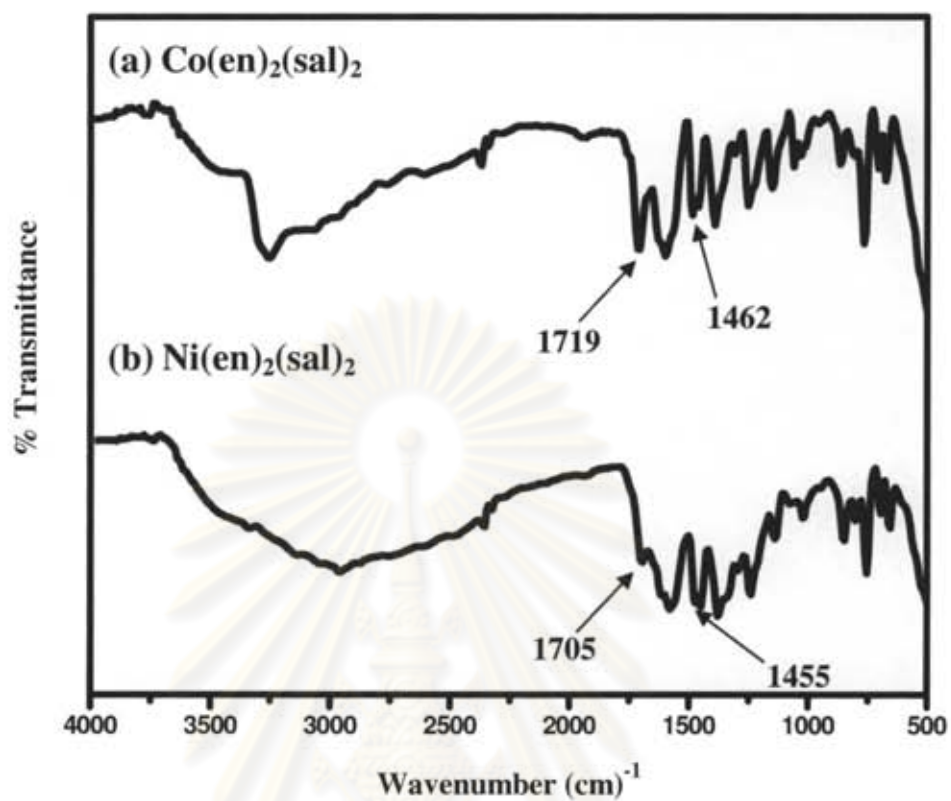
Figure 4.5 IR spectra of (a) Co(en)$_2$(sal)$_2$; (b) Ni(en)$_2$(sal)$_2$
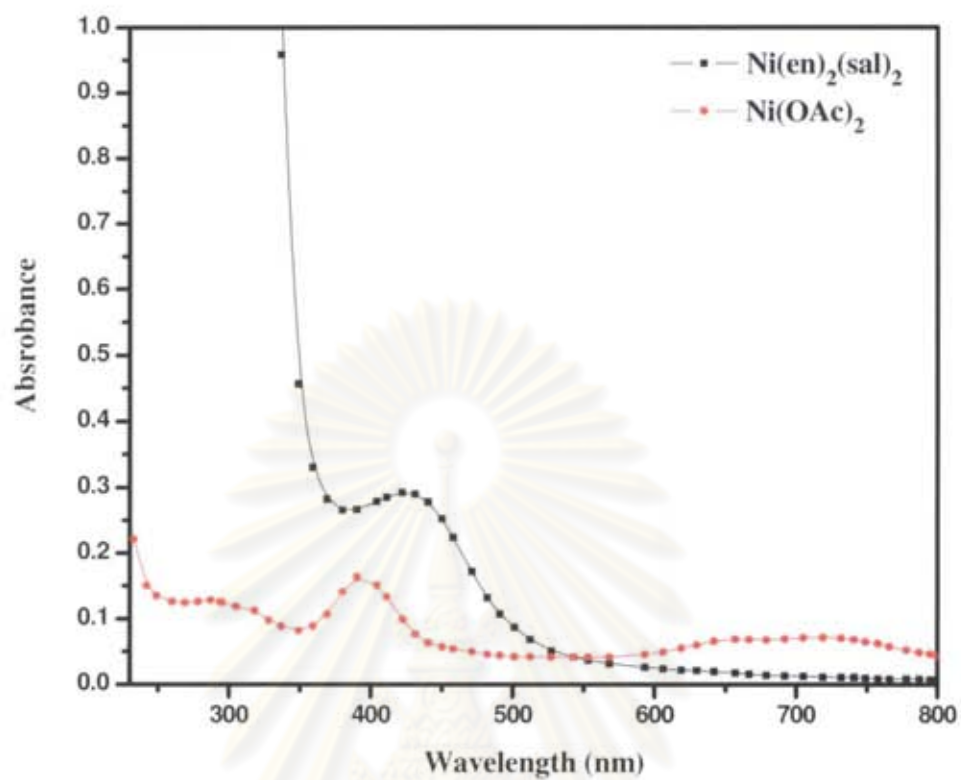
Figure 4.6 UV-Vis spectra of Ni(OAc)$_2$ and Ni(en)$_2$(sal)$_2$
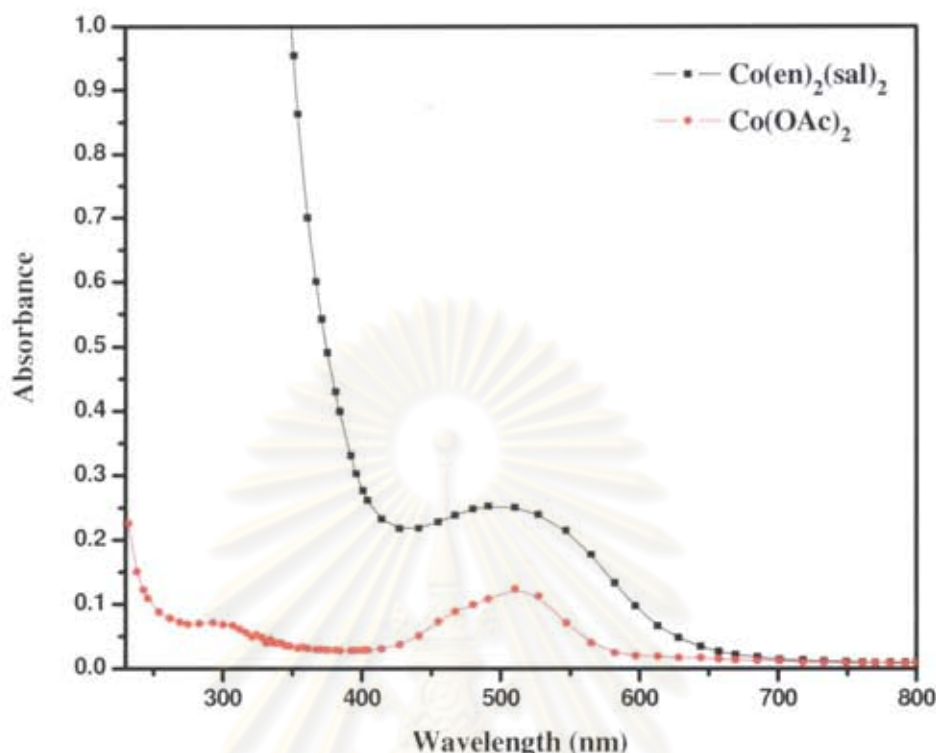
Figure 4.7 UV-Vis spectra of Co(OAc)$_2$ and Co(en)$_2$(sal)$_2$

4.1.3.1 IR spectroscopy of M(trien) complexes

M(trien) (where M = Ni and Co) show similar IR spectra are shown in Figures 4.8 and 4.9. Absorption bands are observed at 3213-3441 cm^{-1} (NH stretching), 2938-2986 cm^{-1} (CH stretching), 1402 cm^{-1} (CN stretching) and 1024-1056 cm^{-1} (CO stretching), which shifted from typical absorption band of Ni(OAc)$_2$ and Co(OAc)$_2$ at 1027 cm^{-1} and 1023 cm^{-1}, respectively. The carbonyl (C=O stretching) of M(trien) complexes appeared in the range 1546-1573 cm^{-1} (asymmetric C=O stretching) and 1409-1466 cm^{-1} (symmetric C=O stretching), which were different from those of Ni(OAc)$_2$, which normally appear at 1535 cm^{-1} (asymmetric C=O stretching) and 1417 cm^{-1} (symmetric C=O stretching) and those of Co(OAc)$_2$, which normally appear at 1544 cm^{-1} (asymmetric C=O) and 1422 cm^{-1} (symmetric C=O stretching). These results suggested that the M(trien) complexes were formed.

4.1.3.2 UV-Visible spectroscopy of M(trien) complexes

UV-Vis spectra of M(trien) complexes are shown in Figures 4.10 and 4.11. The maximum wavelength of Ni(trien) and Co(trien) complexes appeared at 348 and 505 nm, respectively. They are different form the maximum wavelength of $Ni(OAc)_2$ and $Co(OAc)_2$ at 394 and 513 nm, respectively. It was found that the maximum wavelength of Ni(trien) and Co(trien) complexes shifted from those of $Ni(OAc)_2$ and $Co(OAc)_2$, which indicated the complexes were obtained.
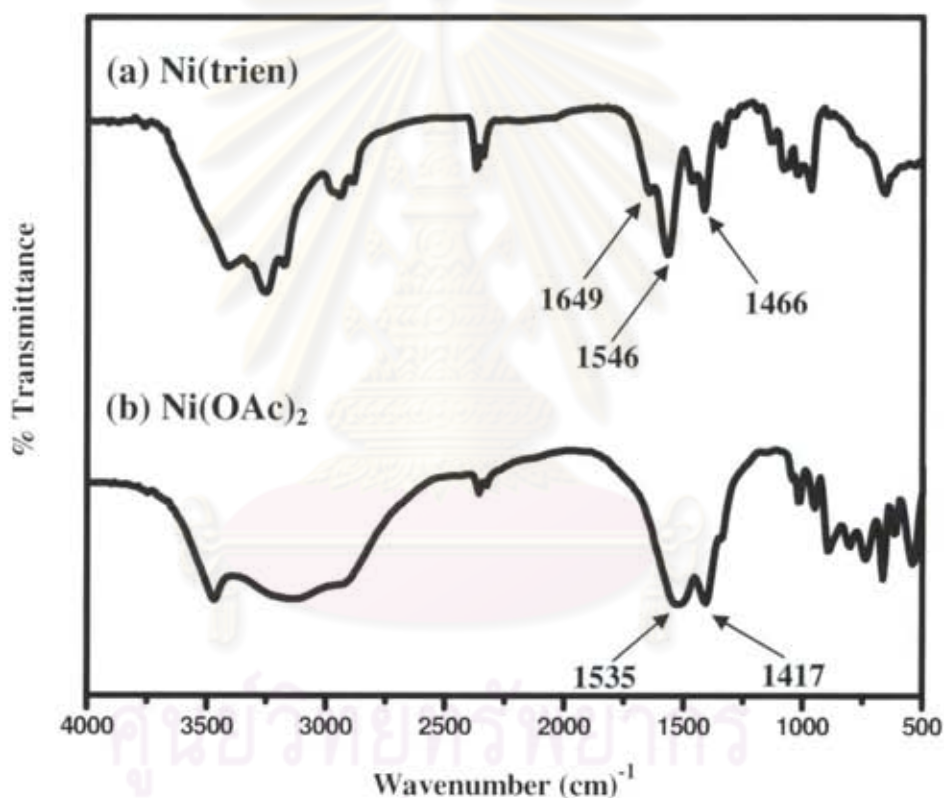
Figure 4.8 IR spectra of (a) Ni(trien); (b) $Ni(OAc)_2$
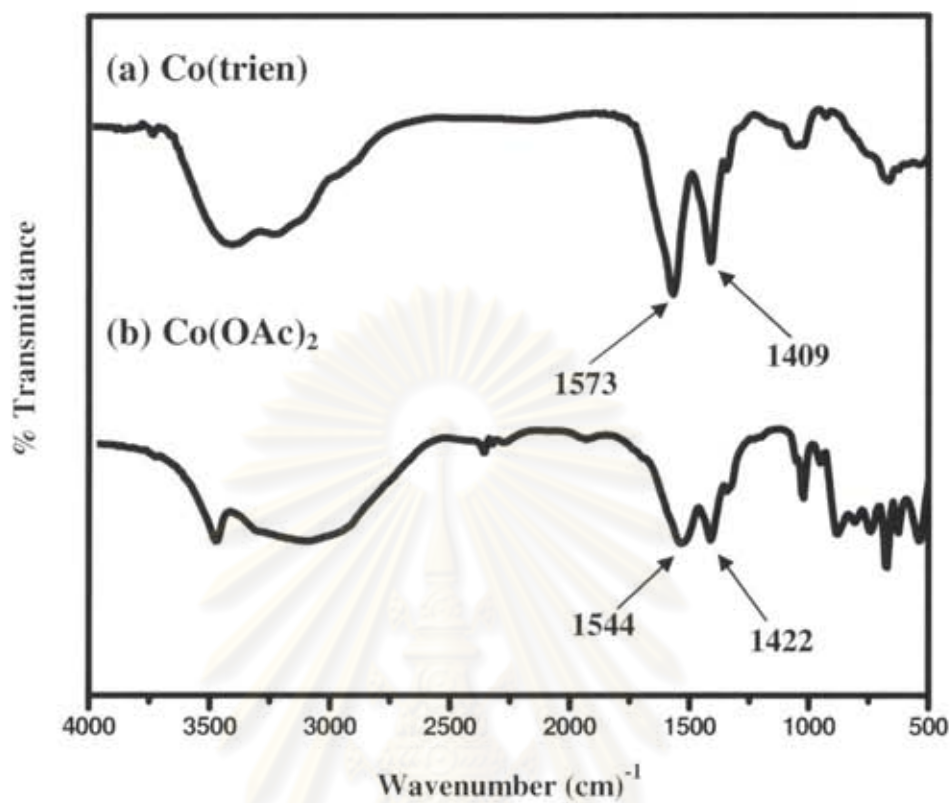
Figure 4.9 IR spectra of (a) Co(trien); (b) Co(OAc)$_2$
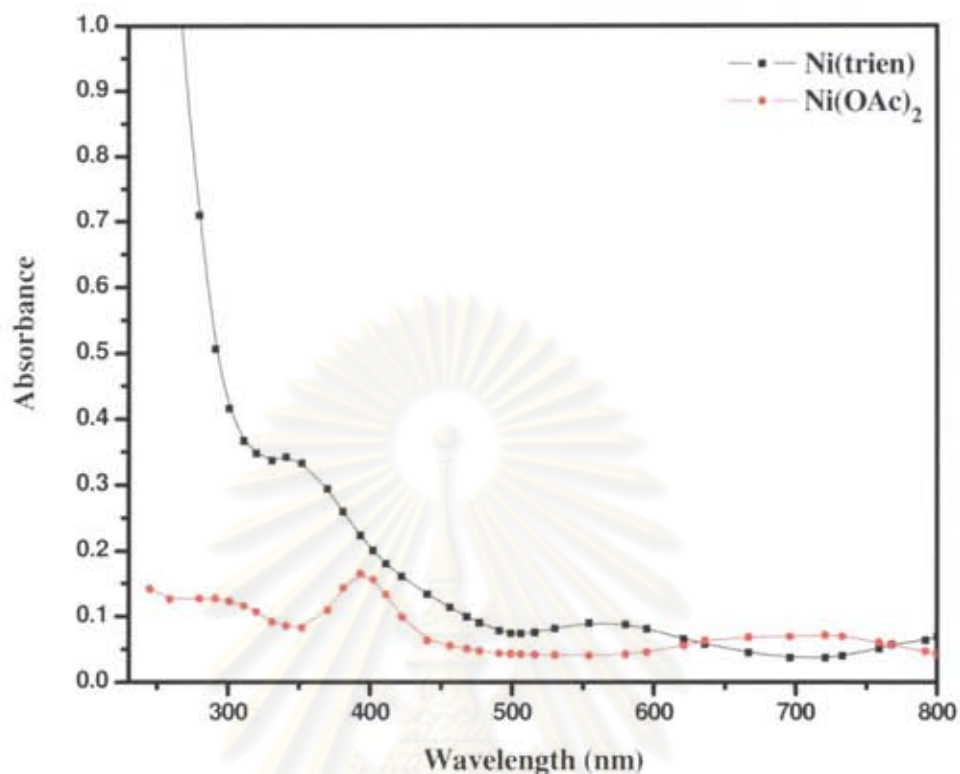
Figure 4.10 UV-Vis spectra of Ni(OAc)$_2$ and Ni(trien)

4.1.4 Synthesis of metal-triethylenetramine-salicylate complexes [M(trien)(sal)$_2$]

M(trien)(sal)$_2$ were synthesized from the reaction between metal (II) acetate, triethylenetetramine (trien) and salicylic acid (Scheme 4.4) by modification of the synthetic method reported in the literature [19]. Ni(trien)(sal)$_2$ and Co(trien)(sal)$_2$ complexes were obtained as blue and red-brown viscous liquid, respectively.
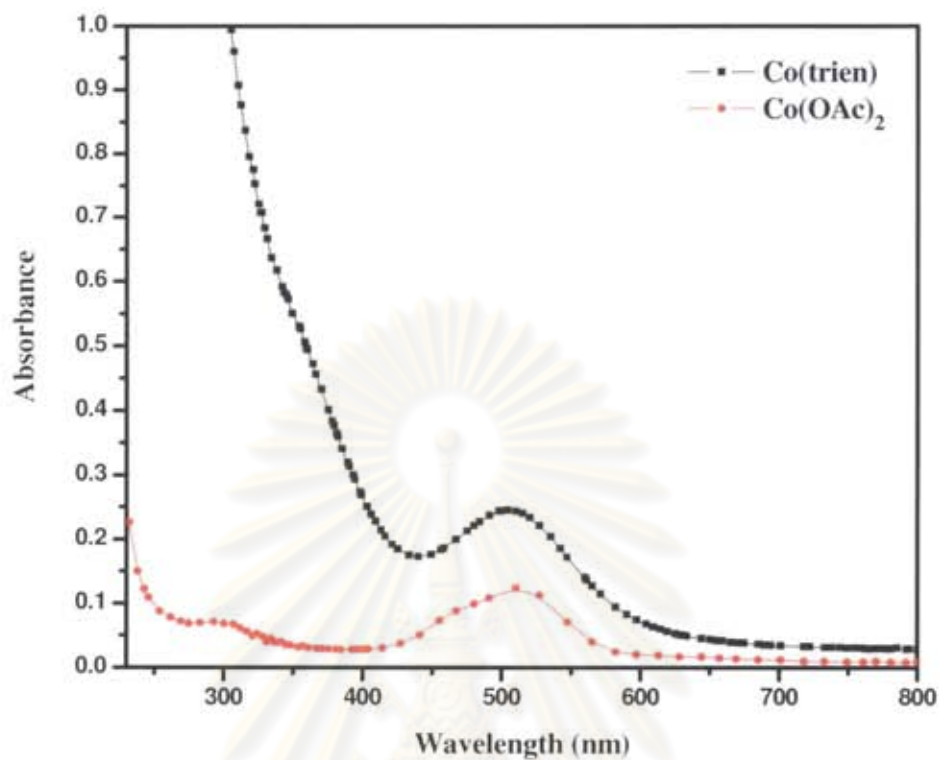
Figure 4.11 UV-Vis spectra of Co(OAc)₂ and Co(trien)
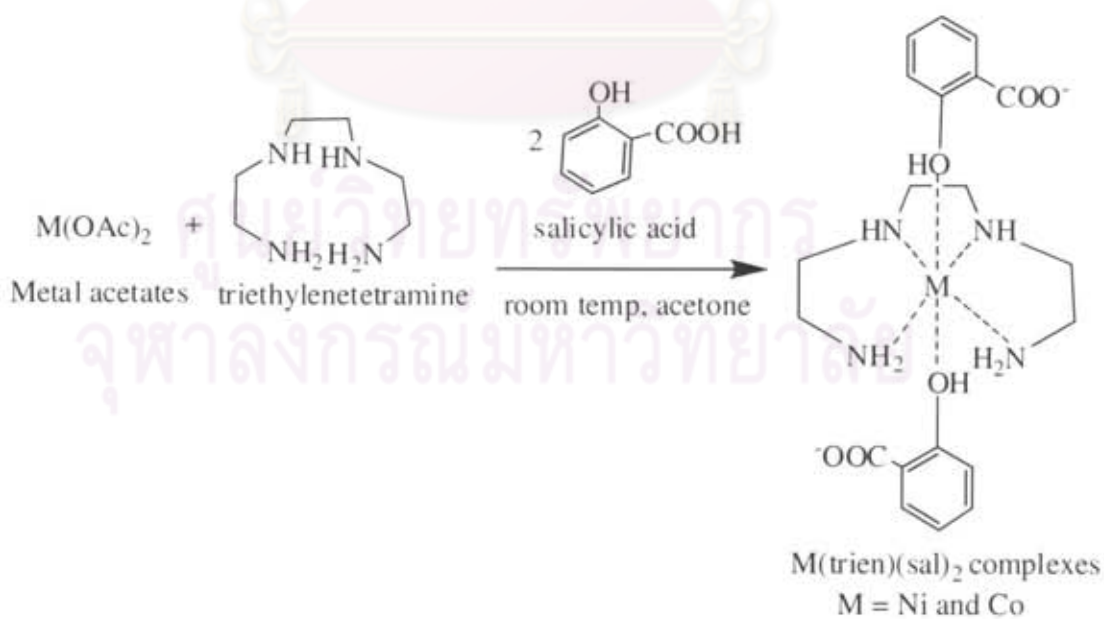
Scheme 4.4 Synthesis of metal-triethylenetetramine-salicylate complexes
[M(trien)(sal)₂]
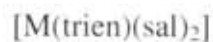
4.1.4.1 IR spectroscopy of M(trien)(sal)$_2$ complexes

M(trien)(sal)$_2$ (where M = Ni and Co) show similar IR spectra are shown in Figure 4.12. Absorption bands are observed at 3090-3218 cm^{-1} (NH stretching), 2938-2943 cm^{-1} (CH stretching). The carbonyl (C=O stretching) of M(trien)$_2$(sal)$_2$ complexes appear in the range 1466-1471 cm^{-1} (symmetric C=O stretching). The important absorption bands were observed at 1717-1721 cm^{-1} (C=O stretching, salicylate). 1588-1591 cm^{-1} (Ar-H stretching), 1380-1387 cm^{-1} (CN stretching), 761-862 cm^{-1} (Ar-H stretching)
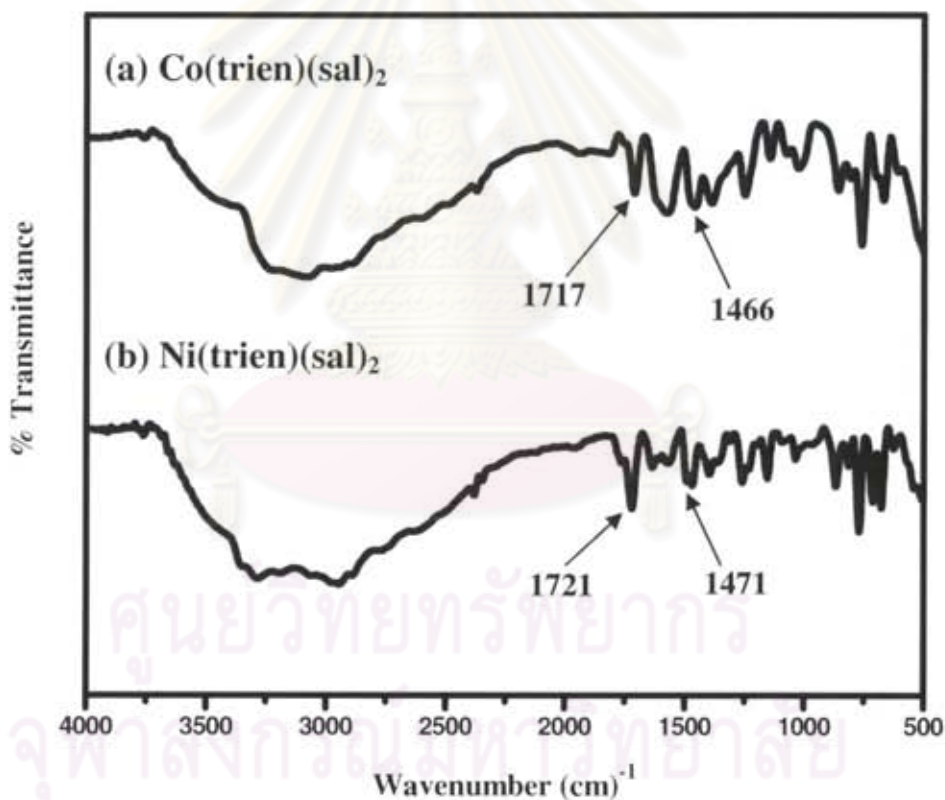
Figure 4.12 IR spectra of (a) Co(trien)(sal)$_2$; (b) Ni(trien)(sal)$_2$

4.1.4.2 UV-Visible spectroscopy of M(trien)(sal)$_2$ complexes

UV-Vis spectra of M(trien)(sal)$_2$ complexes are shown in Figures 4.13 and 4.14. The maximum wavelength of Ni(trien)(sal)$_2$ and Co(trien)(sal)$_2$ complexes appeared at 295 and 496 nm, respectively. They are different form maximum wavelength of Ni(OAc)$_2$ and Co(OAc)$_2$ at 394 and 513 nm, respectively. It was found that the maximum wavelength of Ni(trien)(sal)$_2$ and Co(trien)(sal)$_2$ complexes shifted from those of Ni(OAc)$_2$ and Co(OAc)$_2$, which indicated the complexes were obtained.
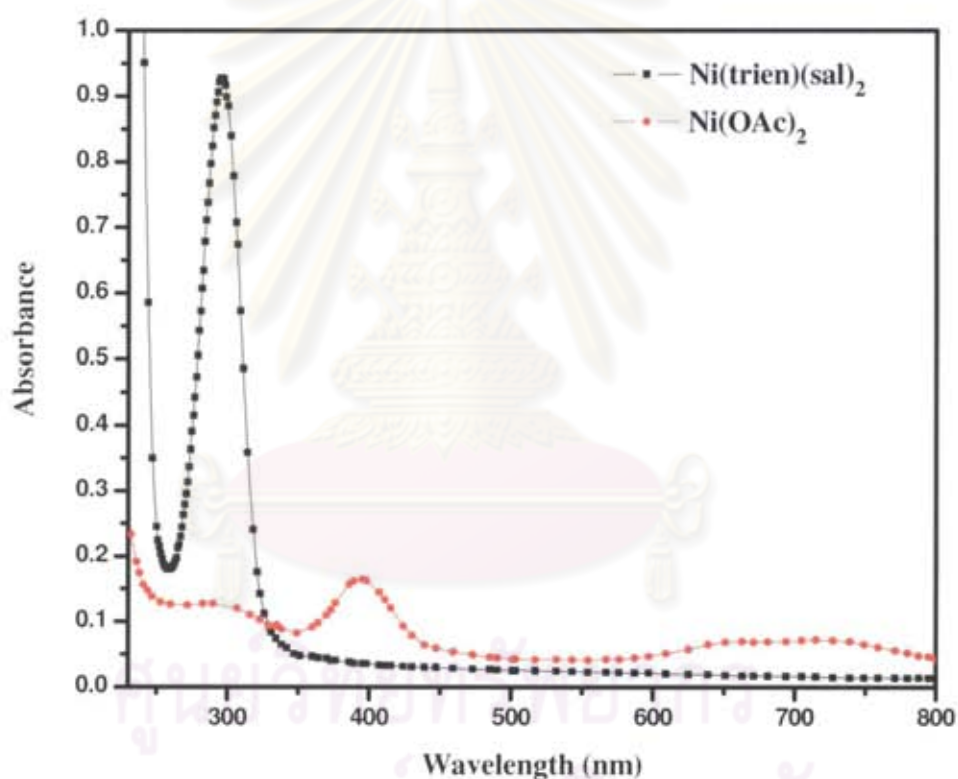
Figure 4.13 UV-Vis spectra of Ni(OAc)$_2$ and Ni(trien)(sal)$_2$
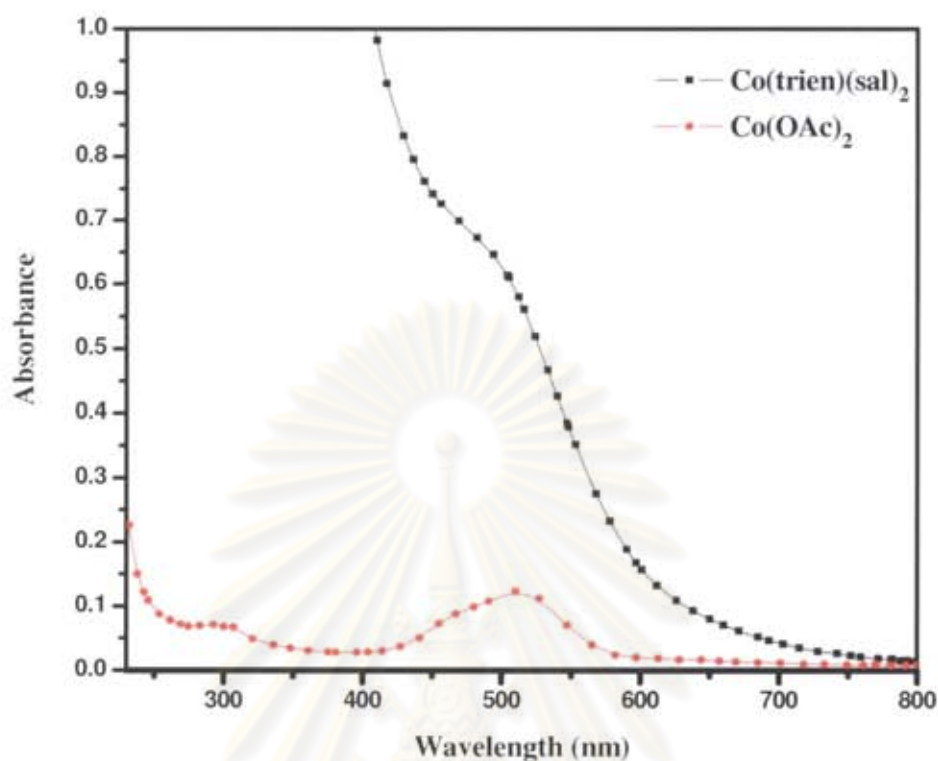
Figure 4.14 UV-Vis spectra of $Co(OAc)_2$ and $Co(trien)(sal)_2$

Table 4.1 shows the yield (%) of metal complexes which were obtained in the range 68-92%. All metal complexes showed different color from metal acetates. UV-Vis spectra of the metal complexes were obtained in water at 1000 ppm. λ_{max} of the metal complexes were found in the range 295 and 505 nm.

Molar absorptivity of $M(en)_2$ and $M(trien)$ is in the range 40-60 while that of $M(en)_2(sal)_2$ and $M(trien)(sal)_2$ is in the range 399-521. The presence of salicylic acid in the structure of $M(en)_2(sal)_2$ and $M(trien)(sal)_2$ increased their molar absorptivities.

Table 4.1 Yield (%) and UV-Vis data of metal complexes

Metal complexes	Yield (%)	Color	λ_{max} (nm)	Molar absorptivity
Ni(en)$_2$	68	purple-red	344	60
Ni(en)$_2$(sal)$_2$	95	yellow-brown	427	399
Ni(trien)	90	purple	348	46
Ni(trien)(sal)$_2$	88	blue	295	429
Ni(OAc)$_2$	-	green	394	25
Co(en)$_2$	74	deep-red	470	40
Co(en)$_2$(sal)$_2$	90	red	497	452
Co(trien)	76	light-brown	505	40
Co(trien)(sal)$_2$	92	red-brown	496	521
Co(OAc)$_2$	-	red	513	19

4.2 Rigid polyurethane foams catalyzed by metal complexes

4.2.1 Preparation of rigid polyurethane foams

Rigid polyurethane foams (PURFs) catalyzed by transition metal complexes: M(en)$_2$; M(en)$_2$(sal)$_2$; M(trien) and M(trien)(sal)$_2$ (where M = Ni and Co) were prepared by one step and the foams formulations are shown in Table 3.2. The polyol, silicone surfactant (B8460), blowing agent (water) and catalysts (transition metal complexes) were first mixed well in paper cup (8.5×16.5 cm) by hand mixing and then PMDI was added. The mixture was stirred by using high speed mechanical stirrer (2000 rpm) for 30 seconds at room temperature and foams were allowed to rise. During the expansion, cream time, gel time, tack-free time, rise time and foaming temperatures were recorded. Cream time is the time of the beginning of reaction or blowing reaction. Gel time is the time needed for the mass to reach the gel point or gelling reaction. Tack free time is the time of the foams could not tack with other

materials or crosslink reaction. Rise time is the time when the foams stop rising. After preparation, the foams were kept at room temperature for 48 h to complete the polymerization reaction and 7 days before investigation of their properties. Samples were cut into specific shapes by cutter and then the different properties of the foams were analyzed. In this study, the amount of polyol, blowing agent, surfactant and catalysts were fixed. The NCO indexes used in the preparation of foams were 100 and 150. The foam formulation and the foam appearances are shown in Tables 4.2, Figures 4.15 and 4.16, respectively. Most foam showed good appearances. When the foams were prepared at increased NCO index, the foams were more brittle than those prepared at lower NCO index.

Table 4.2 PURFs formulations at different NCO indexes [20]

Formulation (pbw)	NCO index	100	150
	NCO:OH	2.5:1	3.75:1
	(mole ratio)		
Polyols (Raypol®4221)		10	10
Catalysts (metal complexes and DMCHA)		0.12	0.12
Surfactant (TEGOTAB B8460)		0.25	0.25
Blowing agent (H_2O)		0.4	0.4
Polymeric MDI (MR-200)		13.3	25

Figure 4.15 Foam prepared using DMCHA as a catalyst at different times (a) after all starting materials were mixed; (b) at cream time; (c) at gel time; (d) at tack-free time

During the foam preparation, Figure 4.15 (a) shows the reaction mixture appearance after all starting materials were mixed. Figure 4.15 (b) shows the reaction mixture at cream time, which is the reaction between isocyanate and water to give CO_2 and results in foam rising. Figure 4.15 (c) shows the reaction mixture at gel time, which is the reaction between isocyanate and hydroxyl group to form polyurethane. Figure 4.15 (d) shows the foam appearance at tack free time, which is the time when the polymerization reaction is completed and the foam does not stick to the other materials.
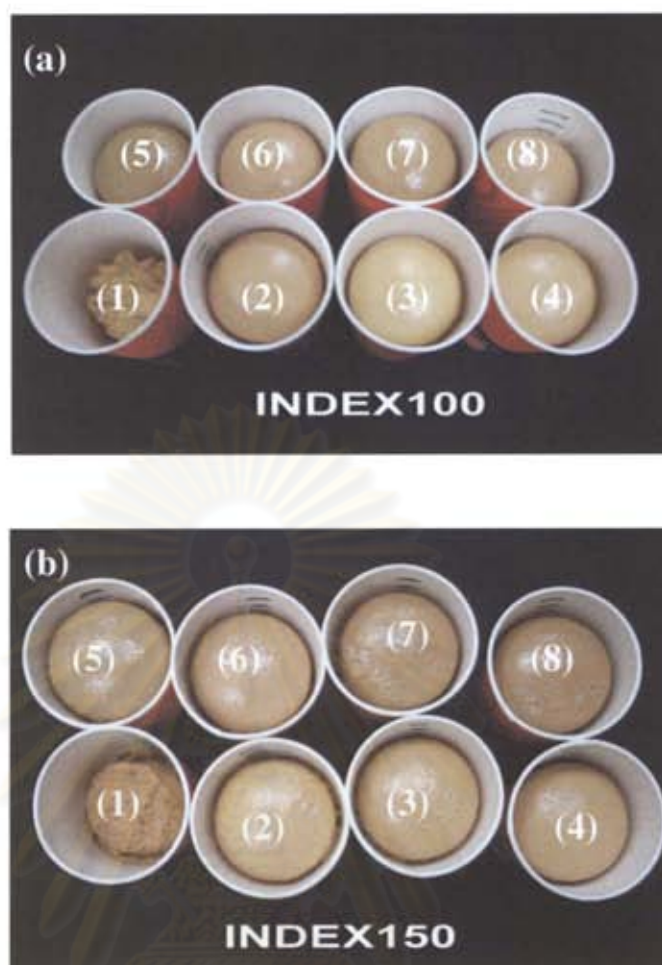
Figure 4.16 Foam appearances at NCO indexes of (a) 100 and (b) 150

Figure 4.16 shows PURFs catalyzed from different catalysts at NCO indexes of 100 and 150. Figure 4.16 (a) and (b) (1) shows the PURFs prepared from $Ni(en)_2$, which had poor external appearance. Figure 4.16 (a) and (b) (2), (3), (4), (5), (6), (7) and (8) show the those foams prepared from $Ni(en)_2(sal)_2$, $Ni(trien)$, $Ni(trien)(sal)_2$ $Co(en)_2$, $Ni(en)_2(sal)_2$, $Co(trien)$ and $Co(trien)(sal)_2$ respectively. All metal complexes, except $Ni(en)_2$, gave PURFs with similar to appearance.

4.2.2 The reaction time of rigid polyurethane foams

Table 4.3 and Figure 4.17-4.18 show cream time, gel time, tack free time and rise time of the foams prepared at the NCO indexes of 100 and 150. The obtained results showed that all transition metal complexes gave similar cream time at NCO index of 100 and 150. This suggested that catalytic activity of the reaction between

isocyanate and water to give CO_2 (blowing reaction) of all catalysts were similar. Both $Ni(en)_2$ and $Co(en)_2$ were good catalysts since the reaction time were short, however, morphology of the foam prepared by use of $Ni(en)_2$ was not good since the foam had less volume than those prepared using other metal complex catalysts. This indicated that $Ni(en)_2$ catalyzed gelling reaction, which was the reaction between isocyanate and hydroxyl groups, to form urethane groups very well but the catalytic activity of $Ni(en)_2$ towards blowing reaction to give CO_2 was not good. The blowing reaction of PURFs had effect to the foam density since this reaction released CO_2 and caused the form rise toward the top of a mold. The blowing reaction of $Ni(en)_2$ was not good since small amount of CO_2 was released therefore the density of PURFs catalyzed by $Ni(en)_2$ was high. The reaction time of PURFs catalyzed by DMCHA showed better catalytic activity than metal complex catalysts.

The metal complexes synthesized could catalyzed PURFs polymerization since the metal complexes (metal-based catalysts) acted as a Lewis acid, primarily coordinated to the oxygen atom of the NCO group and activated the electrophilic nature of the carbon and amine interacting with the proton of hydroxyl group in polyol, which then reacts with the isocyanate (Schemes 4.6) while the tertiary amine coordinate to the positive electron charged carbon of the NCO group or hydrogen of the OH group and forms a transition state to activate urethane formation reaction. It is postulated that a tertiary amine can be varied by maximizing its ability to form a hydrogen bond with alcohol to activate the O–H bond and therefore it can attach to the isocyanate more easily. The mechanism of tertiary amine catalysts are shown in Scheme 4.5.

Table 4.3 Cream times, gel times, tack-free times and rise times of PURFs catalyzed by different metal complexes

Catalysts	Cream time (sec)	Gel time (min)	Tack-free time (min)	Rise time (min)	Volume
NCO index = 100					
DMCHA	2	0.1	4.4	3.4	8/8
Ni(en)$_2$	5	0.2	5.4	4.5	6/8
Ni(en)$_2$(sal)$_2$	7	1.2	12.5	8.1	7/8
Ni(trien)	6	1.2	13.1	7.4	7/8
Ni(trien)(sal)$_2$	6	1.7	11.5	7.3	7/8
Co(en)$_2$	6	0.9	6.3	6.2	7/8
Co(en)$_2$(sal)$_2$	6	1.75	8.1	6	7/8
Co(trien)	7	1	8.2	4.5	7/8
Co(trien)(sal)$_2$	6	1.8	8.4	7.3	7/8
NCO index = 150					
DMCHA	1	0.1	5.5	3.2	8/8
Ni(en)$_2$	4	1	9.4	6.5	6/8
Ni(en)$_2$(sal)$_2$	5	2.5	13.5	9.1	7/8
Ni(trien)	6	1.7	13.3	9.1	7/8
Ni(trien)(sal)$_2$	5	2.8	14.1	8.5	7/8
Co(en)$_2$	4	1.4	7.2	7.5	7/8
Co(en)$_2$(sal)$_2$	5	1.8	9.5	6.6	7/8
Co(trien)	5	1.4	8.5	7	7/8
Co(trien)(sal)$_2$	6	2	9.5	6.4	7/8
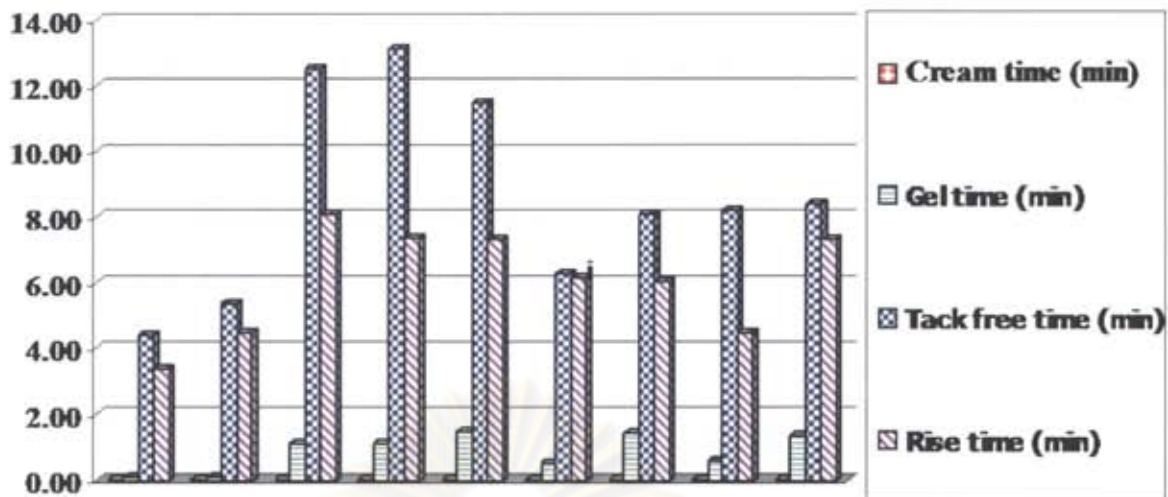
Figure 4.17 Reaction time of PURFs at NCO index 100
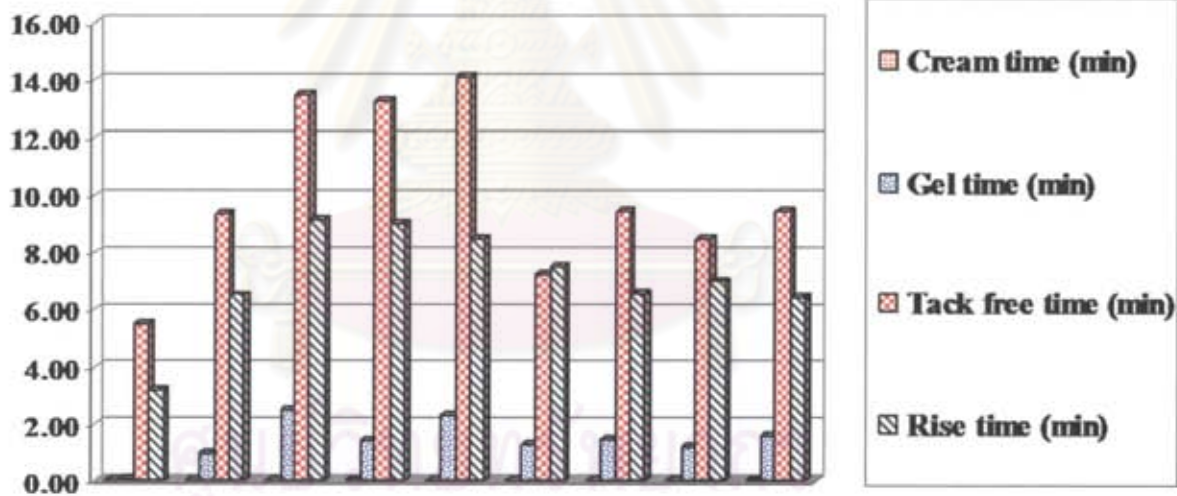
Figure 4.18 Reaction time of PURFs at NCO index 150

Baker mechanism

Farka mechanism

Scheme 4.5 Reaction mechanism of tertiary amine catalysts
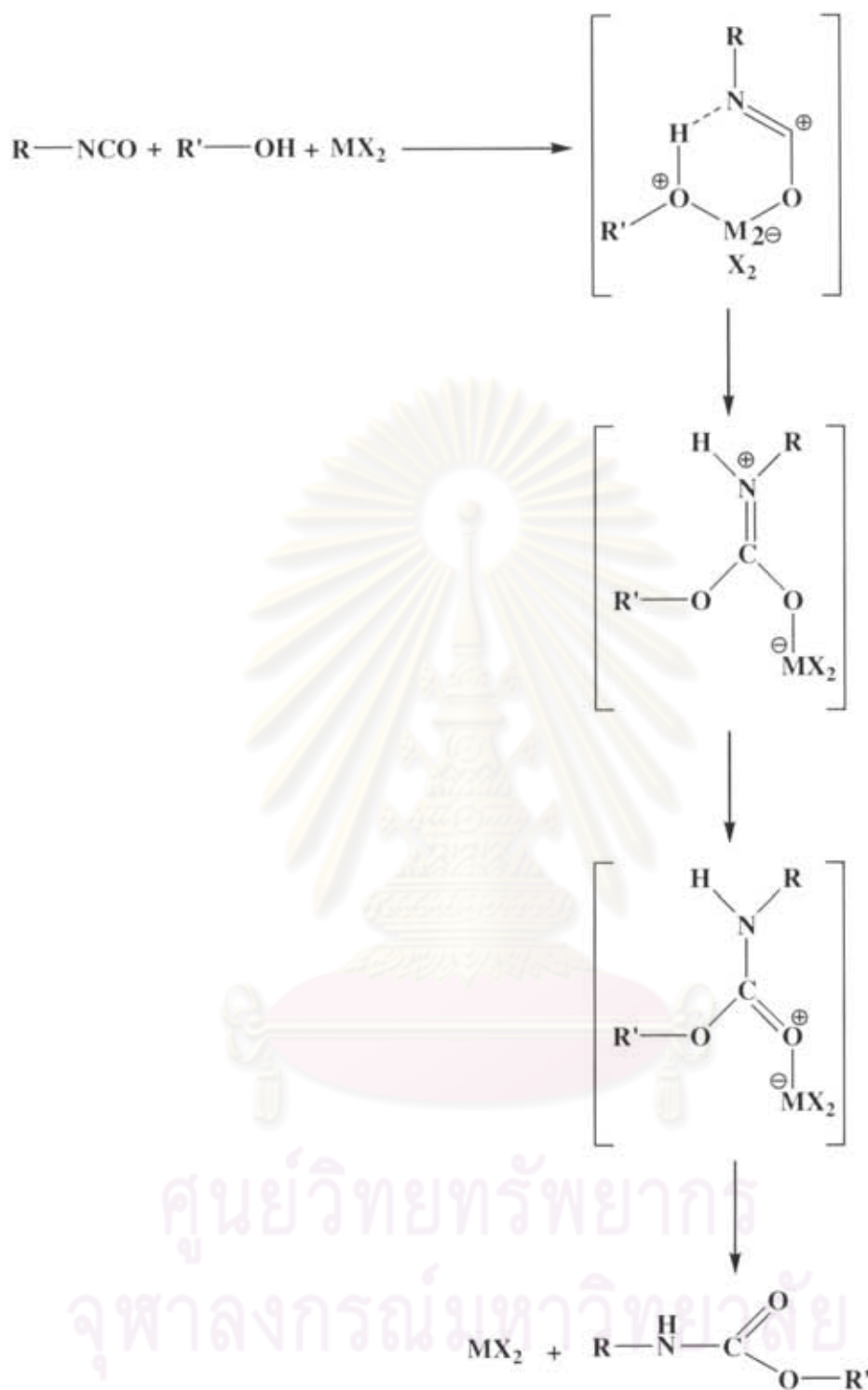
Scheme 4.6 Activation mechanism of metal-based catalyst on urethane formation
reaction

When salicylic acid was added into the structure of metal complexes to yield
$M(en)_2(sal)_2$ and $M(trien)(sal)_2$, the reaction time of these metal complex catalysts

were slower than those synthesized without salicylic acid, M(en)$_2$ and M(trien). This might be because salicylic acid formed complex with the metal and therefore steric effect from salicylic acid hindered the interaction of both metal and amine parts in metal complexes with the hydroxyl group in polyol.

PURFs catalyzed by metal complexes at NCO index of 100 showed the shorter reaction than those prepared at NCO index of 150. Only Co(en)$_2$ catalyst showed long rise time, which was as long as tack-free time. This was good for foam preparation since the foam continued to rise when the polymerization reaction was almost completed. After the reaction was completed, the foam would not collapse.

The maximum rise rates were calculated by differential at secondary stage of rise profile (which is maximum slope) as shown in Figure 4.19. The results obtained show that Ni(en)$_2$ gave the highest maximum rise rate of PURF. Catalytic activity of Ni(en)$_2$ was good but PURFs catalyzed by Ni(en)$_2$ had poor morphology. All metal complexes synthesized showed higher maximum rise rate than that DMCHA. This indicated that the metal complexes showed better catalytic activity towards blowing reaction than DMCHA.
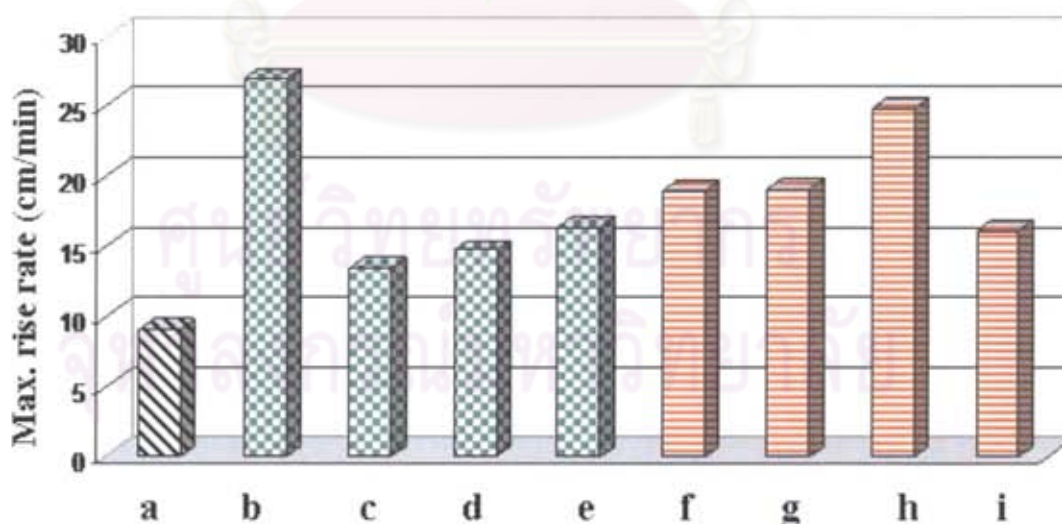
Figure 4.19 Maximum rise rates of PURFs catalyzed by different metal
complexes (a) DMCHA (ref); (b) Ni(en)$_2$; (c) Ni(en)$_2$(sal)$_2$; (d) Ni(trien);
(e) Ni(trien)(sal)$_2$; (f) Co(en)$_2$; (g) Co(en)$_2$(sal)$_2$; (h) Co(trien); (i)
Co(trien)(sal)$_2$

4.2.3 Density and compressive strength of rigid polyurethane foams

The apparent density of PURFs was measured according to ASTM D 1622. After foam preparation, PURFs were kept at room temperature for 48 hours, and then the foams were cut into cubic shape with 3.0 cm x 3.0 cm x 3.0 cm dimensions before apparent density of foams were measured.

The reaction time, especially blowing reaction of PURFs had effect on the foam density. Ni(en)$_2$ gave the foam with higher density than the foam catalyzed by other catalysts. This indicated that the blowing reaction of PURFs catalyzed by Ni(en)$_2$ was not good. Density of PURFs catalyzed by different metal complexes, M(en)$_2$, M(en)$_2$(sal)$_2$, M(trien) and M(trien)(sal)$_2$ (where M = Ni and Co), at NCO indexes of 100 and 150 are in the range 42.3-62.2 kg/m^3 and 49.7-73.9 kg/m^3, respectively as shown in Table 4.4 (b) and (e). The results showed that all metal complexes, except Ni(en)$_2$, gave PURFs with suitable density. The desirable density for rigid polyurethane foam applications is 40-50 kg/m^3 [22, 23].

As expected, the density of PURFs increased with increasing NCO index because the excess of isocyanate in PURFs system could undergo further polymerization to give polyisocyanurate, which was a crosslinked structure [20]. If PURFs were prepared over the NCO index of 150, the foam would be brittle and therefore the density could not measured.

In comparison between the density of PURFs prepared from metal complexes and DMCHA, it was found that the foams prepared from nickel complexes showed higher density than those prepared from DMCHA while the foams prepared form Co(trien) showed similar density to those prepared from DMCHA.

Table 4.4 (a) Density and compressive strength of PURFs prepared at the NCO index of 100

PURFs catalyzed by	Index 100	
	Density (kg/m^3)	Compressive strength (MPa)
DMCHA	39.6	0.19
Ni(en)$_2$	69.2	-
Ni(en)$_2$(sal)$_2$	47.5	0.12
Ni(trien)	46.7	0.07
Ni(trien)(sal)$_2$	46.9	0.23
Co(en)$_2$	39.8	0.12
Co(en)$_2$(sal)$_2$	44.2	0.16
Co(trien)	46.6	0.05
Co(trien)(sal)$_2$	55.6	0.19

Table 4.4 (b) Density and compressive strength of PURFs prepared at the NCO index of 150

PURFs catalyzed by	Index 150	
	Density (kg/m^3)	Compressive strength (MPa)
DMCHA	50.3	0.32
Ni(en)$_2$	71.8	-
Ni(en)$_2$(sal)$_2$	67.5	-
Ni(trien)	63.9	-
Ni(trien)(sal)$_2$	68.1	-
Co(en)$_2$	56.5	-
Co(en)$_2$(sal)$_2$	56.2	-
Co(trien)	46.8	0.25
Co(trien)(sal)$_2$	55.3	-

Compressive strength of PURFs is an important parameter which determined its application. PURFs were subjected to compressive stress at 10% strain [24]. The yield point of a material is defined in engineering and materials science as the stress at which a material begins to deform plastically. Prior to the yield point the material will deform elastically and will return to its original shape when the applied stress is removed. Once the yield point is passed some fraction of the deformation will be permanent and non-reversible.

Compressive strength of PURFs catalyzed by different metal complexes at NCO indexes of 100 and 150 were in the range 0.13-0.24 MPa and 0.25 MPa, respectively (Table 4.4 (a) and (b) and Figures 4.20-4.21). Compressive strength of PURFs with the maximum density of 50 kg/m^3 was measured. It was found that compressive strength increased with increasing density of PURFs.
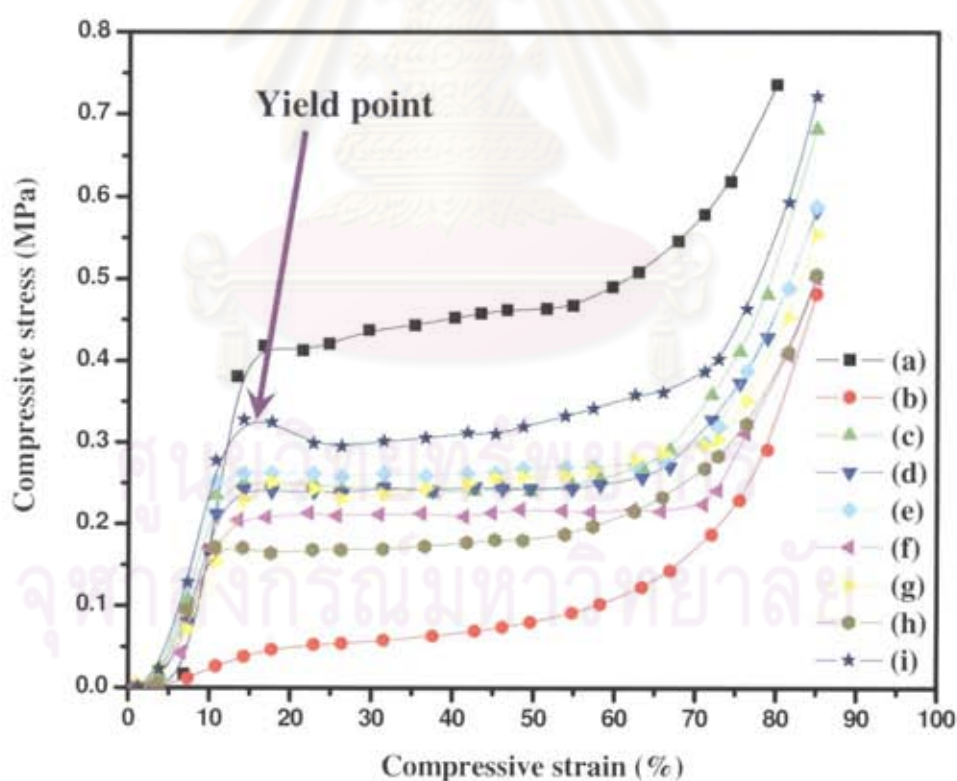
Figure 4.20 Compressive strength of PURFs catalyzed by different metal
complexes at NCO index of 100 (a) DMCHA (ref); (b) Ni(en)$_2$;
(c) Ni(en)$_2$(sal)$_2$; (d) Ni(trien); (e) Ni(trien)(sal)$_2$; (f) Co(en)$_2$; (g)
Co(en)$_2$(sal)$_2$; (h) Co(trien); (i) Co(trien)(sal)$_2$
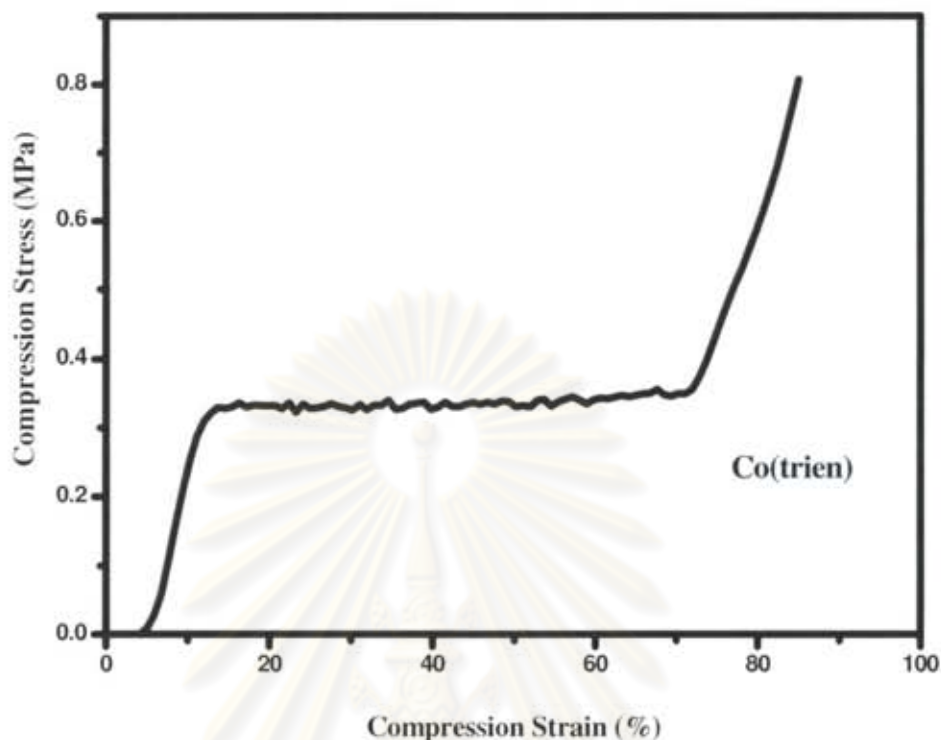
Figure 4.21 Compressive strength of PURF catalyzed by Co(trien) at NCO index of
150

The compression curves showed three stages of deformation; initial linear
behavior, linear plateau region and densification in the final stage. The initial slope
was used to calculate the compressive modulus of foam and intersection point
between the initial slope and plateau slope was used to calculate the compressive
strength [25]. It was observed that slope of the initial linear part are the same for all
PURFs. All PURFs had the same compressive modulus. The shape of plateau region
depends on the morphology of cell in PURFs foam. For linear plateau, cell
deformation occurs as combination of cell bending and collapse.

4.2.4 The temperature profile of rigid polyurethane foams

The reaction between polymeric MDI and polyol is exothermic reaction that
gives a rapid increase in both the temperature and the viscosity of the mixtures [26].
The maximum foaming temperatures of PURFs catalyzed by transition metal

complexes at NCO indexes of 100 and 150 showed high temperatures and were in the range 114-126 $^{\circ}$C and 118-125 $^{\circ}$C, respectively (Table 4.5). Figure 4.22-4.23 shows the relationship between the temperature profile and the reaction time, namely cream time, gel time, and tack-free time that tack-free time showed maximum temperature. The maximum core temperature of almost PURFs decreased with increasing the NCO index, except for Ni(trien)(sal)$_2$ and Co(en)$_2$, which the maximum core temperature increased with increasing the NCO index. PURFs catalyzed by Co(trien)(sal)$_2$ and Ni(trien)(sal)$_2$ showed the highest maximum temperature at NCO index of 100 and 150, respectively. In comparison between DMCHA and metal complexes catalysts, it was found that foams catalyzed by metal complexes showed higher maximum core temperature than foams catalyzed by DMCHA. This result indicated that the reaction between isocyanate groups and hydroxyl groups (gelling reaction) of PURFs catalyzed by metal complexes was better than that catalyzed by DMCHA.

Table 4.5 Maximum core temperature in the preparation of rigid polyurethane foams

Catalysts	Maximum Core Temperature ($^{\circ}$C)	
	NCO Index	
	100	150
DMCHA (ref)	109	108
Ni(en)$_2$	126	123
Ni(en)$_2$(sal)$_2$	121	118
Ni(trien)	124	124
Ni(trien)(sal)$_2$	121	126
Co(en)$_2$	114	127
Co(en)$_2$(sal)$_2$	121	123
Co(trien)	121	122
Co(trien)(sal)$_2$	128	123
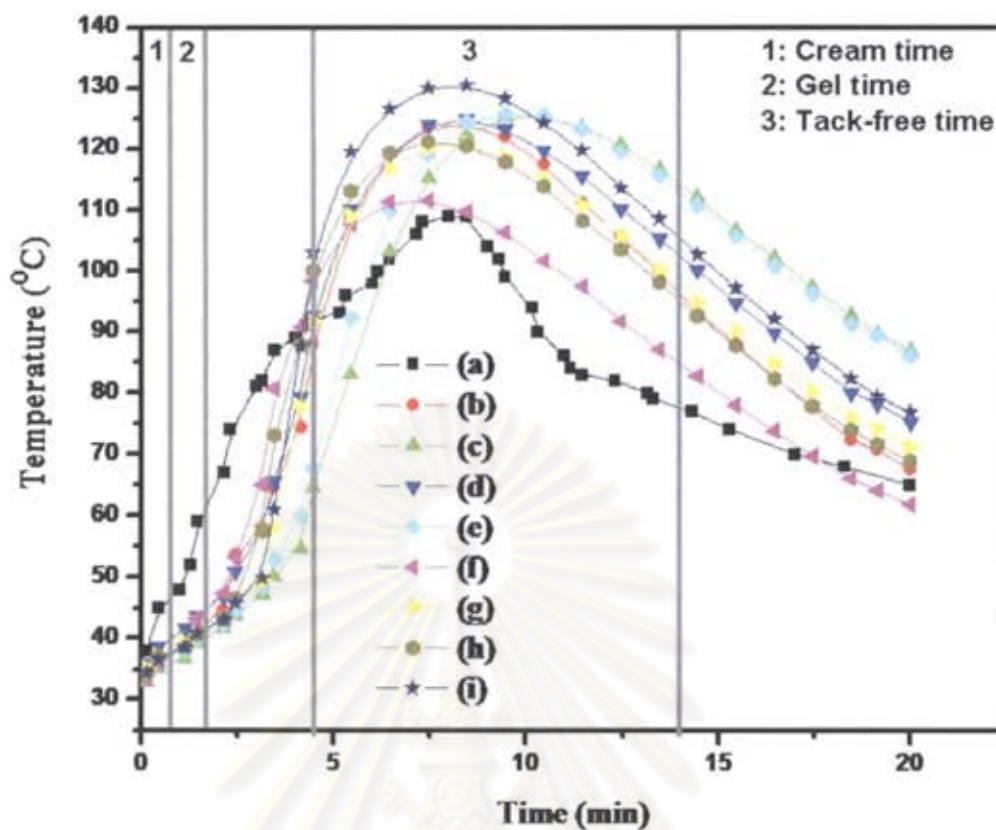
Figure 4.22 Core temperature profiles of PURFs catalyzed by different metal complexes synthesized at NCO index of 100 (a) DMCHA (ref); (b) Ni(en)$_2$; (c) Ni(en)$_2$(sal)$_2$; (d) Ni(trien); (e) Ni(trien)(sal)$_2$; (f) Co(en)$_2$; (g) Co(en)$_2$(sal)$_2$; (h) Co(trien); (i) Co(trien)(sal)
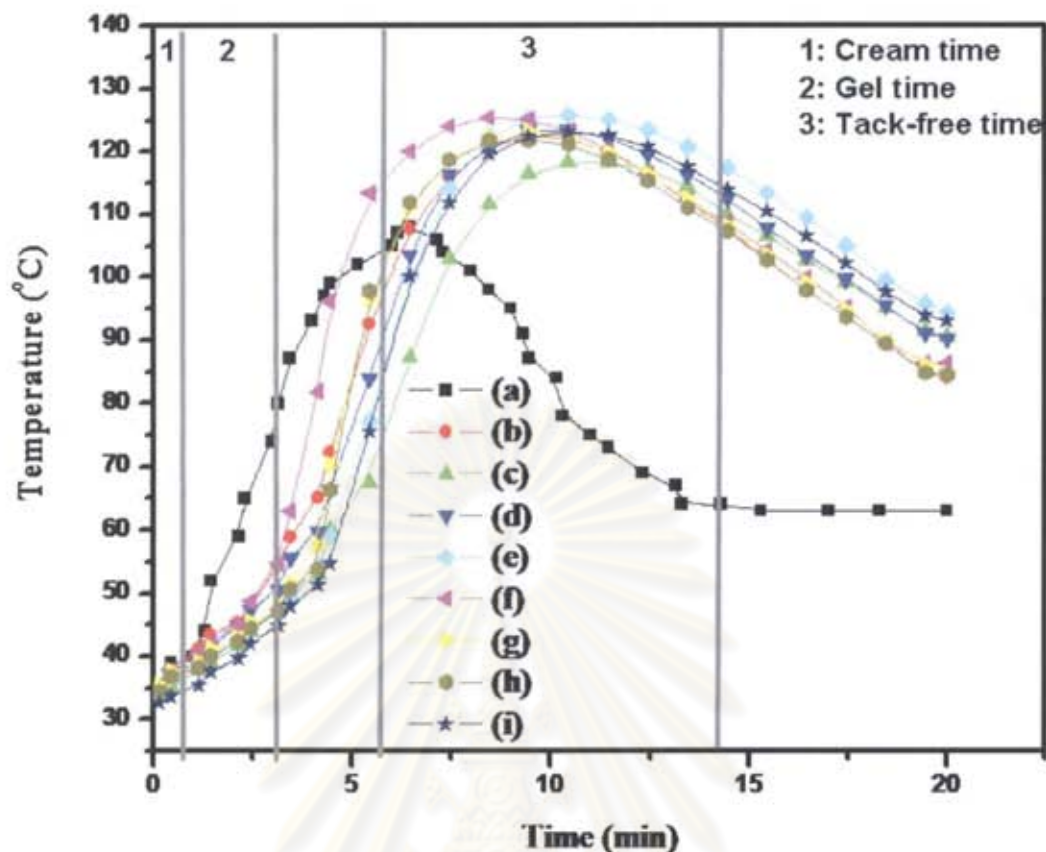
Figure 4.23 Core temperature profiles of PURFs catalyzed by different metal
complexes synthesized at NCO index of 150 (a) DMCHA (ref); (b)
Ni(en)$_2$; (c) Ni(en)$_2$(sal)$_2$; (d) Ni(trien); (e) Ni(trien)(sal)$_2$; (f) Co(en)$_2$; (g)
Co(en)$_2$(sal)$_2$; (h) Co(trien); (i) Co(trien)(sal)
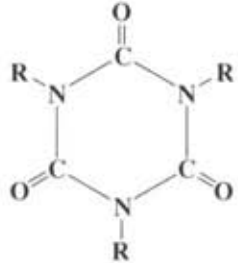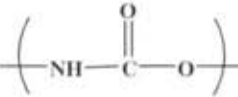
4.2.5 Isocyanate conversions of rigid polyurethane foams

The calculation of NCO conversion referred to IR spectra of polyurethane
catalyzed by transition metal complexes, M(en)$_2$, M(en)$_2$(sal)$_2$, M(trien) and
M(trien)(sal)$_2$ (where M = Ni and Co).

All PURFs catalyzed by metal complexes at NCO index of 100 and 150
showed similar IR spectra. The important absorption bands used to calculate
isocyanate conversion are free NCO (isocyanate stretching band) observed at 2269
cm^{-1}, phenyl group as a reference group 1595 cm^{-1}, the C-N stretching band of
isocyanurate ring at 1406-1420 cm^{-1}, which directly indicates the potency of the

catalysts to result in high trimer conversion, and urethane C-O stretching at 1216-1238 cm^{-1}.

Table 4.6 Wavenumber of PURFs used in calculation [21]

Functional groups	Wavenumber (cm^{-1})	Chemical structure
Isocyanate	2277	N=C=O
Phenyl	1595	Ar-H
Isocyanurate (PIR)	1415	
Urethane (PUR)	1220	

The NCO conversion is defined as the ratio between isocyanate peak area at time t and isocyanate peak area at time 0 as shown in following equation [27]:

$$\text{Isocyanate conversion } (\%) = \left[1 - \frac{\text{NCO}^f}{\text{NCO}^i} \right] \times 100$$

where;

NCO^f is the area of isocyanate absorbance peak area at time t

NCO^i is the area of isocyanate absorbance peak area at initial time 0

Quantity of free NCO in RPUR foams were normalized by aromatic ring absorption band at 1595 cm^{-1}.

IR spectra of PURFs catalyzed by DMCHA and Co(trien) at NCO index of 100 are shown in Figure 4.24.
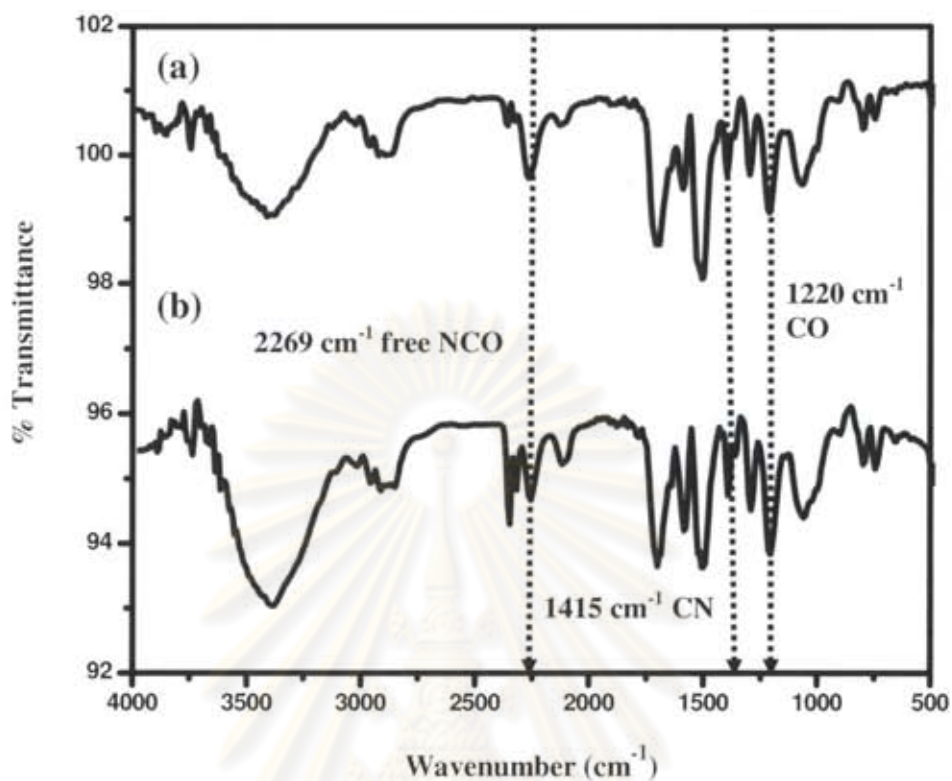
Figure 4.24 IR spectra of PURFs catalyzed by (a) Co(trien); (b) DMCHA at NCO index of 100

NCO conversion of PURFs could be quantitatively determined by IR spectroscopy following method described in the literature [27] as shown in Table 4.7 and Figure 4.25.

Table 4.7 NCO conversion of PURFs catalyzed by transition metal complexes

PURFs catalyzed by	% NCO Conversion		PIR/PUR	
	Index 100	Index 150	Index 100	index 150
DMCHA	99	98	0.21	0.20
Ni(en)$_2$	97	96	0.19	0.62
Ni(en)$_2$(sal)$_2$	97	96	0.21	0.21
Ni(trien)	99	98	0.18	0.27
Ni(trien)(sal)$_2$	99	98	0.17	0.18
Co(en)$_2$	99	97	0.19	0.29
Co(en)$_2$(sal)$_2$	99	97	0.17	0.18
Co(trien)	98	97	0.22	0.31
Co(trien)(sal)$_2$	99	88	0.17	0.43

The results obtained that NCO conversion decreased with increasing of the content of NCO indexes due to the excess amount of isocyanate in polymerization reaction. The access isocyanate could not undergo trimerization to give isocyanurate group since metal complex catalysts were not specific towards the isocyanurate formation. The NCO conversion was in the range 88-99%. The ratio of polyisocyanurate/polyurethane (PIR/PUR) in PURFs is shown in Figure 4.26. The results revealed that PIR/PUR ratio increased at the higher isocyanate index.

ศูนย์วิทยทรัพยากร
จุฬาลงกรณ์มหาวิทยาลัย
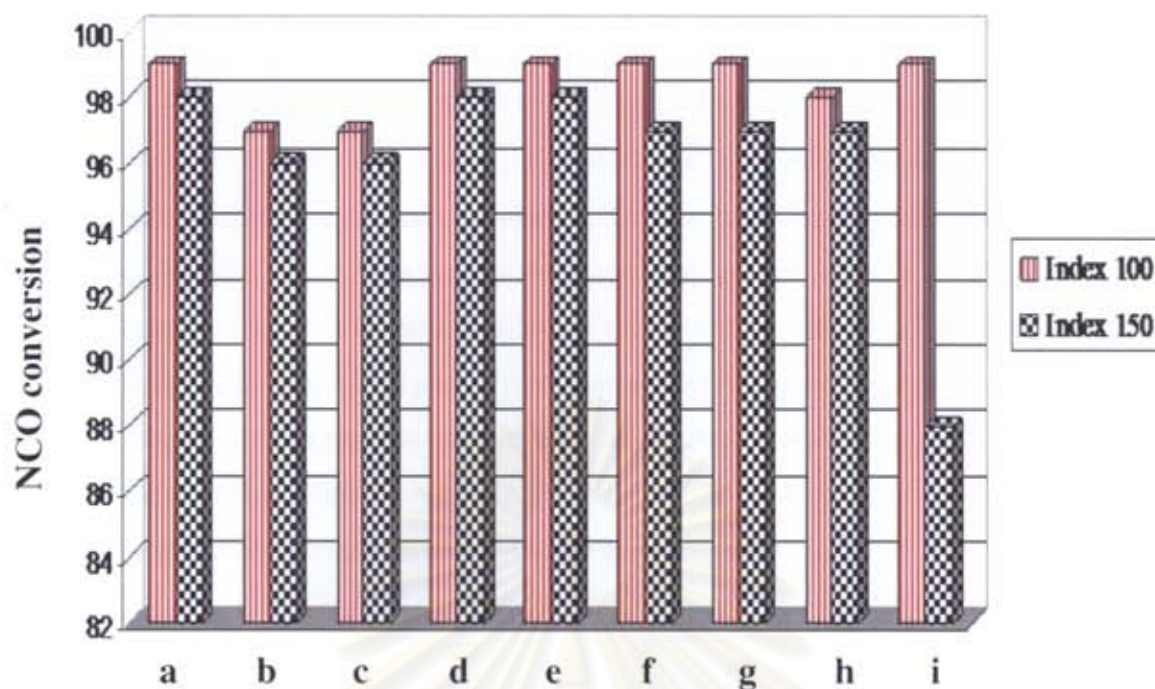
Figure 4.25 NCO conversions of PURFs catalyzed by different metal
complexes (a) DMCHA (ref); (b) Ni(en)$_2$; (c) Ni(en)$_2$(sal)$_2$; (d) Ni(trien);
(e) Ni(trien)(sal)$_2$; (f) Co(en)$_2$; (g) Co(en)$_2$(sal)$_2$; (h) Co(trien); (i)
Co(trien)(sal)$_2$
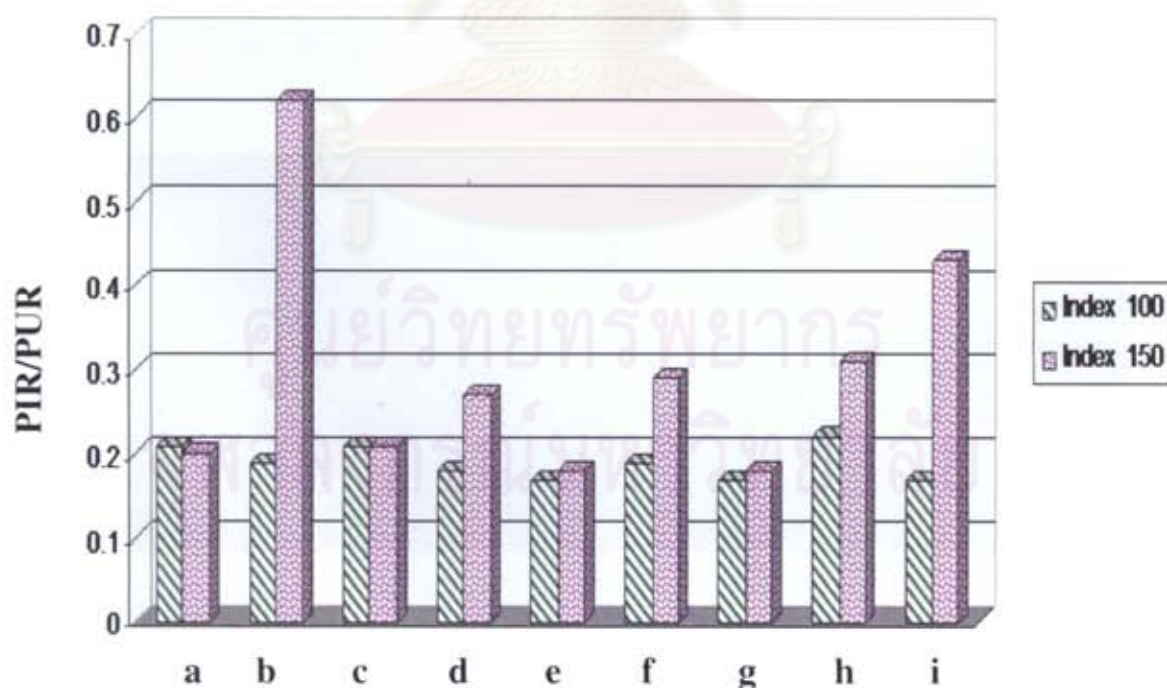
Figure 4.26 PIR/PUR of PURFs catalyzed by different metal
complexes (a) DMCHA (ref); (b) Ni(en)$_2$; (c) Ni(en)$_2$(sal)$_2$; (d) Ni(trien);
(e) Ni(trien)(sal)$_2$; (f) Co(en)$_2$; (g) Co(en)$_2$(sal)$_2$; (h) Co(trien); (i)
Co(trien)(sal)$_2$

From these results, PIR/PUR of all PURFs slightly increased with increasing NCO index. Therefore, this result indicated that the metal complexes were not good catalyst for polyisocyanurate formation. On the other hand, these metal complexes could catalyze gelling reaction to form urethane groups. PURFs catalyzed by nickel and cobalt complexes showed similar NCO conversion and PIR/PUR ratio. It could be concluded that both nickel and cobalt complexes were good catalysts for polyurethane formation and blowing reaction but were unsuitable catalyst for trimerization reaction. The catalytic behavior was the same as that of DMCHA, which is a suitable catalysts for polyurethane formation and blowing reaction.

Morphology of PURFs catalyzed by Co(en)$_2$ in parallel and perpendicular direction of foam rising is shown in Figure 4.27. It was found that cell morphology showed spherical cell. SEM micrographs shown in Figures 4.27 and 4.28 show that both PURFs prepared from Co(en)$_2$ and Ni(en)$_2$ catalysts had closed cell like to DMCHA as shown in Figure 4.29. PURFs catalyzed by Ni(en)$_2$ showed poor external appearance when analyzed by SEM which indicted that cell size was not uniform although Ni(en)$_2$ had good catalytic activity.
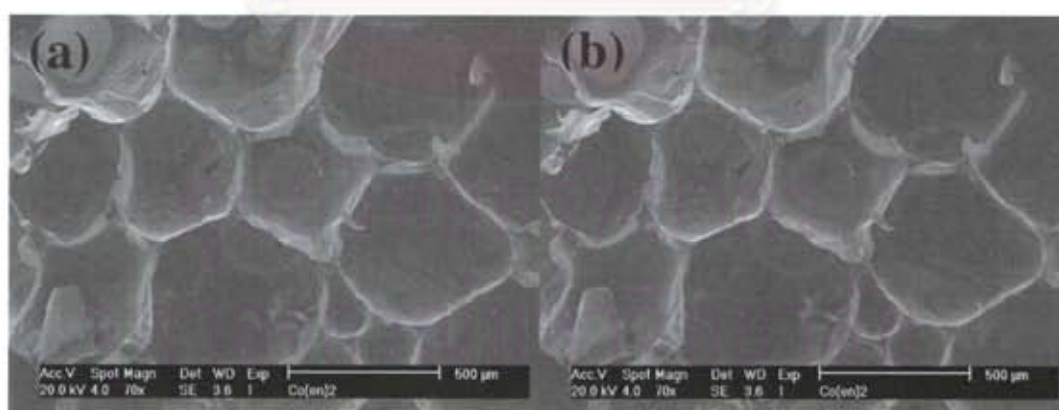
Figure 4.27 SEM of PURFs catalyzed by Co(en)$_2$; (a) top view; (b) side view (70x)
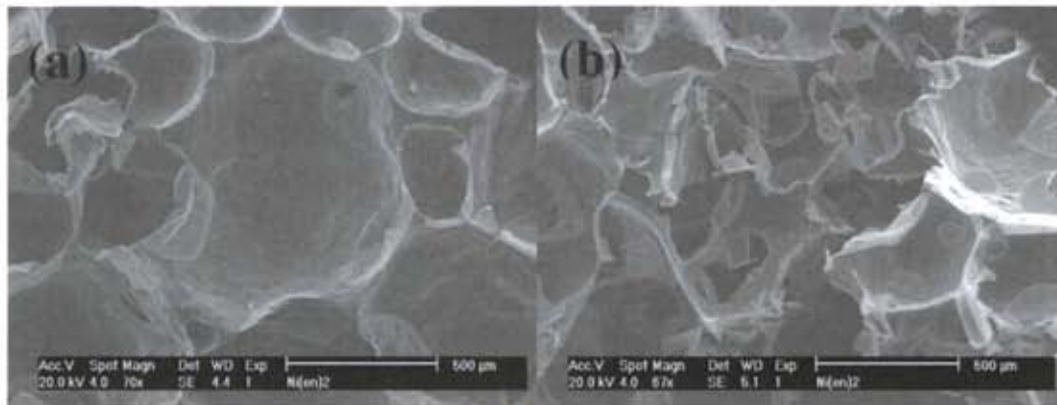
Figure 4.28 SEM of PURFs catalyzed by Ni(en)$_2$; (a) top view; (b) side view (70x)
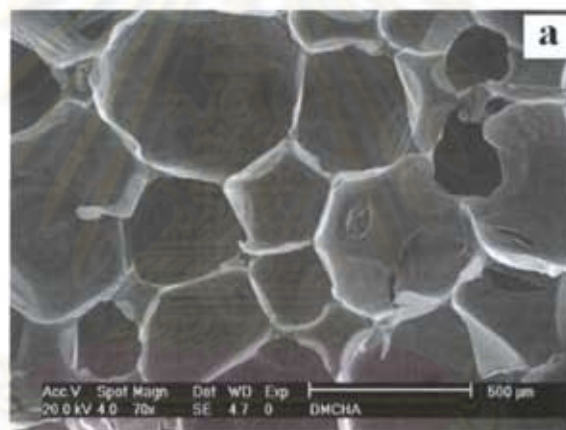
Figure 4.29 SEM of PURFs catalyzed by DMCHA (70x)

In the comparison of PURFs cell size between those prepared from DMCHA, Ni(en)$_2$ and Co(en)$_2$, DMCHA gave PURF with smaller cell size and more uniform cell than those prepared from Ni(en)$_2$ and Co(en)$_2$. Since the smaller PURFs cell size gave more strength to the PURFs [28], the PURF catalyzed by DMCHA had higher compressive strength than those catalyzed by Ni(en)$_2$ and Co(en)$_2$.

4.2.6 Thermal stability

Thermal stability of PURFs catalyzed by Ni(en)$_2$, Co(en)$_2$, and DMCHA (ref.) at NCO index of 150 were investigated by thermogravimetric analysis under nitrogen atmosphere (Figure 4.30). TGA thermograms of all PURFs showed the decomposition of foams in one step. The initial composition temperature (IDT), which is the temperature at 5% weight loss was found in the range 267-285 ^{o}C. The residual weights at 600°C were in the range 38-42%. PURFs catalyzed by Ni(en)$_2$, Co(en)$_2$, and DMCHA showed their maximum decomposition temperature (Tmax) values in the range 331-337°C. The foams prepared from Ni(en)$_2$ and Co(en)$_2$ showed similar thermal decomposition with that prepared from DMCHA catalyst. This indicated that the Ni(en)$_2$ and Co(en)$_2$ showed similar catalytic reaction with that of DMCHA.
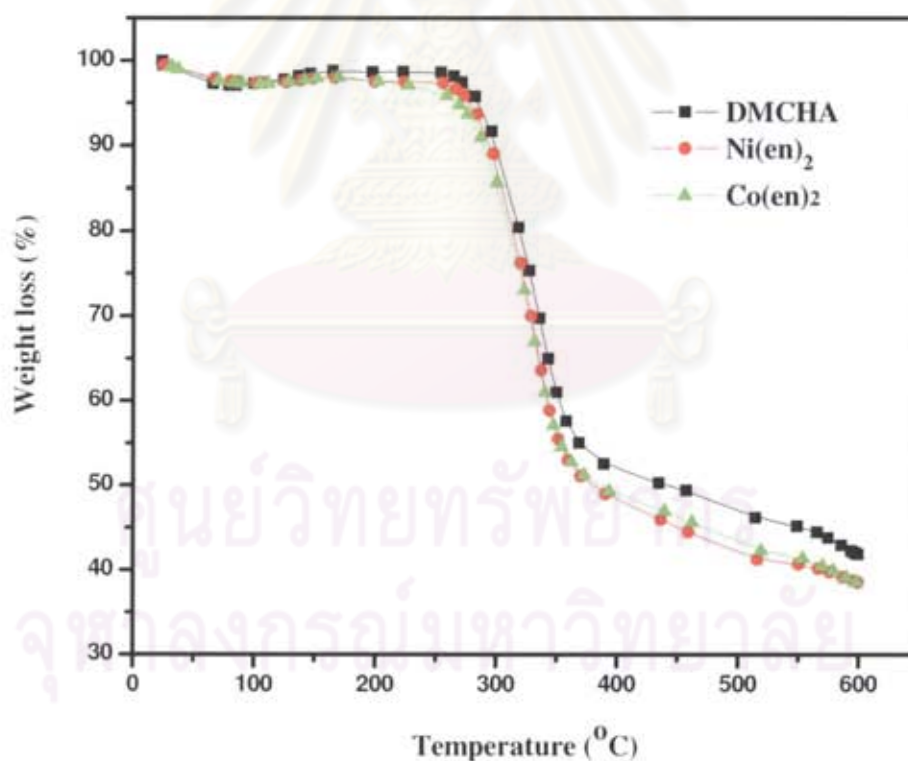
Figure 4.30 TGA thermograms of PURFs catalyzed by (a) DMCHA (ref.);
(b) Ni(en)$_2$; (c) Co(en)$_2$ at the NCO index of 150

4.2.7 Thermal conductivity

Thermal conductivity is the ability to transmit heat through the foam matrix. Thermal conductivity of PURFs catalyzed by DMCHA, Co(trien) and Co(en)$_2$ were investigated by thermal constant analysis (TCA) at room temperature (Table 4.8). Thermal conductivity of foams is usually controlled by its density. Thermal conductivity of foams increases as the density decreases [29]. This is because of the higher proportion of gas in the foam and therefore radiant heat transfer is the dominant heat transfer process. As the foam density increases, the heat transfer become increasingly governed by conduction through the solid component of the foam.

The results in Table 4.8 showed that PURFs catalyzed by Co(trien) and Co(en)$_2$ gave thermal conductivity similar to that of DMCHA.

Table 4.8 Thermal conductivity of PURFs

Catalysts	NCO index	Density (kg/m^3)	Thermal conductivity (W/m K)
Co(trien)	100	39.6	0.0391
Co(en)$_2$	150	47.1	0.0386
DMCHA	150	50.3	0.0377

Thermal conductivity of PURFs related to cell size [30]. It was found that small cell size had lower thermal conductivity. The smaller cell size improved the thermal insulation property of the PURFs.

For comparison, PURFs were prepared by use of metal acetates, amines and salicylic acid as catalysts. It was found that the polymerization reaction was slow and the PURFs had poor appearance as shown in Figures 4.31.

Non-catalyst $Ni(OAc)_2$ $Co(OAc)_2$

en   trien   Salicylic acid
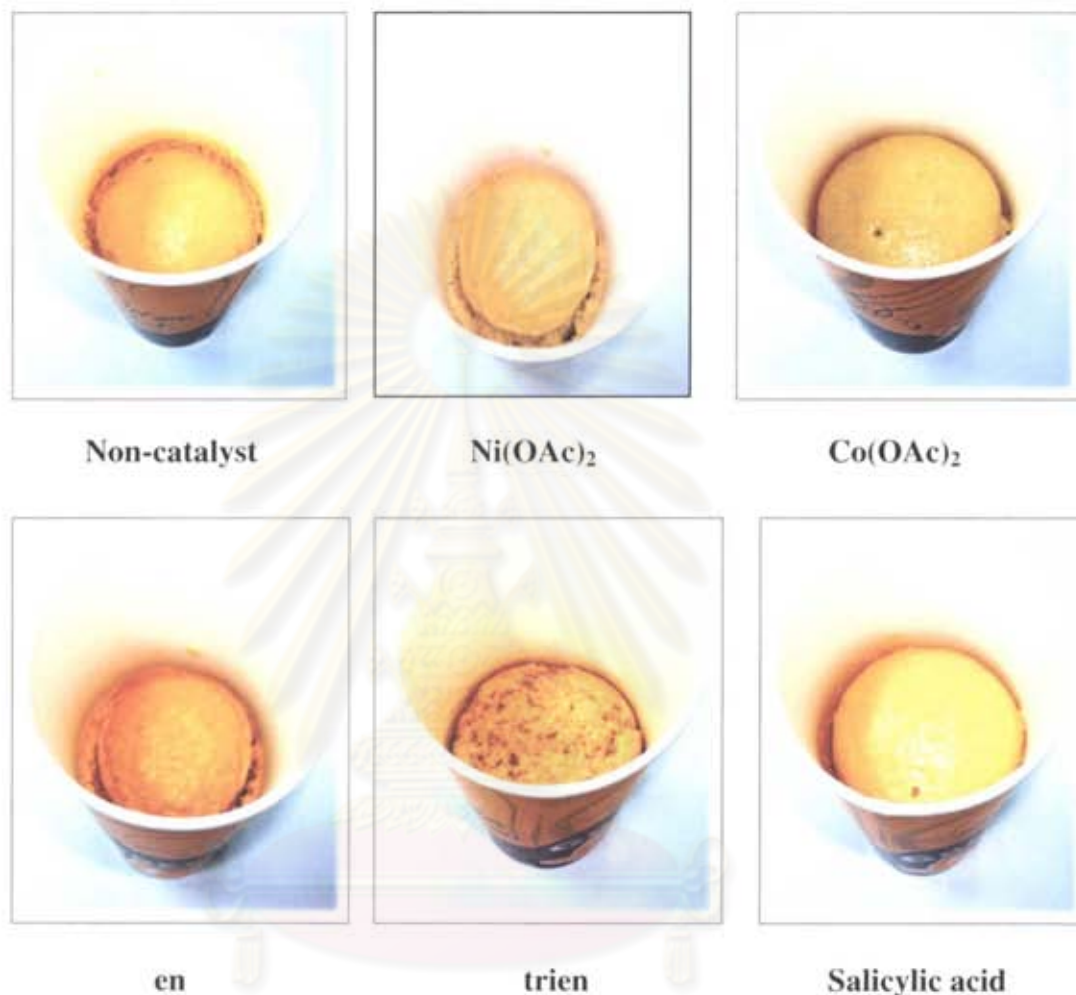
Figure 4.31 External appearance of PURFs catalyzed by metal acetates, amines and
salicylic acid

CHAPTER V
CONCLUSION

5.1 Conclusion

Transition metal complexes, namely $M(en)_2$, $M(en)_2(sal)_2$, $M(trien)$ and $M(trien)(sal)_2$ (M = Ni and Co) were synthesized and used as catalysts for the preparation of rigid polyurethane foams. All metal complexes were synthesized by use of acetone as a solvent. Metal complexes were characterized by IR and UV-vis spectroscopy. IR spectra of nickel and cobalt complexes showed different absorption bands from those in metal acetate starting materials. UV spectra also showed that the maximum wavelength of both nickel and cobalt complexes shifted from that of metal acetate. This indicated metal complexes between metal acetate, amines (ethylenediamine and triethylenetetramine) and salicylic acid were formed.

Rigid polyurethane foams (PURFs) were prepared by two short method (Scheme 3.5). $Ni(en)_2$ was a good catalyst for gelling reaction since PURFs catalyzed by $Ni(en)_2$ had short reaction time. However, $Ni(en)_2$ was a poor catalyst for blowing reaction, which is the reaction between isocyanate and water (blowing agent) to give CO_2. Therefore, the foam catalyzed by $Ni(en)_2$ had less volume than those prepared using other metal complex catalysts and the foam external appearance was not good. Form the reaction times, cobalt complexes, especially $Co(en)_2$, showed better catalytic activity than nickel complexes. DMCHA showed better catalytic activity than metal complexes catalysts. $M(en)_2(sal)_2$ and $M(trien)(sal)_2$ showed longer reaction time than $M(en)_2$ and $M(trien)$ because of the steric effect. The reaction time, especially blowing reaction of PURFs, had an effect on the foam density. $Ni(en)_2$ gave the foams with higher density than those catalyzed by other catalysts. Density of PURFs catalyzed by different metal complexes was in the range 42.3-73.9 kg/m^3. The results showed that all metal complexes, except $Ni(en)_2$, gave PURFs with suitable density. Compressive strength of PURFs was in the range 0.13-0.25 MPa. Compressive strength increased with increasing density of PURFs.

The polymerization was an exothermic reaction. The maximum core temperature of PURFs were in the range of 114-125°C. The maximum core temperature of most PURFs decreased with increasing the NCO index. In comparison

between DMCHA and metal complexes catalysts, it was found that foams catalyzed by metal complexes showed higher maximum core temperature than those catalyzed by DMCHA. This result indicated that the reaction between isocyanate groups and hydroxyl groups (gelling reaction) of PURFs catalyzed by metal complexes was better than that catalyzed by DMCHA.

IR spectra of all PURFs showed similar characteristic absorption band. IR spectroscopy was used to determine the NCO conversion and polyisocyanurate/polyurethane (PIR/PUR) ratio. The results indicated that NCO conversion decreased with increasing of the content of NCO indexes. PIR/PUR ratio slightly increased with increasing of NCO content in foam formulations. Thus, the metal complexes could not catalyze the trimerization formation. SEM micrographs of PURFs catalyzed by Ni(en)$_2$, Co(en)$_2$ and DMCHA showed that the foams had closed cell structure which was the property of rigid foams. TGA thermograms of PURFs showed the decomposition of foams in one step. The foams prepared from Ni(en)$_2$ and Co(en)$_2$ showed similar thermal decomposition with that prepared from DMCHA catalyst. This indicated that the catalytic reaction of Ni(en)$_2$ and Co(en)$_2$ was similar catalytic to that of DMCHA. Thermal conductivity of PURFs increased as the density decreased. PURFs catalyzed by Co(trien) and Co(en)$_2$ gave thermal conductivity similar to that of DMCHA.

5.2 Suggestion for future work

The advantage of Ni and Co complexes as catalysts for rigid polyurethane foam preparation is their catalytic activities are similar to the reference catalyst, DMCHA. Although Ni(en)$_2$ had bad external appearance but it gave shorter reaction time than Co(en)$_2$ while Co(en)$_2$ gave better external appearance than Ni(en)$_2$. The suggestion for future work is to synthesize the catalyst mixture between nickel and cobalt complexes to improve the catalytic activity and blowing reaction of nickel-based catalyst.

Table 5.1 Summary of data in PURFs preparations

Parameters	Conclusion				
Reaction times	**Ni complexes**				
	Ni(en)$_2$	Ni(trien)	Ni(en)$_2$(sal)$_2$	Ni(trien)(sal)$_2$	DMCHA
Cream time (sec)	5.0	7.0	6.0	6.0	2.0
Gel time (min)	0.2	1.2	1.2	1.7	0.1
Tack-free time (min)	**5.4**	**12.5**	**13.1**	**11.5**	**4.4**
Rise time (min)	4.5	8.1	7.4	7.3	3.4
	Co complexes				
	Co(en)$_2$	Co(trien)	Co(en)$_2$(sal)$_2$	Co(trien)(sal)$_2$	DMCHA
Cream time (sec)	6.0	6.0	7.0	6.0	2.0
Gel time (min)	0.9	1.75	1	1.8	0.1
Tack-free time (min)	**6.3**	**8.1**	**8.2**	**8.4**	**4.4**
Rise time (min)	6.2	6	4.5	7.3	3.4
Catalytic activity	Co complexes > Ni complexes				
	DMCHA > all metal complexes				
Catalytic reaction	Blowing and gelling reaction				
Polymerization temperature	114-125°C				
Density (kg/m^3)	**NCO index = 100**		**NCO index = 150**		
	42.3-62.2		49.7-73.9		
Compressive strength (MPa)	Ni(trien)(sal)$_2$ > DMCHA				
	NCO index = 100		**NCO index = 150**		
Ni(trien)sal$_2$	0.23		-		
DMCHA	0.19		0.32		

REFERENCES

[1] D. Klempner.; K.C. Frich. *Handbook of polymeric foams and foam technology.* New York: Oxford University Press, 1991.

[2] R. Herrington.; K. Hock. *Flexible polyurethane foams.* United State of America: The Dow Chemical, 1991.

[3] Pentrakoon, D.; Ellis, J.W. *An introduction to plastic foams.* Chulalongkorn University Press, 2005.

[4] N.C. Hilyard.; A. Cunningham. *Low density cellular plastics: physical basis of behavior.* London: 1994.

[5] ASTM D 3576-98 Standard test method for cell size of rigid cellular plastic.

[6] G.L.A. Sims.; C. Khunniteekool. *J.Cell. Polym.* 13(1994): 137-146.

[7] ASTM D 2856-94 (1988) Standard test method for open-cell content of rigid cellular plastics by the air pycnometer.

[8] R.L. Sandridge.; P.G. Gemeinhardt.; R.H. Sauders. American Chemical Society Meeting. Chicago: 1961.

[9] BS 4443: Part 6: Methods of test or flexible cellular materials: Determination of air flow value. British Standard Institute, 1991.

[10] ASTM D2842-1 Standard test method for water absorption of rigid cellular plastics.

[11] BS 4334: Part 1: Method of test for flexible cellular materials: Determination of apparent density. British Standard Institute, 1988.

[12] ASTM D1621-04 Standard test method for compressive properties of rigid cellular plastics.

[13] Sh. I. Inoue.; Y. Nagai.; H. Okamoto. Amine-manganese complexes as a efficient catalyst for polyurethane syntheses. *Polym. J.* 34 (2002): 298-301.

[14] R. V. Maris.; Y. Tamano.; H. Yoshimura.; K. Gay. Polyurethane catalysis by tertiary amines. *J. Cell. Plast.* 41 (2005): 305-322.

[15] S. Murayama.; K. Fukuda.; T. Kimura.; T. Sasahara. Water-blown polyurethane rigid foam modified with maleate. *J. Cell. Plast.* 41 (2005): 373-378.

[16] A. Strachota.; B. Strachotova.; M. Spirkova. Comparison of environmentally friendly, selective polyurethane catalysts. *Mater. Manuf. Process.* 23 (2008): 566-570.

[17] H. Sardon.; L. Irusta.; M.J. Fernández-Berridi. Synthesis of isophorone diisocyanate (IPDI) based waterborne polyurethanes: Comparison between zirconium and tin catalysts in the polymerization process. *Prog. Org. Coat.* 66 (2009): 291–295.

[18] S. Okuzono.; K. Tokumoto.; Y. Tamano.; D. W. Lowe. New Polyisocya-nurate catalysts which exhibit high activity at low temperature. *J. Cell. Plast.* 37 (2001): 72-89.

[19] A. V. Kurnoskin. Metalliferous epoxy chelate polymers: 1. synthesis and properties. *Polymer. J.* 34 (1993): 1060-1067.

[20] M. Modesti.; A. Lorenzetti.; F. Simioni.; M. Checchin. Thermal stable hybrid foams based on cyclophosphazene and polyrethanes. *Polym. Degrad. Stabil.* 87 (2005): 287-292.

[21] M. Modesti.; A. Lorenzetti.; F. Simioni.; M. Checchin. An experimental method for evaluating isocyanate conversion and trimer formation in polyisocyanurate-polyurethane foams. *Eur. Polym. J.* 37 (2001): 949-954.

[22] H. Landrock. *Handbook of plastic foams.* USA: Noyes, 1995.

[23] D. Randall.; S. Lee. *The polyurethane book.* London: Jonh Wiley & Sons, 2002.

[24] M. C. Saha.; M. E. Kabir.; S. Jeelani. Enhancement in thermal and mechanical properties of polyurethane foam infused with nanoparticles, *Mat. Sci. Eng.* 479 (2008): 213–222.

[25] S. Jones.; K. W. Scott.; B. G. Willoughby.; E. A. Sheard. Monitoring of polyurethane foam cure. *J. Cell. Plast.* 38 (2002): 285-299.

[26] G. Oertel. *Polyurethane handbook.* New York: Hanser, 1985.

[27] G. Wood. *The ICI polyurethane book.* 2nd Edition. London: Jonh Wiley & Sons, 1990.

[28] M. C. Hawkins.; B. O'Toole.; D. Jackovich. Cell morphology and mechanical properties of rigid polyurethane foam. *J. Cell. Plast.* 41 (2005): 267-285.

[29] M. Thirumal.; D. Khastgir.; N. K. Singha.; B. S. Manjunath. Effect of a Nanoclay on theMechanical, Thermal and Flame Retardant Properties of Rigid Polyurethane Foam. *J.Macrom. Sci.* 46 (2009): 704-712.

[30] H. Lim.; S. H. Kim.; B. K. Kim. Effects of silicone surfactant in rigid polyurethane foams. *Express. Polym. Lett.* 2 (2008): 194-200.

APPENDICES

Appendix A
NCO index and NCO conversion Calculations

NCO index calculation

#Example Calculate the parts by weight (pbw) of pure PMDI (MR-200), molar mass = 365.8, functionality = 2.7 at an isocyanate indexes of 80, 100, 120, 140, 150, 160 and 200 required to react with the following formulation:

Table A1 Formulation of PURFs

Formulation (pbw)	Part by weight (g)
Raypol® 4221 (OHV = 440 mgKOH/ g, functionality = 4.3)	100.0
Catalysts	1.0
Surfactant	2.5
Blowing agent (water, M_w = 18 g/mole, functionality = 2)	4.0
PMDI (MR-200), NCO indexes of 80, 100, 120, 140, 150, 160 and 200	???

$$\text{Hydroxyl value} = \frac{56.1 \times \text{functionality} \times 1000}{\text{Molar mass}} = \frac{56.1 \times 1000}{\text{Equivalentweight}}$$

$$\text{Equivalent weight} = \frac{\text{Molar mass}}{\text{functionality}}$$

$$\text{Equivalent weight of raypol 4221} = \frac{56.1}{440} \times 1000 = 127.5$$

$$\text{Equivalent weight of water} = \frac{18}{2} = 9.0$$

Note: Surfactants and catalysts are neglected in stoichiometric calculations because they do not react with NCO groups.

$$\text{Number of equivalent in formulation} = \frac{\text{parts by weight (pbw.)}}{\text{equivalent weight}}$$

Equivalent in the above formulation:

$$\text{Polyol (Raypol 4221)} = \frac{100}{127.5} = 0.784$$

$$\text{Water (blowing agent)} = \frac{4.0}{9.0} = 0.444$$

$$\text{Total equivalent weight} = 1.228$$

For stoichiometric equivalence, PMDI pbw is total equivalent x equivalent weight because PMDI reacts with polyol and water.

thus:

$$\text{PMDI (pbw)} = 1.228 \text{ x } \frac{\text{PMDI molar mass}}{\text{functionality}} = 1.228 \text{ x } \frac{365.8}{2.7} = 166.37$$

Note: 166.37 defines the isocyanate quantity at 100 index

where;

$$\text{Isocyanate index} = \frac{\text{actual amount of isocyanate}}{\text{theoretical amount of isocyanate}} \text{ x } 100$$

thus:

Isocyanate index = 80;

$$\text{Isocyanate actual} = \frac{166.37}{100} \text{x } 80 = 133 \text{ pbw}$$

Isocyanate index = 100;

$$\text{Isocyanate actual} = \frac{166.37}{100} \text{x } 100 = 166.37 \text{ pbw}$$

Isocyanate index = 120;

$$\text{Isocyanate actual} = \frac{166.37}{100} \text{x } 120 = 200 \text{ pbw}$$

Isocyanate index = 140;

$$\text{Isocyanate actual} = \frac{166.37}{100} \text{x } 140 = 233 \text{ pbw}$$

Isocyanate index = 150;

$$\text{Isocyanate actual} \quad = \frac{166.37}{100} \times 150 = 249.5 \text{ pbw}$$

Isocyanate index = 160;

$$\text{Isocyanate actual} \quad = \frac{166.37}{100} \times 160 = 266 \text{ pbw}$$

Isocyanate index = 200;

$$\text{Isocyanate actual} \quad = \frac{166.37}{100} \times 200 = 333 \text{ pbw}$$

NCO conversion calculation

The NCO conversion can be calculated by FTIR method, defined as the ratio between isocyanate peak area at time t and isocyanate peak area at time 0, following equation:

$$\text{Isocyanate conversion (\%)} = \left[1 - \frac{NCO^f}{NCO^i} \right] \times 100$$

where;

NCO^f is the area of isocyanate absorbance peak area at time t

NCO^i is the area of isocyanate absorbance peak area at time 0

Quantity of free NCO in RPUR foams were normalized by aromatic ring absorption band at 1595 cm^{-1}.

Table A2 Free NCO absorbance peak area in PMDI (MR-200) from ATR-IR

PMDI (MR-200) spectra	NCO Absorbance peak area Normalized @ 1.0 Ar-H peak area
1	79.378
2	81.635
3	78.262
4	79.499
5	79.491
Average (NCO^i); ATR-IR	79.65
NCO^i (FTIR)	98.0

 # _Example_ Calculate the conversion of isocyanate (α) and PIR/PUR of rigid polyurethane foams catalyzed by DMCHA catalyst at NCO index 150

Conversion of isocyanate (%)

Data at **Table A1**

Absorbance peak area of initial NCO = 98 = NCO^i

The data from **Table A2** at NCO index 100, absorbance peak area of free NCO was normalized by aromatic ring quantity:

Absorbance peak area of final NCO = 0.79195 = NCO^f

thus,

$$\text{Conversion of isocyanate (\%)} = \left[1 - \frac{NCO^f}{NCO^i}\right] \times 100$$

$$= \left[1 - \frac{0.79195}{98}\right] \times 100$$

% NCO conversion = 99.2

PIR/PUR

Absorbance peak area of PIR (polyisocyanurate) = 11.505

Absorbance peak area of PUR (polyurethane) = 55.536

thus, PIR/PUR $= \dfrac{11.505}{55.536} = 0.207$

Table A3 NCO conversion of PURFs catalyzed by DMCHA at different NCO indexes

DMCHA	Peak Area					NCO	
NCO index	NCO 2277 cm^{-1}	Ar-H 1595 cm^{-1}	PIR 1415 cm^{-1}	PUR 1220 cm^{-1}	NCO^f Ar-H=1	conversion (%)	PIR/PUR
100	29.07	36.707	11.505	55.536	0.79195	99.2	0.207
150	44.259	22.363	8.508	42.857	1.97912	98.9	0.199
160	63.65	29.382	12.389	68.298	2.16629	98.0	0.181
200	29.07	36.707	11.505	55.536	0.79195	97.5	0.207

Table A4 NCO conversion of PURFs catalyzed by Ni(en)$_2$ at different NCO indexes

F-Ni(en)$_2$	Peak Area					NCO	
NCO index	NCO 2277 cm^{-1}	Ar-H 1595 cm^{-1}	PIR 1415 cm^{-1}	PUR 1220 cm^{-1}	NCO^f Ar-H=1	conversion (%)	PIR/PUR
80	49.508	22.257	10.835	45.433	2.22438	97.7	0.238
100	50.398	20.846	6.775	35.492	2.41763	97.5	0.191
120	32.838	23.601	8.778	46.239	1.39138	98.6	0.189
140	35.379	13.336	4.563	21.37	2.65289	97.3	0.214
150	30.006	10.262	16.948	27.231	2.92399	97.0	0.622
160	99.434	25.991	10.412	36.964	3.82571	96.1	0.282
200	30.625	22.526	10.348	17.586	1.35954	98.6	0.588

Table A5 NCO conversion of PURFs catalyzed by Ni(en)$_2$(sal)$_2$ at different NCO
indexes

| F-Ni(en)$_2$(sal)$_2$ | Peak Area | | | | | NCO | |
NCO index	NCO 2277 cm^{-1}	Ar-H 1595 cm^{-1}	PIR 1415 cm^{-1}	PUR 1220 cm^{-1}	NCO^f Ar-H=1	conversion (%)	PIR/PUR
80	26.801	31.822	7.878	34.535	0.84222	99.1	0.228
100	65.586	21.396	9.187	43.129	3.06534	96.8	0.213
120	39.176	15.155	6.243	30.231	2.58502	97.4	0.207
140	33.939	8.521	7.667	22.414	3.98298	95.9	0.342
150	51.464	28.010	5.045	23.310	1.83734	98.1	0.216
160	143.702	27.51	10.935	49.15	5.22363	94.7	0.222
200	15.416	18.537	16.746	54.28	0.83163	99.2	0.309

Table A6 NCO conversion of PURFs catalyzed by Ni(trien) at different NCO
indexes

| F-Ni(trien) | Peak Area | | | | | NCO | |
NCO index	NCO 2277 cm^{-1}	Ar-H 1595 cm^{-1}	PIR 1415 cm^{-1}	PUR 1220 cm^{-1}	NCO^f Ar-H=1	conversion (%)	PIR/PUR
80	34.302	21.441	6.889	39.507	1.59983	98.4	0.174
100	24.767	32.089	8.940	50.569	0.77182	99.2	0.177
120	49.355	19.518	10.125	26.157	2.52869	97.4	0.387
140	31.829	3.955	3.673	10.661	8.04779	91.8	0.345
150	36.502	26.771	10.660	38.943	1.36349	98.6	0.274
160	326.717	32.462	12.808	63.051	10.0646	89.7	0.203
200	51.302	25.842	7.095	34.931	1.98522	97.9	0.203

Table A7   NCO conversion of PURFs catalyzed by Ni(trien)(sal)$_2$ at different NCO indexes

F-Ni(trien)(sal)$_2$ NCO index	Peak Area					NCO conversion (%)	PIR/PUR
	NCO 2277 cm^{-1}	Ar-H 1595 cm^{-1}	PIR 1415 cm^{-1}	PUR 1220 cm^{-1}	NCO^f Ar-H=1		
80	6.157	6.068	4.322	14.158	1.01467	98.9	0.305
100	24.747	25.430	5.641	32.957	0.97314	99.0	0.171
120	91.408	32.603	12.475	59.015	2.80367	97.1	0.211
140	12.795	17.342	14.905	68.403	0.7378	99.2	0.218
150	50.001	29.140	5.222	28.228	1.71589	98.2	0.185
160	395.084	29.955	10.685	45.406	13.1893	86.5	0.235
200	105.156	36.684	14.405	61.651	2.86654	97.1	0.234

Table A8   NCO conversion of PURFs catalyzed by Co(en)$_2$ at different NCO indexes

F-Co(en)$_2$ NCO index	Peak Area					NCO conversion (%)	PIR/PUR
	NCO 2277 cm^{-1}	Ar-H 1595 cm^{-1}	PIR 1415 cm^{-1}	PUR 1220 cm^{-1}	NCO^f Ar-H=1		
80	19.147	22.091	7.309	32.754	0.86673	99.1	0.223
100	16.145	19.521	5.265	27.202	0.82706	99.2	0.194
120	56.356	24.472	9.21	47.212	2.30288	97.7	0.195
140	54.867	30.557	5.769	28.471	1.79556	98.2	0.203
150	31.342	14.183	9.472	33.123	2.20983	97.7	0.286
160	339.351	30.066	13.12	67.424	11.2869	88.5	0.195
200	56.894	27.015	7.804	35.549	2.10602	97.9	0.220

Table A9 NCO conversion of PURFs catalyzed by Co(en)$_2$(sal)$_2$ at different NCO indexes

F-Co(en)$_2$(sal)$_2$ NCO index	Peak Area					NCO conversion (%)	PIR/PUR
	NCO 2277 cm^{-1}	Ar-H 1595 cm^{-1}	PIR 1415 cm^{-1}	PUR 1220 cm^{-1}	NCO^f Ar-H=1		
80	37.688	34.645	7.996	36.842	1.08783	98.9	0.217
100	14.346	22.222	6.460	37.717	0.64558	99.3	0.171
120	71.566	22.693	15.233	36.385	3.15366	96.8	0.419
140	37.836	5.329	5.137	19.553	7.10002	92.8	0.263
150	39.473	19.474	4.561	25.535	2.02696	97.9	0.179
160	220.316	26.41	11.12	54.173	8.34214	91.5	0.205
200	198.63	27.87	23.264	53.685	7.12702	92.7	0.433

Table A10 NCO conversion of PURFs catalyzed by Co(trien) at different NCO indexes

F-Co(trien) NCO index	Peak Area					NCO conversion (%)	PIR/PUR
	NCO 2277 cm^{-1}	Ar-H 1595 cm^{-1}	PIR 1415 cm^{-1}	PUR 1220 cm^{-1}	NCO^f Ar-H=1		
80	17.184	1.18	3.863	12.867	14.5627	85.1	0.300
100	42.452	19.676	9.826	43.988	2.15755	97.8	0.223
120	96.499	22.704	9.382	39.57	4.25031	95.7	0.237
140	47.645	31.472	9.085	50.245	1.51389	98.5	0.181
150	19.233	10.830	11.934	38.553	1.7759	98.2	0.310
160	346.69	27.636	10.063	46.309	12.5449	87.2	0.217
200	123.733	36.794	9.088	41.848	3.36286	96.6	0.217

Table A11 NCO conversion of PURFs catalyzed by Co(trien)(sal)$_2$ at different NCO indexes

F-Co(trien)sal$_2$ NCO index	Peak Area					NCO conversion (%)	PIR/PUR
	NCO 2277 cm^{-1}	Ar-H 1595 cm^{-1}	PIR 1415 cm^{-1}	PUR 1220 cm^{-1}	NCO^f Ar-H=1		
80	31.068	19.942	10.52	65.733	1.55792	98.4	0.160
100	25.717	24.015	11.045	65.785	1.07087	98.9	0.168
120	75.892	26.329	9.525	42.743	2.88245	97.1	0.223
140	25.144	11.947	4.586	17.949	2.10463	97.9	0.256
150	81.246	8.662	14.490	33.585	9.37959	90.4	0.431
160	204.151	29.424	9.377	40.048	6.93825	92.9	0.234
200	104.307	29.31	16.772	72.304	3.55875	96.4	0.232

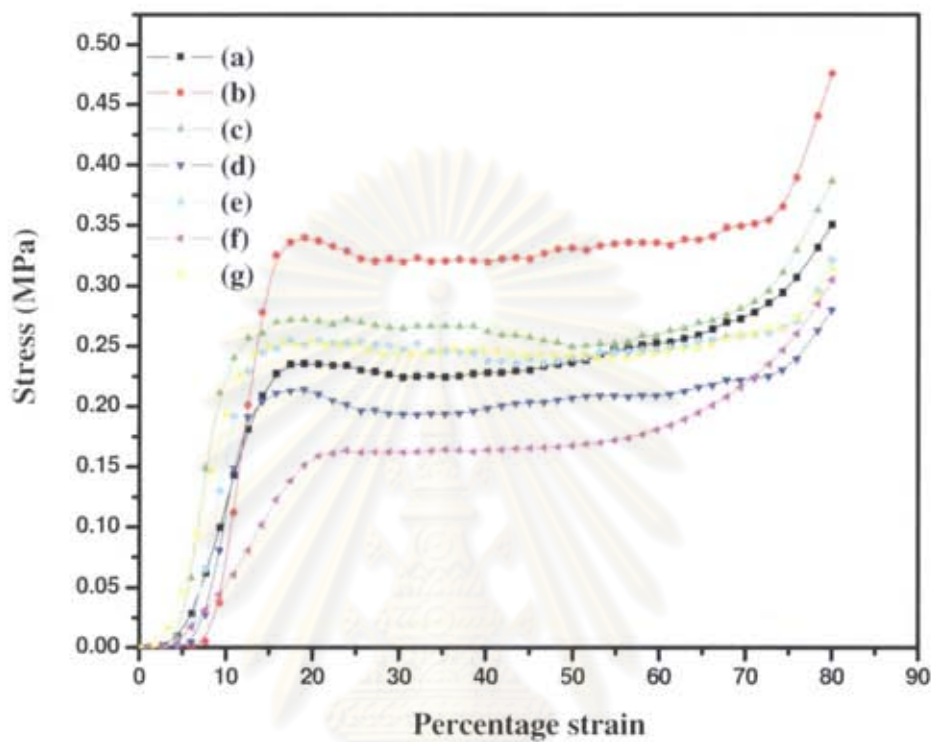# Appendix B

Compressive strength and data

Figure B1 Compression stress-strain curve of PURFs catalyzed by different catalysts at NCO index of 80 (a) $Ni(en)_2(sal)_2$; (b) $Ni(trien)$; (c) $Ni(trien)(sal)_2$; (d) $Co(en)_2$ (e) $Co(en)_2(sal)_2$; (f) $Co(trien)$; (g) $Co(trien)(sal)_2$

ศูนย์วิทยทรัพยากร

จุฬาลงกรณ์มหาวิทยาลัย

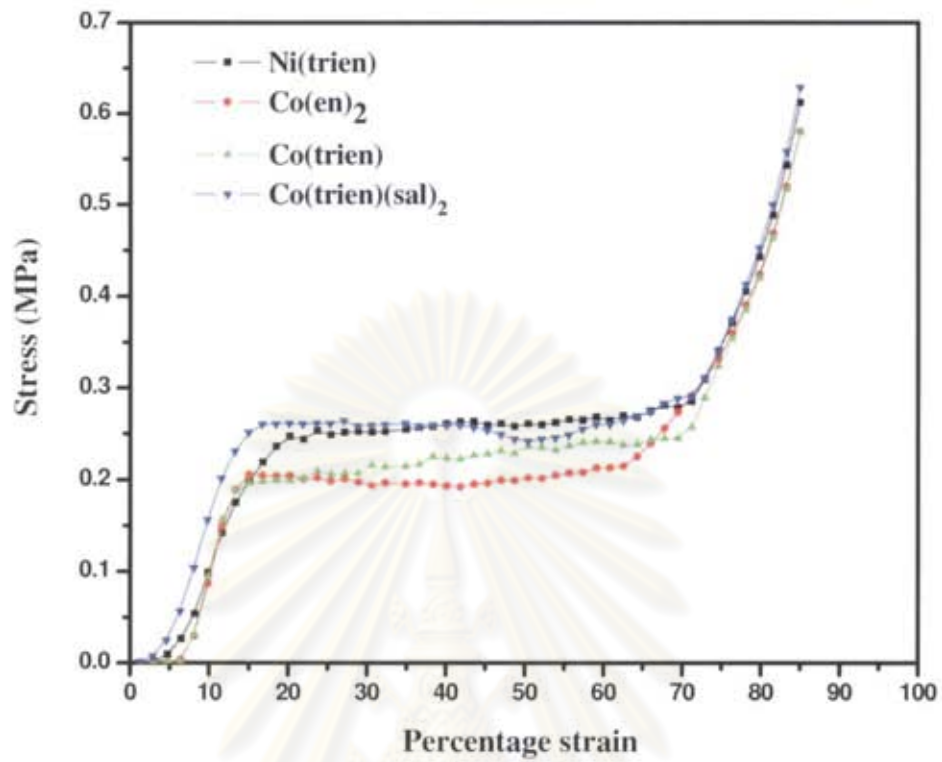**Figure B2** Compression stress-strain curve of PURFs catalyzed by different catalysts at index of 120
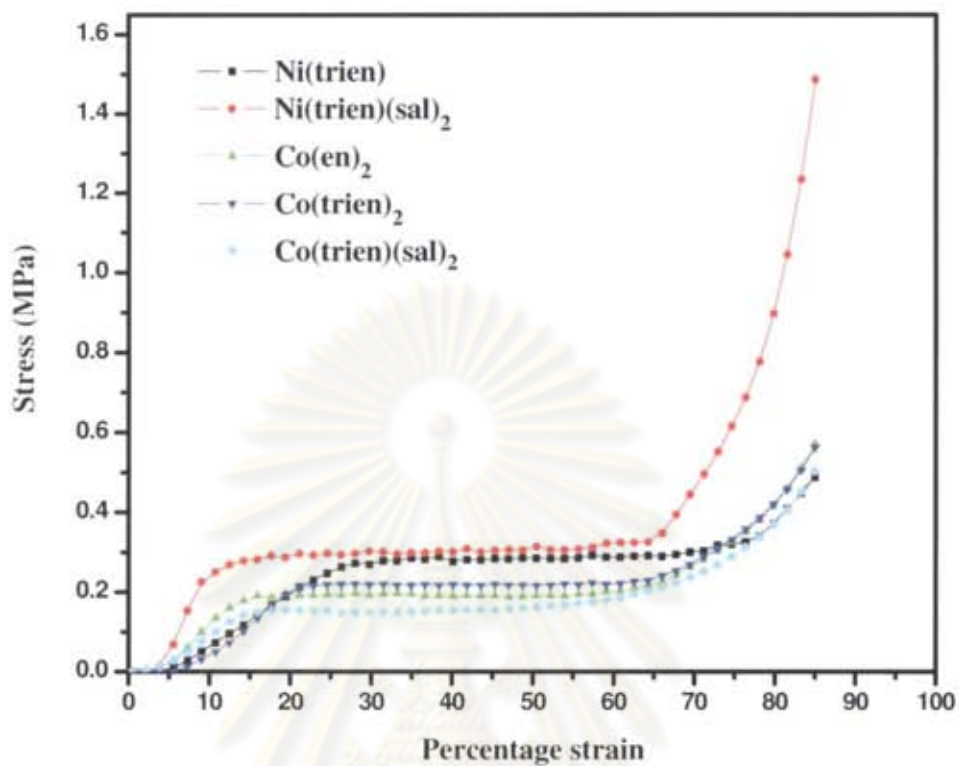
Figure B3 Compression stress-strain curve of PURFs catalyzed by different catalysts
at index of 140

ศูนย์วิทยทรัพยากร
จุฬาลงกรณ์มหาวิทยาลัย

VITAE

Name	:	MISS BHATTARIN SAENGFAK
Date of birth	:	August 20, 1984
Nationality	:	Thai
Address	:	17/50 Moo 1, Seekan, Donmuang, Bangkok, 10210

University Education: Master's Degree from Program in Petrochemistry and Polymer Science, Faculty of Science, Chulalongkorn University, 2008-2010

Bachelor's Degree from Department of Materials Science and Engineering, Program in Petrochemicals and Polymeric Materials, Faculty of Engineering and Industrial Technology, Silpakorn University, 2003-2008

Scholarship:

2009-2010 The NCE-PPAM (National Center of Excellence for Petroleum, Petrochemicals and Advanced Materials)

Conference attendance: Poster presentation "Preparation of rigid polyurethane foam catalyzed by nickel and cobalt complexes" at The 3rd Silpakorn University Research Fair on Creative Economy Conference in Nakhon Pathom, Thailand.

Poster presentation "Preparation of rigid polyurethane foam catalyzed by nickel and cobalt complexes" at The 7th International Symposium on Advanced Materials in Asia-Pacific and JAIST International Symposium on Nano Technology September 30- October 1, 2010 at Ishikawa, Japan.